

THE FUNCTION OF THE MONOMERIC FORM OF THE MU-OPIOID RECEPTOR:  
G PROTEIN-MEDIATED ALLOSTERIC REGULATION OF AGONIST BINDING  
AND STIMULATION OF NUCLEOTIDE EXCHANGE

by

Adam John Kuszak

A dissertation submitted in partial fulfillment  
of the requirements for the degree of  
Doctor of Philosophy  
(Pharmacology)  
in The University of Michigan  
2009

Doctoral Committee:

Associate Professor Roger K. Sunahara, Chair  
Professor Henry I. Mosberg  
Professor Richard R. Neubig  
Professor John R. Traynor  
Associate Professor John J.G. Tesmer

## DEDICATION

To my parents, my sister Beth, and my fiancée Kristin. Your constant love and support has given me the strength to dream big, overcome adversity, and accomplish my goals.

## ACKNOWLEDGEMENTS

First and foremost I must thank my mentor, Dr. Roger Sunahara, for giving me the opportunity to train in his laboratory. He has been an endless source of enthusiasm and encouragement, and his guidance is greatly appreciated.

I thank all the members of my thesis committee, Drs. Neubig, Traynor, Tesmer, and Mosberg, for offering extensive critical discussions of my work, and always pushing me to not just meet their expectations, but to surpass them. I especially thank Dr. Traynor for not only generously providing reagents crucial for my work, but for entertaining many conversations about opioid receptor pharmacology. Dr. Mosberg lent his expertise, and his laboratory, to guide efforts in developing new methods to visualize ligand binding to opioid receptors.

I would like express my deep gratitude to Jessica Anand and Sethuramasundaram “Sethu” Pitchiya who were instrumental in the single molecule imaging experiments performed with fluorescently-labeled receptor and agonists. Jessica, under the guidance of Dr. Mosberg in the Department of Medicinal Chemistry, synthesized the Cy3-labeled agonist dermorphin and characterized its pharmacology both in cellular membranes and in the HDL reconstitution system. Sethu, in the Department of Chemistry, provided his expertise in visualizing the single molecule interactions with fluorescence microscopy. Beyond their technical expertise, I am grateful for the extensive conversations the three of us had regarding the molecular pharmacology of opioid receptors. I must also thank Dr. Nils Water in the Department of Chemistry, as the single molecule imaging experiments were performed in his laboratory. These experiments benefited greatly from Nils’ critical analysis and input.

I must thank Dr. Matthew Whorton. Dr. Whorton developed the HDL approach to membrane protein reconstitution in our lab, which establishes the foundation for this

work. More importantly, I am his debt for the extensive guidance and training he provided throughout my graduate career.

My first efforts in graduate research were spent investigating the molecular pharmacology of the chemokine receptor CCR5. Several undergraduate students helped tremendously in those studies, including Pamela Okolie, Jeff Marchant, and Theresa Lee. Finally, I would like to thank the many former and current members of the Sunahara lab; Aimee Felczak, Dr. Kannan Vaddakadathmeethal, Margaret Sadoff, Katerina Popova, Dr. Diwahaar Narasimhan, Gisselle Velez Ruiz, Dr. Abishek Bandyopadhyay, Brian Devree, Diane Calinski, and Joseph Nichols. I am greatly appreciative of all their help through the years, and I shall always value their friendship.

## TABLE OF CONTENTS

DEDICATION .....	ii
ACKNOWLEDGEMENTS .....	iii
LIST OF FIGURES .....	viii
LIST OF TABLES .....	x
LIST OF APPENDICES .....	xi
LIST OF ABBREVIATIONS .....	xii
ABSTRACT .....	xiv
CHAPTER 1. INTRODUCTION	
Historical Overview .....	1
Opioid Receptor Signaling .....	4
Allosteric Regulation of Opioid Receptors .....	9
Opioid Receptor Oligomerization .....	11
A challenge to requisite dimers .....	14
Elucidating the function of monomeric MOR .....	15
CHAPTER 2. INSECT CELL EXPRESSION AND PURIFICATION OF FUNCTIONAL $\mu$ -OPIOID RECEPTOR	
Introduction .....	17

Results.....	19
Expression of a functional $\mu$ -opioid receptor fusion protein in insect cells .	19
YMOR purification.....	22
Discussion.....	26
Materials Methods .....	31

CHAPTER 3. RECONSTITUTION OF A  $\mu$ -OPIOID RECEPTOR INTO HIGH DENSITY LIPOPROTEIN PARTICLES: THE MONOMER FUNCTIONALLY COUPLES G PROTEINS

Introduction.....	38
Results.....	40
Reconstitution of YMOR into High Density Lipoprotein particles.....	40
Lipid composition influences reconstituted YMOR activity .....	43
YMOR is monomeric when incorporated into HDL.....	45
Monomeric YMOR binds antagonists with appropriate affinities.....	48
Monomeric YMOR functionally couples G proteins.....	49
Discussion.....	52
Materials and Methods.....	55

CHAPTER 4. INVESTIGATING DIFFERENTIAL G PROTEIN ACTIVATION AND AGONIST BINDING TO MONOMERIC  $\mu$ -OPIOID RECEPTOR

Introduction.....	61
Results.....	62
DAMGO and morphine differentially activate $G\alpha_{i3}$ coupled to monomeric YMOR.....	62
DAMGO can differentially activate $G\alpha_{i2}$ , $G\alpha_{i3}$ and $G\alpha_{oA}$ coupled to monomeric YMOR .....	63

$G\alpha_{oA}$ exhibits higher basal nucleotide binding compared to $G\alpha_{i2}$ .....	65
DAMGO and morphine appear equipotent at activating $G\alpha_{i2}$ coupled to monomeric YMOR .....	67
Morphine appears equipotent at activating $G\alpha_{i2}$ and $G\alpha_{oA}$ coupled to monomeric YMOR .....	67
Naloxone does not significantly alter basal activity of $G\alpha_{i2}$ or $G\alpha_{oA}$ .....	68
$G_{i2}$ and $G_{oA}$ heterotrimers regulate high affinity morphine binding to monomeric YMOR .....	69
Discussion.....	71
Materials and Methods.....	75
 CHAPTER 5. CONCLUSIONS	
Summary .....	77
A potential role for opioid receptor oligomerization .....	78
Direct analysis of opioid receptor organization in cells.....	82
Isolation and reconstitution of opioid receptor dimers .....	85
 APPENDICES .....	 88
REFERENCES .....	104

## LIST OF FIGURES

### Figure

1-1	The G protein cycle .....	5
1-2	Overview of opioid receptor signaling .....	8
1-3	Activation of transducin by monomeric rhodopsin in HDL particles .....	15
2-1	Modification of MOR for insect cell expression .....	20
2-2	YMOR functionally binds ligands and couples to G proteins .....	21
2-3	YMOR expression increases in the presence of naltrexone .....	22
2-4	Detergent solubilization of YMOR from insect cells .....	23
2-5	Naltrexone increases coordinated-cobalt retention of YMOR .....	23
2-6	Inclusion of cholesteryl hemissuccinate (CHS) during n-dodecyl- $\beta$ -D-maltoside (DDM) solubilization stabilizes YMOR .....	24
2-7	Purification of YMOR from High Five <sup>TM</sup> insect cells .....	25
2-8	Detergent solubilization disrupts high affinity [ <sup>3</sup> H]DPN binding to YMOR ..	26
3-1	Schematic overview of GPCR reconstitution into HDL particles .....	40
3-2	Reconstitution of YMOR into rHDL particles .....	42
3-3	The ratio of POPC to POPG in rHDL particles influences the binding properties of incorporated YMOR .....	43
3-4	The presence of brain lipid extract during YMOR reconstitution into HDL increases [ <sup>3</sup> H]DPN binding levels .....	44
3-5	HDL reconstitution of Cy3- and Cy5-labeled YMOR .....	46
3-6	YMOR is monomeric when reconstituted into HDL particles .....	47
3-7	Opioid antagonists bind YMOR in rHDL with affinities equivalent to those observed for membrane preparations .....	48



## LIST OF FIGURES, CONTINUED

### Figure

3-8	Binding of agonists to rHDL•YMOR is allosterically regulated by G proteins.....	50
3-9	HDL reconstituted YMOR activates G <sub>12</sub> in response to agonist binding .....	51
4-1	Morphine is less efficacious than DAMGO towards activation of G $\alpha_{13}$ coupled to monomeric YMOR.....	64
4-2	G $\alpha_{oA}$ exhibits higher basal nucleotide binding than G $\alpha_{12}$ when coupled to rHDL•YMOR.....	66
4-3	Ligand dose-response for [ <sup>35</sup> S]GTP $\gamma$ S binding to G <sub>12</sub> coupled monomeric YMOR.....	68
4-4	Ligand dose-response for [ <sup>35</sup> S]GTP $\gamma$ S binding to G <sub>oA</sub> coupled monomeric YMOR.....	69
4-5	Allosteric regulation of morphine binding to monomeric YMOR by G <sub>12</sub> and G <sub>oA</sub> .....	70
5-1	Visualization of Bodipy TR-conjugated opioids binding to live cells .....	84
5-2	Anti-FLAG Western Blot analysis of YDOR enrichment.....	86
A-1	[Lys <sup>7</sup> , Cys <sup>8</sup> ]dermorphin-Cy3 structure .....	89
A-2	[Lys <sup>7</sup> , Cys <sup>8</sup> ]dermorphin-Cy3 preparation.....	90
A-3	[Lys <sup>7</sup> , Cys <sup>8</sup> ]dermorphin-Cy3 retains agonist properties.....	91
A-4	Single molecule imaging of Cy3-labeled agonist binding to rHDL•YMOR coupled to G <sub>12</sub> .....	92
A-5	Single molecule TIRF imaging of [Lys <sup>7</sup> , Cys <sup>8</sup> ]dermorphin-Cy3 binding is competed by naltrexone and dependent on G protein coupling.....	94
B-1	Analysis of ( $\Delta$ 1-43)His <sub>6</sub> -apoA-1 purification.....	98
B-2	Analysis of G <sub>12</sub> , G <sub>13</sub> , and G <sub>oA</sub> heterotrimer purifications .....	99
B-3	Size exclusion chromatography resolution of rHDL•YMOR particles .....	100
B-4	Na <sup>+</sup> ions modulate [ <sup>3</sup> H]DPN binding to monomeric YMOR .....	101
B-5	Allosteric regulation of CTAP binding to YMOR.....	103

## LIST OF TABLES

### Table

1-1	Relative receptor selectivity of representative opioids .....	2
1-2	Opioid receptor differences in mediating behavioral responses .....	4
3-1	[ <sup>3</sup> H]DPN binding parameters of YMOR reconstituted with varying lipid ratios.....	44
3-2	Components of porcine polar lipid brain extract .....	44
4-1	DAMGO stimulation of [ <sup>35</sup> S]GTPγS binding to G protein heterotrimers coupled to rHDL•YMOR.....	65

LIST OF APPENDICES

**Appendix**

A.....	88
B.....	98

## LIST OF ABBREVIATIONS

AC	adenylyl cyclase
apoA-1	apolipoproteinA-1
Arr3	Arrestin3
BLE	polar brain lipid extract
BRET	bioluminescence resonance energy transfer
BSA	bovine serum albumin
C <sub>12</sub> E <sub>10</sub>	polyoxyethylene lauryl ether
cAMP	cyclic adenosine monophosphate
CHAPS	3-[(3-Chloramidopropyl)dimethylammonio]-1-propanesulfonate hydrate
CHO	Chinese hamster ovary
CHS	cholesteryl hemisuccinate
CTAP	D-Phe-Cys-Tyr-D-Trp-Arg-Thr-Pen-Thr-NH <sub>2</sub>
DAG	diacylglycerol
DAMGO	[D-Ala <sup>2</sup> , N-MePhe <sup>4</sup> -Gly-ol <sup>5</sup> ]enkephalin
DDM	n-dodecyl-β-D-maltoside
DOR	δ-opioid receptor
DPDPE	[D-Pen <sup>2,5</sup> ]enkephalin
DPN	diprenorphine
DTT	dithiothreitol
EC <sub>50</sub>	molar concentration of agonist which produces 50% maximal response
ERK	extracellular signal-regulated kinase
FRET	fluorescence resonance energy transfer
G protein	guanine nucleotide binding protein
GDP	guanosine diphosphate
GFP	green fluorescent protein

## LIST OF ABBREVIATIONS, CONTINUED

GPCR	G protein-coupled receptor
GRK	G protein-coupled receptor kinase
GTP	guanosine triphosphate
GTP $\gamma$ S	guanosine 5'-( $\gamma$ -thio) triphosphate
HDL	high density lipoprotein
HEK	human embryonic kidney
High Five <sup>TM</sup>	<i>Trichoplusia ni</i>
K <sub>d</sub>	equilibrium dissociation constant of a ligand in saturation studies
K <sub>i</sub>	equilibrium dissociation constant of a ligand in competition studies
KOR	$\kappa$ -opioid receptor
LDAO	lauryldimethylamine N-oxide
MOR	$\mu$ -opioid receptor
N-O $\beta$ G	n-octyl- $\beta$ -glucoside
NP40	Nonidet P-40
NTX	naltrexone
POPC	1-palmitoyl-2-oleoyl-sn-glycero-3-phosphocholine
POPG	1-palmitoyl-2-oleoyl-sn-glycero-3-[phosphor-rac-(1-glycerol)]
rHDL	reconstituted HDL particles
rHDL•YMOR	reconstituted HDL particles containing YMOR
SDS-PAGE	sodium dodecyl sulfate polyacrylamide gel electrophoresis
SEC	size exclusion chromatography
SEM	standard error of the mean
Sf9	<i>Spodoptera frugiperda</i>
SM-TIRF	single molecule total internal reflection fluorescence microscopy
YDOR	YFP-DOR
YFP	yellow fluorescent protein
YMOR	YFP-MOR

## ABSTRACT

Opioids have been the mainstays to alleviate pain for millennia. The opioid receptors responsible for analgesia are G protein-coupled receptors (GPCRs) which bind several endogenous ligands and couple to multiple isoforms of the  $G_{i/o}$  family of G proteins. Numerous studies have promoted the hypothesis that opioid receptors function as requisite homo- and heterodimers. However, recent reports have illustrated that prototypical GPCRs are fully capable of activating their cognate G proteins as monomers. This thesis investigates the capacity of monomeric MOR to efficiently couple to and activate multiple G protein isoforms. Furthermore, the capacity of monomeric MOR to bind both alkaloid and peptide agonists with high affinity that is subject to allosteric regulation is determined. Finally, it is proposed that differential activation of multiple  $G_{i/o}$  protein isoforms can be promoted by monomeric MOR. To study these questions a yellow fluorescent protein-MOR fusion protein (YMOR) was constructed and expressed in insect cells to facilitate high expression levels. YMOR displays appropriate function, as it binds ligands with high affinity, induces agonist-stimulated [ $^{35}$ S]GTP $\gamma$ S binding to  $G\alpha_i$ , and is allosterically regulated by coupled  $G_i$  protein heterotrimer in insect cell membranes. A novel purification scheme was developed to purify active YMOR, which was then reconstituted into a phospholipid bilayer in the form of high density lipoprotein (HDL) particles. Single particle imaging of fluorescently-labeled YMOR confirmed the receptor was monomeric in HDL particles. Just as in membrane preparations, monomeric YMOR binds alkaloid and peptide antagonists and agonists with high affinity, activates coupled  $G_i$  and  $G_o$  heterotrimers, and is subject to allosteric regulation by both  $G_i$  and  $G_o$ . Furthermore, experiments measuring  $G\alpha$  stimulation suggest that monomeric YMOR can support differential activation of  $G_i$  protein heterotrimers. These data illustrate that the monomeric form of MOR is indeed the minimal functional unit for G protein coupling. In additional studies, single molecule imaging of a Cy3-labeled MOR agonist, [Lys<sup>7</sup>,

Cys<sup>8</sup>]dermorphin, illustrate a novel method for investigating GPCR-ligand binding and suggests that one molecule of agonist binds per monomeric YMOR. While the role of homo-(and hetero)dimerization of opioid receptors continues to be debated, this work has shown that oligomerization is not essential for G protein coupling *in vivo*. It is possible that opioid receptor oligomerization is involved in differential arrestin recruitment and/or desensitization and internalization, where it may play a role in the development of tolerance to opioids *in vivo*.

# CHAPTER 1

## INTRODUCTION

### **Historical Overview**

For millennia humans have used opioid compounds to alleviate pain. Opioids take their name from the opium poppy plant (*Papaver somniferum*), from which the analgesics were first prepared. The active compounds of these preparations were not identified until the first half of the 19<sup>th</sup> century with the extraction of the alkaloids morphine, codeine, and papaverine by Sertürner, Robiquet, and Merck (1). Morphine was later identified as the main active compound, and purified preparations quickly became the drug of choice for the treatment of chronic pain in the early 20<sup>th</sup> century. In addition to analgesia, opioids cause euphoria, nausea, respiratory depression, decreased bowel motility, and exhibit a high level of rewarding/addictive properties. Despite these adverse effects, opioids continue to be used as the mainstay treatment for pain today (2). Yet even with their extensive use in the clinical settings, as well as high incidence of abuse, it was not until the early 1970s that researchers started to unravel the endogenous system at which opioids mediate their effects.

First, specific endogenous opioid binding sites were identified in rat brain homogenates (3-5). The identification of several endogenous opioid peptides, the enkephalins, endorphins, and dynorphins soon followed (6). These compounds were



found in distinct brain regions and are derived from precursor proteins. Shortly thereafter three distinct opioid receptors ( $\mu$ ,  $\kappa$ , and  $\sigma$ ) were proposed to exist based on behavioral responses to morphine, ketocyclazocine, and ( $\pm$ )SKF-10,047 (7). While the  $\sigma$  receptor was later refuted, molecular cloning revealed that opioid binding sites indeed consisted of three isoforms:  $\mu$  (8),  $\delta$  (9, 10), and  $\kappa$  (11). These receptors share ~60% sequence identity, with the greatest diversity found in the ligand binding regions. Recently the nociceptin/orphanin FQ receptor was identified as an opioid receptor based on sequence homology (12), however its role in the opioid system and pain modulation remains unclear. From these findings the diversity and heterogeneity of the opioid system began to emerge, as the multiple receptor isoforms were soon shown to bind to an even larger number of endogenous ligands. Furthermore, the endogenous opioids were noted to bind the different receptor isoforms with some selectivity (Table 1-1).

**Table 1-1**  
**Relative receptor selectivity of representative opioids<sup>a</sup>**

	Opioid Receptor		
	$\mu$	$\delta$	$\kappa$
Endogenous peptides			
Met-enkephalin	++	+++	
Leu-enkephalin	++	+++	
Dynorphin A	++		+++
Dynorphin B	+	+	+++
$\beta$ -endorphin	+++	+++	
Synthetic peptides			
DAMGO <sup>b</sup>	+++		
DPDPE <sup>c</sup>		++	
DADLE <sup>d</sup>	+	++	
Alkaloids			
morphine	+++		+
etorphine	+++	+++	+++

<sup>a</sup> The number of “+” symbols represents relative agonist potency

<sup>b</sup> [D-Ala<sup>2</sup>, MePhe<sup>4</sup>, Gly<sup>5</sup>-ol]enkephalin

<sup>c</sup> [D-Pen<sup>2,5</sup>]enkephalin

<sup>d</sup> [D-Ala<sup>2</sup>, D-Leu<sup>5</sup>]enkephalin

Further investigations into the pharmacology of opioid receptors generated a vast number of synthetic opioids with a wide variety of activity and selectivity profiles. Studies using these various ligands revealed that activation of the individual  $\mu$ ,  $\delta$ , and  $\kappa$  opioid receptor isoforms caused distinct behavioral responses (Table 1-2). In particular, although morphine can bind to all three receptor isoforms ( $\mu > \delta > \kappa$ ) it is believed that its analgesic effects, as well as adverse effects, are mediated mainly through the  $\mu$ -opioid receptor.

Differences between the opioid receptor isoforms continued to be elucidated with studies using radiolabeled opioid ligands. These labeled opioids allowed characterization of binding sites at very low ligand concentrations and revealed a large number of distinct binding sites, more than were expected based on three receptor isoforms. Indeed, extensive reports have culminated in proposals of multiple subtypes for the  $\mu$ ,  $\delta$ , and  $\kappa$  opioid receptors (13). In the case of the  $\mu$  receptor two subtypes have been proposed,  $\mu_1$  and  $\mu_2$ . The  $\mu_2$  site appeared to be selective for morphine binding, while the  $\mu_1$  site poorly discriminated between  $\mu$  and  $\delta$  selective ligands (14). Moreover, careful analysis of behavioral responses following administration of highly selective ligands has led to the proposal that  $\mu_1$  and  $\mu_2$  may contribute to opioid actions such as induction of analgesia and development of dependence in a differential manner (15). However, despite extensive cloning efforts researchers have been unable to identify DNA transcripts coding for multiple receptor subtypes of the  $\mu$ ,  $\delta$ , and  $\kappa$  receptors. As a result, some have questioned the specificity of the ligands used in binding studies which identified multiple receptor subtypes (16). Although the exact nature opioid receptor subtypes remained elusive, the molecular function of the receptors began to be unraveled.

**Table 1-2**  
**Opioid receptor differences in mediating behavioral responses**

Pharmacology in vivo	Opioid Receptor		
	$\mu$	$\delta$	$\kappa$
Antinociception	+++	+/-	+/-
Respiratory Depression	+	-	-
Rewarding Effects	+	-	-
Tolerance	+	+	+
Dependence	+	-	+/-

The number of “+” symbols represents relative amount receptor isoforms contribute to each response

### Opioid Receptor Signaling

Opioid receptors are members of the G protein-coupled receptor (GPCR) superfamily of membrane proteins, belonging to the rhodopsin-like class A family. Approximately one thousand genes in the human genome have been identified as GPCRs, and they are crucial components in a multitude of physiological systems. GPCRs function to bind extracellular agonists and transmit activating signals to intracellular signaling cascades via guanine nucleotide binding proteins (G proteins). GPCRs are integral membrane proteins consisting of a seven helical transmembrane domain topology. G proteins are heterotrimeric complexes comprised of an  $\alpha$  ( $G\alpha$ ),  $\beta$  ( $G\beta$ ), and  $\gamma$  ( $G\gamma$ ) subunit. The concept of guanine nucleotide regulated signaling proteins was initially proposed by Rodbell in 1971 (17), and vast amount of research since has provided a rather thorough understanding of G protein interactions with GPCRs (18, 19), which will be briefly discussed here (Figure 1-1).

Agonist binding stabilizes specific conformations of the transmembrane helices of the receptor, which in turn promote conformational changes in the nucleotide binding domain of the coupled  $G\alpha$  subunit. Ligand binding to opioid receptors is believed to

involve residues in the transmembrane domains for both alkaloids and peptides, and residues in the extracellular loops for peptides (20). The receptor-induced conformational changes in  $G\alpha$  cause nucleotide exchange of a bound guanosine diphosphate (GDP) for guanosine triphosphate (GTP). GTP binding activates the  $G\alpha$ , resulting in a dissociation of the G protein from the receptor. Both the  $GTP\cdot G\alpha$  and  $G\beta\gamma$  dimer complex can then activate or inhibit downstream effector proteins. The signaling activity is terminated by hydrolysis of the GTP via the intrinsic GTPase enzymatic activity of  $G\alpha$ . The  $GDP\cdot G\alpha$  and  $G\beta\gamma$  can then re-couple to receptors, resetting the system for further stimulation.

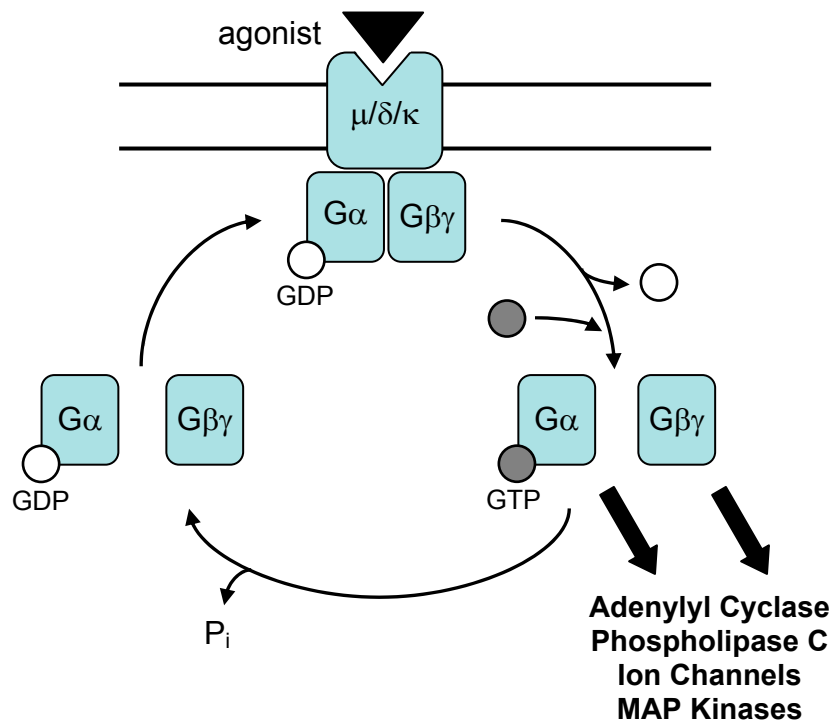


**Figure 1-1.** The G protein cycle. Schematic overview of G protein activation and signaling. G protein heterotrimers are composed of an  $\alpha$ ,  $\beta$  and  $\gamma$  subunit. In the basal state  $G\alpha$  is bound to GDP and the heterotrimer can couple to GPCRs, in this case an opioid receptor. When agonist binds to the receptor it promotes nucleotide exchange at  $G\alpha$ , which then binds GTP. The GTP-bound  $G\alpha$  dissociates from the receptor and both  $GTP\cdot G\alpha$  and  $G\beta\gamma$  can regulate signaling effectors such as adenylyl cyclase, phospholipase C, ion channels, and mitogen activated protein kinases (MAP kinases). Hydrolysis of GTP to GDP by the intrinsic GTPase activity of  $G\alpha$  terminates G protein activity and allows for the subunits to re-associate with receptor.

A critical aspect to regulation of G protein signaling is receptor desensitization following activation by agonist. After G protein dissociation, the receptor C-tail (and for GPCRs the third intracellular loop) is phosphorylated at specific residues by G protein-coupled receptor kinases (GRKs). The phosphorylated C-tail then serves as a recognition site for arrestins, adapter proteins that bind the phosphorylated receptor, promote its internalization and effectively terminate any further receptor signaling. Recently, the GPCR-arrestin interaction has been implicated in new roles, as it has also been shown to mediate signaling through effectors like extracellular signal-regulated kinase 1/2 (ERK1/2) (21). The molecular determinants of GPCR internalization versus signal via arrestin coupling are still being delineated.

There are 23 known mammalian isoforms of  $G\alpha$  subunits, which are divided into four families:  $G_s$ ,  $G_i$ ,  $G_q$ , and  $G_{12}$  (22). They are all highly related by sequence, as all families share approximately 45% amino acid identity and members of a single family can share greater than 90% identity (23).  $G\alpha$  subunits also share a common structure and mechanism of nucleotide binding (24). In all  $G\alpha$  subunits, the binding of GTP induces conformation changes in so-called 'switch' regions, which interact with effectors to regulate their activity (25, 26). G protein heterotrimers interact with GPCRs via their C-terminal tails and the intracellular loops. N-terminal palmitoylation, and also myristoylation in the case of  $G\alpha_i$  and  $G\alpha_o$ , maintains  $G\alpha$  subunits at the plasma membrane. The  $G\beta\gamma$  dimer is bound to the membrane via geranylgeranylation of  $G\gamma$ 's C-terminus. Debate remains over whether or not activated  $G\alpha$  and  $G\beta\gamma$  subunits dissociate completely from the receptor, or if they even fully dissociate from each other.

A considerable amount of work has investigated opioid receptor coupling to G proteins and the resulting signaling events (Figure 1-2). Studies which showed that opioid receptor activation causes inhibition of adenylyl cyclase and a reduction in cellular cAMP levels were the first indication that these receptors coupled to  $G\alpha_i$  (27). Numerous investigations have subsequently focused on opioid receptor regulation of adenylyl cyclase, yet it remains unclear how decreasing cyclic AMP concentration plays a role in analgesia. Decreased cAMP is, however, thought to be involved in the development of tolerance during chronic opioid use. In addition, the higher amount of cAMP seen with removal of the chronic stimulation, termed ‘supersensitization,’ is thought to be a cellular model for withdrawal and dependence (28).

Opioid receptor coupling to  $G\alpha_o$  was first revealed in studies which showed DADLE ([D-Ala<sup>2</sup>, D-Leu<sup>5</sup>]enkephalin) inhibition of  $Ca^{2+}$  current in neuroblastoma x glioma hybrid cells (29). While both  $G_i$  and  $G_o$  could mediate this effect,  $G_o$  was found to be ten-fold more potent. Shortly thereafter  $\mu$ - and  $\delta$ -opioid receptors (MOR and DOR) were found to activate  $K^+$  channels via  $G_o$  coupling (30). The ability of opioid receptors to regulate ion channels in neurons clearly allows them to modulate excitatory neurotransmission, and is likely directly related to their analgesic effects. Although expressed at very high levels in the brain (0.2-0.5% of the total protein), the function of  $G\alpha_o$  is still somewhat unclear. In fact, it is believed that the  $G\beta\gamma$  partners of  $G\alpha_o$  may be responsible for opioid receptor regulation of ion channels (31-33). In addition,  $G\beta\gamma$  subunits have been proposed to activate phospholipase C $\beta$  isoforms (33), although the link between their activation and opioid-induced analgesia remains unclear.

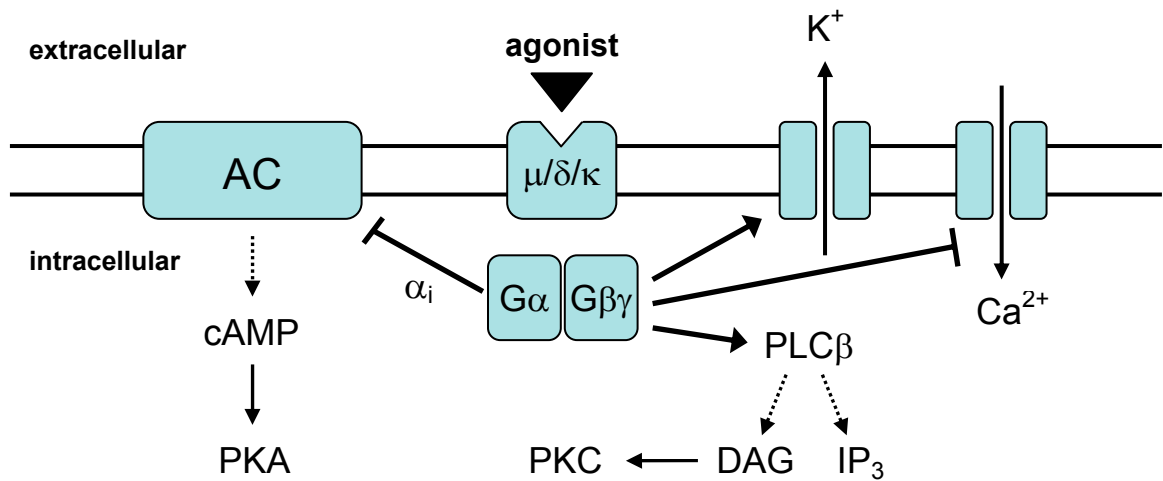


**Figure 1-2.** Overview of opioid receptor signaling. A simplified schematic representation of the signaling cascades induced by agonist binding to  $\mu$ ,  $\delta$ , and  $\kappa$  opioid receptors coupled to  $G_{i/o}$  heterotrimeric G proteins. Solid arrows represent stimulation of effector proteins. Blunt-end lines represent inhibition of effector proteins. Dotted arrows indicate generation of second messenger signaling molecules. Abbreviations used are:  $\mu/\delta/\kappa$ , one of the three opioid receptor isoforms; AC, adenylyl cyclase; cAMP, cyclic adenosine monophosphate; PKA, protein kinase A; PLC, phospholipase C; DAG, diacylglycerol; IP<sub>3</sub>, inositol triphosphate; PKC, protein kinase C.

Multiple isoforms have been identified for each  $G\alpha$  of the  $G_{i/o}$  family, including  $G\alpha_{i1}$ ,  $G\alpha_{i2}$ ,  $G\alpha_{i3}$ ,  $G\alpha_{oA}$ , and  $G\alpha_{oB}$  (23). Adding a further level of complexity to opioid receptor activation of  $G_i$  and  $G_o$ , all five isoforms have been shown to couple to MOR (34), and multiple studies provide evidence that activation of the receptor results in differential activation of the individual isoforms (35). However, the rank-order of  $G\alpha$  activation varies greatly depending on the experimental system (endogenous or transfected receptors and/or G proteins). This large diversity in signaling partners may allow for fine control over the cellular responses to opioids, depending on which G protein-effector signaling complexes are present in particular CNS regions and cells.

## Allosteric Regulation of Opioid Receptors

Just as ligand binding to opioid receptors has been found to initiate multiple protein interactions and cellular responses, ligand binding is modulated by several mechanisms. GPCRs exist in multiple conformational states and binding of an agonist stabilizes the conformation that activates G proteins. Likewise, G protein coupling to the receptor stabilizes a distinct conformation of the agonist binding site, or orthosteric site. This change in the orthosteric site decreases the agonist dissociation rate, which translates to a decrease in the dissociation constant ( $K_d$ ) and an increase in the affinity of the agonist for the receptor. Thus, the binding of an agonist at the orthosteric site is influenced by the binding of G proteins at a separate site via an allosteric mechanism. In this way, when a GPCR is not coupled to a G protein heterotrimer the binding affinity of agonists is considerably lower than when the receptor is coupled. This allosteric regulation is a defining characteristic of GPCR function (36). The opioid receptors are no exception, as an important aspect of MOR function is the ability of  $G_i$  and  $G_o$  coupling to regulate agonist binding affinity. This has been demonstrated unequivocally by studies analyzing agonist binding to MOR in the absence and presence of various nucleotide conditions to uncouple G protein from the receptor (37-43).

Allosteric regulation of the orthosteric site in GPCRs is not limited to G proteins. Monovalent metal ions have also been shown to be allosteric regulators of opioid binding, and sodium has received the greatest attention. Sodium ions influence the binding of both agonists and antagonists to MOR in an opposing fashion: increasing  $Na^+$  concentrations decrease the binding of agonists, but increase the binding of antagonists (37-39, 44-46). Removing  $Na^+$  has been proposed to destabilize the receptor to some



extent, allowing it to adopt multiple conformations and in turn allow it to more readily adopt a conformation capable of binding agonist (44). This influence over agonist binding is not unique to opioid receptors, as ligand binding to many GPCRs has been found to be regulated by metal ions (36). An aspartate in the second transmembrane domain which is conserved among most GPCRs, including  $\mu$ ,  $\delta$ , and  $\kappa$  opioid receptors, is believed to be critical for the  $\text{Na}^+$  effects (47, 48). The carboxyl moiety of this aspartate residue is thought to be accessible to  $\text{Na}^+$  in the cytoplasm. Similar to G proteins, the binding of  $\text{Na}^+$  to this allosteric site alters the ligand dissociation rate at the orthostatic site. Recently, a determination of the crystal structure of the  $\beta_1$ -adrenergic receptor found a  $\text{Na}^+$  ion was important in stabilizing the second extracellular loop of the receptor by coordinating cysteine and aspartate residues (49). While no such interaction has been identified for opioid receptors, this finding nonetheless suggests another potential way GPCR function (or stability) can be regulated by sodium.

Finally, ligand binding at opioid receptors is known to be allosterically regulated by membrane microfluidity. The plasma membrane environment surrounding the receptor affects its ability to adopt different conformations, and thus influences the orthosteric binding site. Membrane fluidity/rigidity can be modified by the cholesterol and phospholipid components. Alterations of the membrane composition by removal or addition of cholesterol has been shown to have dramatic effects on agonist binding to MOR (50-52). Similarly, agonist binding to MOR is highly sensitive to the content of acidic and unsaturated phospholipids in the membrane (53, 54).

Taken together, it is apparent that MOR function is highly multifaceted. MOR binds multiple relatively small alkaloid and relatively large peptide ligands with eloquent

and nuanced selectivity. MOR is capable of activating multiple G protein isoforms in a differential manner. Finally, ligand binding to MOR is regulated by several allosteric modulators. More recently a further level of complexity was added to MOR function, as the receptor has been proposed to exist in oligomeric complexes.

### **Opioid Receptor Oligomerization**

While the multiple levels of MOR regulation were being elucidated the receptors were traditionally thought to function as a monomeric unit. Since the 1990s, however, considerable evidence has accumulated which suggests GPCRs may exist as dimers or higher order oligomers at the plasma membrane. The ability of GPCRs to form homo- or heterodimers may impart yet another level of signaling diversity and specificity, as the formation of larger oligomeric receptor complexes is postulated to cause conformational changes and generate unique ligand binding and G protein coupling surfaces. The importance of GPCR dimerization is best illustrated by the class C GPCRs such as the metabotropic glutamate and GABA<sub>B</sub> receptors. These receptors function as obligate dimers in which the agonist binds to one member of the dimer pair where as the G protein binding and activation is conferred through the other (55).

A large number of class A GPCRs are purported to dimerize based on multiple studies measuring the interaction of two receptors at the plasma membrane. These studies utilized fluorescence resonance energy transfer (FRET) and bioluminescence resonance energy transfer (BRET) to observe interactions between fluorescently-labeled GPCRs in heterologous over-expression systems (56, 57). This includes the opioid receptors, in which all three isoforms have been observed to both homo- and heterodimerize (58).

Recently these proposed interactions have come under increased scrutiny and debate, as some have argued that a lack of stringency in the interpretation of FRET and BRET data has led to a number of GPCRs being falsely identified as dimers (59).

Even with the debate regarding fluorescence based data concerning GPCR dimerization, multiple other investigations support the existence of oligomerization between opioid receptors based on biochemical and pharmacological measurements. The first suggestion of opioid receptor organization came from studies measuring rhodamine-labeled enkephalin binding to neuroblastoma cells. Crude fluorescence microscopy imaging demonstrated punctate staining at the membrane surface, which was converted to a diffuse signal following treatment with reducing agents (60). From these findings the authors proposed that the DOR may exist in protein complexes at the membrane, although such complexes were not required for ligand binding. It is possible, however, that receptor clustering, resulting from desensitization following treatment with the labeled-agonist, may account for these findings.

The possibility of a hetero-oligomeric complex between MOR and DOR first came under consideration when the two receptor types were demonstrated to be endogenously expressed in the same neuron in both the central and enteric nervous system (61-63). Intriguingly, a series of studies on putative opioid receptor subtypes resulted in the proposal that MOR and DOR may form a complex with altered ligand binding properties (64-68). Following the molecular cloning of the opioid receptors, several groups began to look at the interactions of MOR and DOR in heterologous expression systems. Initial reports of DOR homodimers were based on SDS resistant high molecular weight bands in SDS-polyacrylamide gel electrophoresis analyses and also by

various co-immunoprecipitation approaches (69). Perhaps the most compelling data for opioid receptor dimerization came with studies illustrating altered agonist binding affinities at cells expressing both DOR and KOR or MOR and DOR compared to cells expressing a single isoform (70, 71). Further reports suggested that the DOR-selective agonist [D-Pen<sup>2,5</sup>]enkephalin (DPDPE) could compete with the binding of the MOR-selective agonist [D-Ala<sup>2</sup>, N-MePhe<sup>4</sup>-Gly-ol<sup>5</sup>]enkephalin (DAMGO) with higher affinity in cells expressing both MOR and DOR versus cells expressing only MOR (72). Moreover, cells expressing both MOR and DOR surprisingly showed biphasic binding of agonists in the absence of G protein coupling, with affinities that did not correspond with those observed in cells expressing just one receptor isoform (71). More recently, MOR-DOR heterodimers have been proposed to traffic to the membrane in a pre-assembled form (73) and have been proposed to have altered specificity in arrestin recruitment and subsequent activation of ERK (74).

An important caveat to these studies is the assumed formation of specific heterodimer complexes in the plasma membranes of cultured cells. Little discussion was put forth regarding the fact that cells expressing both MOR and DOR may have a mixed population of receptors at the membrane, including homodimers, heterodimers, and perhaps even monomers or higher order oligomers. Therefore although distinct changes in ligand and receptor pharmacology resulted from co-expressing MOR and DOR, the exact nature of the signaling complexes remains unclear.

Despite these concerns, the idea of opioid receptor oligomerization has gained wide acceptance, and some consider it to be necessary for receptor function. This may stem from the fact that opioid receptor dimerization would nicely account for the

delineation of many receptor subtypes ( $\mu_1$ ,  $\mu_2$ ,  $\delta_1$ ,  $\delta_2$ ,  $\kappa_1$ ,  $\kappa_2$ ) defined pharmacologically compared to the three receptors identified by cloning (13). Furthermore, oligomerization may play a role in opioid receptors' ability to couple multiple  $G_{i/o}$  subtypes and activate them differentially. All told, several groups promote the notion of ubiquitous opioid receptor dimer formation, and much research is currently focused on specifically targeting heterodimers as therapeutic targets (75).

### **A challenge to requisite dimers**

The concept of obligate GPCR dimerization has recently been challenged by a series of biochemical studies on the  $\beta_2$  adrenergic receptor ( $\beta_2$ AR) and rhodopsin (76-80). Critical to these studies was the development of a new methodology for studying the function of isolated GPCRs, namely, reconstitution of purified receptors in high density lipoprotein (HDL) particles. In this approach purified GPCRs are incorporated into a phospholipid bilayer which is constrained inside a dimer of apolipoproteinA-1 (apoA-1). These HDL particles are uniform, mono-dispersed, discoidal complexes. Our laboratory utilized this HDL reconstitution approach to definitively elucidate the capacity of monomeric  $\beta_2$ AR and rhodopsin to efficiently couple to and activate their cognate G proteins  $G_s$  and  $G_t$  (Figure 1-3) (78, 79). The demonstration of functional monomeric class A GPCRs stands in stark contrast to the view that opioid receptor oligomerization is required for function. These receptors may, however, simply function differently. After all, the capacity of MOR to bind multiple endogenous ligands with nuanced selectivity, couple to multiple G protein isoforms, and activate G protein isoforms in a differential

manner are traits not traditionally associated with rhodopsin and the  $\beta_2$ AR. It is possible that these functional characteristics are indeed dependent upon receptor oligomerization.

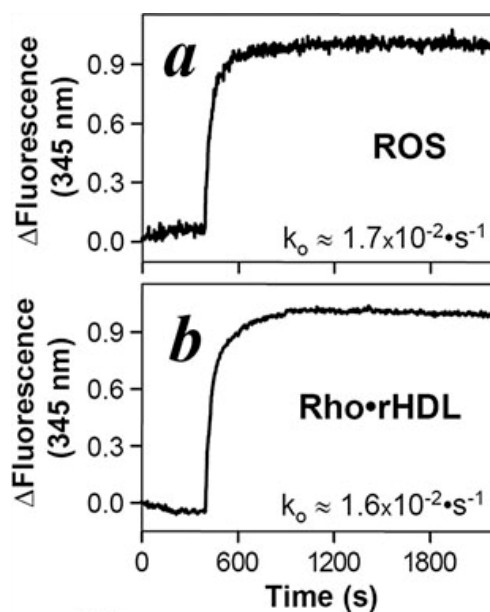


**Figure 1-3.** Activation of transducin by monomeric rhodopsin in HDL particles. Photoactivated oligomeric rhodopsin in rod outer segment (ROS) membranes (**a**) or monomeric rhodopsin in rHDL (**b**) activates transducin at identical rates. Transducin activation was measured by monitoring the tryptophan fluorescence ( $\lambda_{em} = 345$  nm) of the  $G\alpha_i$  subunit. Adapted from Whorton *et al.* 2008, *J Biol Chem* 283:4387-94 (79), with author's permission.

### Elucidating the function of monomeric MOR

An important aspect to our understanding of opioid receptor function therefore faces a critical question: are the multifaceted interactions of MOR with distinct agonists and G protein heterotrimers dependent upon receptor dimerization? This thesis investigates the capacity of monomeric MOR to efficiently couple to and activate multiple G protein isoforms. Furthermore, the capacity of monomeric MOR to bind both alkaloid and peptide agonists with high affinity that is subject to allosteric regulation is

determined. Finally, it is proposed that differential activation of multiple G protein isoforms can be promoted by monomeric MOR.

In order to address these questions, MOR was reconstituted into HDL particles as a monomer, along with distinct G protein heterotrimers. The pharmacology of ligand binding and G protein activation was then determined in this defined system and compared to that of membrane preparations. This approach necessitated the purification of relatively high quantities of active MOR, a task which has to date eluded researchers. A methodology to meet this requirement was developed and is outlined in Chapter 2. Reconstitution of monomeric MOR and G<sub>12</sub> heterotrimer into HDL particles is discussed in Chapter 3, which illustrates that the monomer can not only bind agonists and antagonists with high affinity, but is fully capable of stimulating G $\alpha_i$ . Finally, the capacity of monomeric MOR to support differential activation of multiple G $\alpha$  isoforms is demonstrated in Chapter 4. Additionally, the development of novel single molecule methods for imaging ligand binding to isolated, monomeric GPCRs is presented in Appendix A. Having shown that monomeric MOR is sufficient in several functional measurements, potential physiological roles for oligomerization are discussed in Chapter 5. In conclusion, this thesis establishes that monomeric MOR does indeed display the same level of functional G protein coupling as seen in cellular preparations, providing additional insight to guide our understanding of the cellular and behavioral responses which are potentially influenced by opioid receptor oligomerization.

## CHAPTER 2

### INSECT CELL EXPRESSION AND PURIFICATION OF FUNCTIONAL $\mu$ -OPIOID RECEPTOR

#### **Introduction**

This thesis proposed to investigate the function of an isolated and monomeric  $\mu$ -opioid receptor (MOR), and as such necessitated its purification to homogeneity. Purification of the  $\mu$ - and  $\delta$ -opioid receptors has been attempted many times as investigators tried to understand the heterogeneity and complexity of the opioid receptor system, such as the apparent existence of multiple opioid receptor isoforms (65, 68, 81-83). Several purification schemes from brain homogenates have been reported (84-90) and a common approach in these purifications was the use of immobilized ligand affinity chromatography with ligands selective for MOR (84, 89, 91) or DOR (87). By virtue of the ligand affinity purification, these preparations often resulted in high specific activity for the purified receptor, approaching the theoretical maximum. However, both antagonists and agonists bound the purified component with markedly lower affinity than membrane preparations. Interestingly, Côté and co-workers described a MOR solubilization and purification in which a G protein component was co-purified, resulting in higher affinity agonist binding by the soluble receptor (88, 92). Still, purification of MOR from brain homogenates suffered from relatively low yields, and even with



selective ligand affinity chromatography the endogenous source of receptors can result in a mixed final population of  $\mu$ ,  $\delta$ , and  $\kappa$  opioid receptors.

Following the molecular cloning of the opioid receptors, attempts have been made to address both the relatively low expression levels and heterogeneous receptor starting population by over-expressing MOR in cell culture systems. Human MOR and a green fluorescent protein (GFP)-MOR fusion protein have been expressed in the methylotrophic yeast *Pichia pastoris* with some success (93-96). While the *P. pastoris* expressed MOR was able to bind the opioid antagonist [<sup>3</sup>H]diprenorphine (DPN) with high affinity, the capacity of MOR to couple G proteins was not determined, and relative expression levels were relatively low at ~0.5-1 pmol/mg total membrane protein. Moreover, the GFP-MOR construct was unable to bind opioid agonists (96).

In light of the previous work discussed above, we took a different approach to purify MOR. *Spodoptera frugiperda* (Sf9) and *Trichoplusia ni* (High Five™) insect cells were used to over-express MOR, as these systems are known to produce high levels of recombinant proteins (97). In order to increase expression and aid in purification, a MOR fusion protein was created with a hemagglutinin signal sequence, FLAG epitope, Histidine<sub>10</sub> tag, and yellow fluorescent protein (YMOR). Such fusion protein modifications to GPCRs can potentially alter receptor function by disrupting its ability to bind ligands and undergo conformational changes. Therefore it was critically important to illustrate that YMOR expressed in insect cells was capable of agonist/antagonist binding, G protein activation, and allosteric regulation of agonist binding by G proteins. In this work we demonstrate that insect cells are capable of expressing YMOR in high amounts. This YMOR construct is fully functional in regard to ligand binding and G protein

coupling in insect membranes. Furthermore, we demonstrate a methodology to purify active YMOR to near homogeneity.

## Results

### Expression of a functional $\mu$ -opioid receptor fusion protein in insect cells

A schematic illustration of the yellow fluorescent protein-tagged  $\mu$ -opioid receptor construct, termed YMOR, is shown in Figure 2-1a. This fusion protein was expressed in *Sf9* and High Five<sup>TM</sup> insect cells. Anti-FLAG Western Blot staining of membrane preparations showed the expected molecular weight for YMOR of  $\sim 73$  kDa, as well as higher weight bands of potential SDS-resistant oligomers or protein aggregate (Figure 2-1b). Membrane binding assays showed that YMOR bound the non-specific opioid antagonist [<sup>3</sup>H]DPN with high affinity in a saturable manner ( $K_d = 0.63 \pm 0.08$  nM; Figure 2-2a), in agreement with the ligand binding properties of MOR expressed in mammalian cells (98-100).

The  $\mu$ -selective agonist DAMGO ([D-Ala<sup>2</sup>, N-MePhe<sup>4</sup>, Gly<sup>5</sup>-ol]enkephalin) also bound with high affinity to membranes co-expressing YMOR and  $G\alpha_{i2}$ -His<sub>6</sub>G $\beta_1$ -G $\gamma_2$  G protein heterotrimer ( $G_{i2}$ ) ( $K_d \sim 1.5 \pm 0.3$  nM; Figure 2-2b). DAMGO stimulated [<sup>35</sup>S]GTP $\gamma$ S binding in a concentration dependent manner (Figure 2-2c), eliciting strong activation of  $G_{i2}$ , resulting in [<sup>35</sup>S]GTP $\gamma$ S binding nearly four-fold over basal levels ( $EC_{50} \sim 36 \pm 0.1$  nM). Assays were performed in 100 mM NaCl and 5 mM MgCl<sub>2</sub>. The potency of DAMGO at YMOR expressed in insect cells is well in line with its observed pharmacological characteristics in mammalian cell expression systems (99-101).

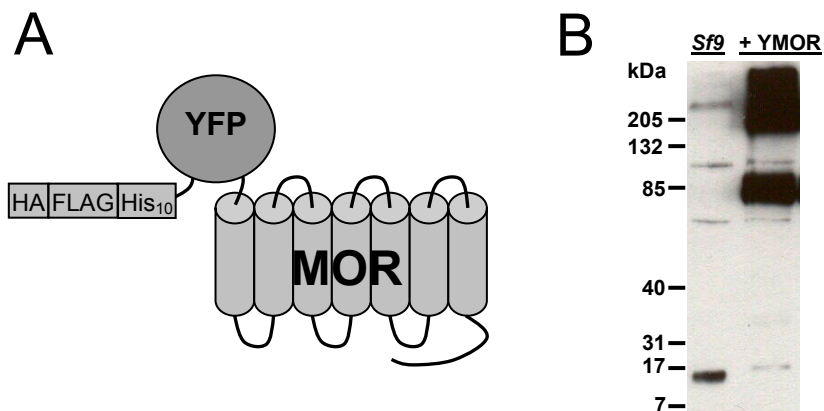


**Figure 2-1.** Modification of MOR for insect cell expression. **(A)** Schematic representation of the modified  $\mu$ -opioid receptor expressed in insect cells. N-terminal modifications included a hemagglutinin signal sequence (HA), FLAG epitope, histidine tag ( $\text{His}_{10}$ ) and a yellow fluorescent protein (YFP). This construct, termed YMOR, was expressed in *Sf9* and High Five<sup>TM</sup> insect cells using a recombinant Baculovirus system. **(B)** Anti-FLAG Western Blot analysis confirmed expression of YMOR in *Sf9* cells at the expected molecular size of 73 kDa. Five mg of total membrane protein was resolved by SDS-PAGE and transferred to nitrocellulose. Higher weight YMOR SDS-resistant oligomers and/or aggregate were also observed.

Allosteric regulation of agonist binding by G proteins (102) was also observed for YMOR expressed in insect cells. In the absence of  $\text{G}_{i2}$ , DAMGO competed with [<sup>3</sup>H]DPN (0.5 nM) binding in a concentration-dependent manner with a  $K_i$  of  $\sim 2.3 \mu\text{M}$  (Figure 2-2d). In membranes expressing both YMOR and  $\text{G}_{i2}$ , DAMGO exhibited a biphasic mode of inhibition of [<sup>3</sup>H]DPN binding with  $K_{i_{hi}} \sim 0.75 \text{ nM}$  and  $K_{i_{lo}} \sim 780 \text{ nM}$  (fraction of  $K_{i_{hi}} = 0.45$ ). The addition of  $10 \mu\text{M}$   $\text{GTP}\gamma\text{S}$  to the YMOR +  $\text{G}_{i2}$  membranes eliminated the high affinity DAMGO binding site ( $K_i \sim 5.2 \mu\text{M}$ ), illustrating that YMOR is allosterically regulated by G proteins. Competition assays were performed in 136 mM NaCl. Taken together, these results demonstrate that YMOR expressed in High Five<sup>TM</sup> cells is fully functional in regards to ligand binding and G protein coupling.

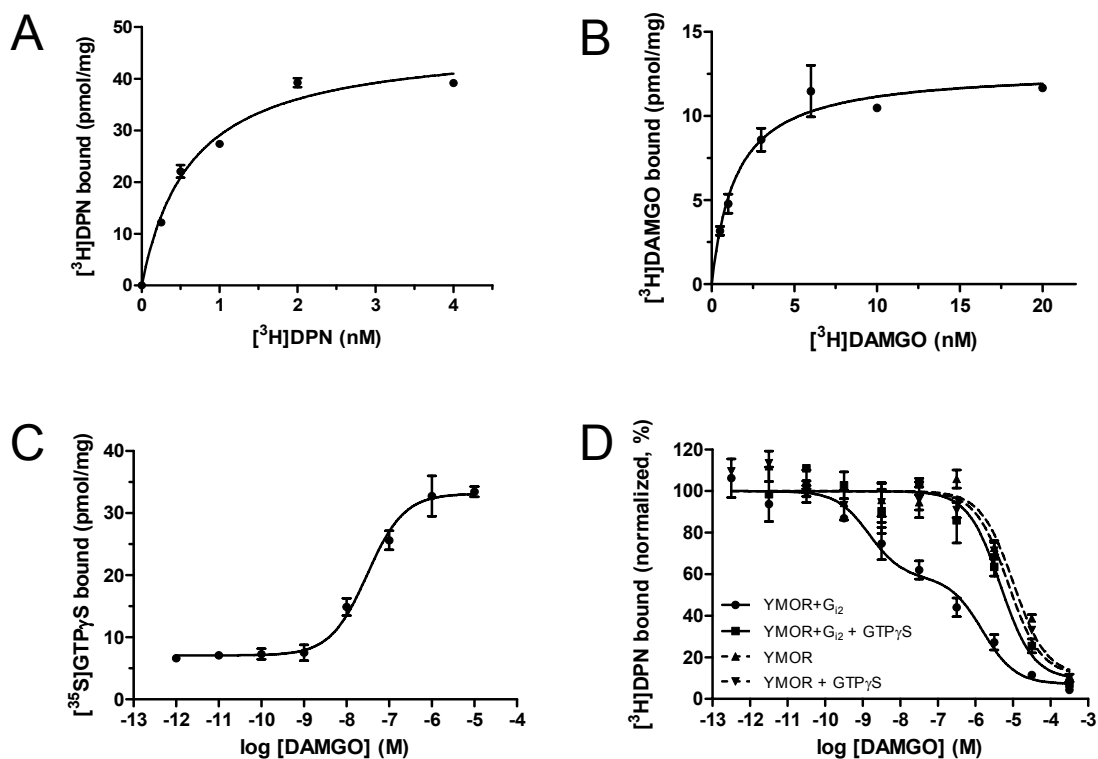


**Figure 2-2.** Y MOR functionally binds ligands and couples to G proteins. Plasma membranes isolated from High Five<sup>TM</sup> cells expressing Y MOR and G<sub>12</sub> heterotrimer were prepared, and 2-5  $\mu\text{g}$  of total membrane protein was used in radioactive binding assays. Y MOR expressed in insect cells exhibits high affinity ligand binding. **(A)** Y MOR bound  $[^3\text{H}]\text{DPN}$  with a  $B_{\text{max}}$  of  $\sim 40$  pmol/mg and a  $K_d$  of  $0.6 \pm 0.1$  nM. **(B)** Y MOR bound  $[^3\text{H}]\text{DAMGO}$  with an  $B_{\text{max}}$  of  $\sim 13$  pmol/mg and a  $K_d$  of  $1.5 \pm 0.3$  nM. **(C)** Y MOR functionally couples to G protein in insect cell membranes. Membrane preparations ( $5 \mu\text{g}$ ) of High Five<sup>TM</sup> cells co-expressing Y MOR and G<sub>12</sub> heterotrimer were incubated with increasing concentrations of the  $\mu$ -opioid agonist DAMGO in the presence of  $0.1$  nM  $[^{35}\text{S}]\text{GTP}\gamma\text{S}$ . DAMGO stimulated  $[^{35}\text{S}]\text{GTP}\gamma\text{S}$  exchange on G $\alpha_{12}$  with an  $\text{EC}_{50}$  of  $36 \pm 0.1$  nM. **(D)** Agonist binding to Y MOR expressed in insect cells is allosterically regulated by G proteins. Y MOR/G<sub>12</sub> membrane preparations were incubated with  $0.5$  nM  $[^3\text{H}]\text{DPN}$  and increasing concentrations of DAMGO in the absence or presence of  $10 \mu\text{M}$  GTP $\gamma$ S. A high affinity binding site for DAMGO ( $\bullet$ ,  $K_{\text{hi}} \sim 0.75$  nM) was disrupted in the absence of G protein coupling (+GTP $\gamma$ S:  $\blacksquare$ ,  $K_i \sim 2.3 \mu\text{M}$ ). DAMGO also displayed low affinity when bound to membranes not expressing G<sub>12</sub> (Y MOR:  $\blacktriangle$ ,  $K_i \sim 5.2 \mu\text{M}$  and Y MOR+GTP $\gamma$ S:  $\blacktriangledown$ ,  $K_i \sim 3.7 \mu\text{M}$ ). Data are representative of at least two experiments performed in duplicate. Error bars represent the SEM.

In an effort to increase the amount of Y MOR at the insect cell plasma membrane, the receptor was expressed in the presence of the general opioid antagonist naltrexone (NTX).  $[^3\text{H}]\text{DPN}$  binding to plasma membrane preparations showed that NTX increased the  $B_{\text{max}}$  of Y MOR in High Five<sup>TM</sup> cells in a concentration dependent manner (Figure 2-

3). Based on these results, subsequent YMOR expressions were performed in the presence of 1  $\mu\text{M}$  NTX. Maximal receptor levels of 20-40 pmol/mg were routinely observed.

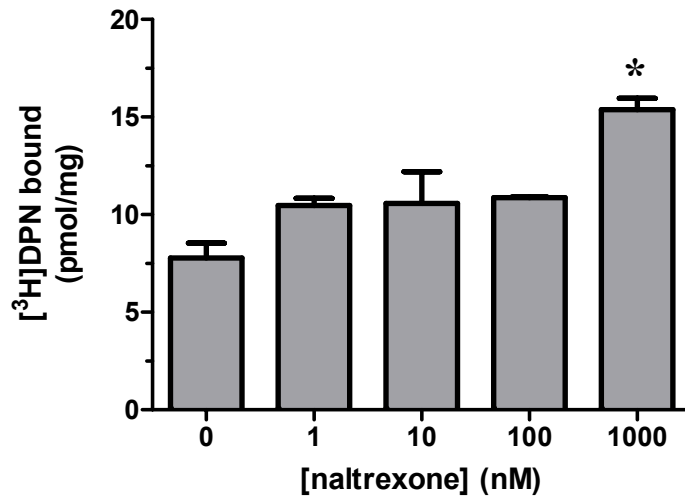


**Figure 2-3.** YMOR expression increases in the presence of naltrexone. High Five<sup>TM</sup> cells expressed YMOR in the absence or presence of increasing amounts of the antagonist naltrexone (NTX). NTX was added 24 hr after infection and 24-30 hr before harvesting. Membrane fractions were prepared and [<sup>3</sup>H]DPN binding to 3  $\mu\text{g}$  of total protein was measured. Due to extensive buffer exchange during membrane preparation, the final NTX concentration in the binding assay was negligible. Infecting cells in the presence of 1  $\mu\text{M}$  NTX approximately doubled the expression of YMOR from  $\sim 7.8$  to  $\sim 15.4$  pmol/mg. Error bars represent the SEM. Experiments were performed in duplicate. \* $P < 0.05$ , significantly different from 0 nM NTX as calculated by a Student's t-test.

### YMOR purification

After verifying that insect expressed YMOR is functional in regards to ligand binding and G protein coupling, efforts were made to purify an active receptor to homogeneity. By necessity, the first step of YMOR purification was extraction of the receptor out of the plasma membrane with detergents. The capacity of a variety of zwitterionic, polar and non-ionic detergents (cholate, n-dodecyl- $\beta$ -D-maltoside (DDM), Triton X-100, lauryldimethylamine *N*-oxide (LDAO), Nonidet P-40 (NP40), 3-[(3-

Chloramidopropyl dimethylammonio]-1-propanesulfonate hydrate(CHAPS), polyoxyethylene lauryl ether (C<sub>12</sub>E<sub>10</sub>), and n-octyl-β-glucoside (N-OβG)) to solubilize YMOR from insect cell membranes was assessed (Figure 2-4). Extraction of YMOR with DDM proved to be most efficient by comparing YMOR levels in detergent soluble and insoluble fractions with anti-FLAG Western Blot staining.

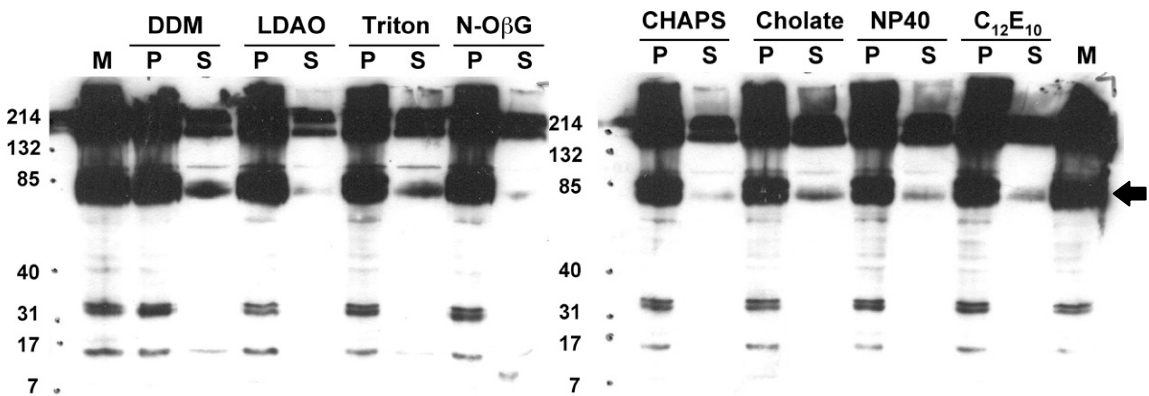


**Figure 2-4.** Detergent solubilization of YMOR from insect cells. *Sf9* cell membrane fractions were prepared at final protein concentration of 5 mg/mL and incubated with detergents at a final concentration of 1% w/v. Samples were subjected to a 100,000 x g spin for 30 min and separated with SDS-PAGE. Anti-FLAG Western Blotting was used to compare the amount of YMOR in the membrane (M), detergent insoluble pellet fraction (P) and the detergent soluble supernatant fraction (S). Equal volumes of pellet and supernatant fractions were loaded. N-dodecyl-β-D-maltoside (DDM) extracted the highest fraction of the ~73 kDa YMOR (arrow).

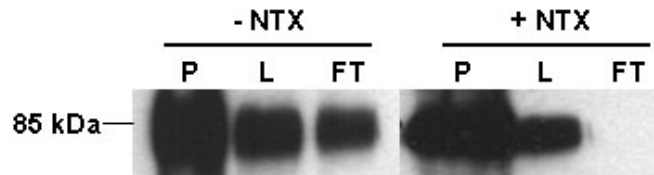


**Figure 2-5.** Naltrexone increases coordinated-cobalt retention of YMOR. Membrane fractions were prepared from High Five<sup>TM</sup> cells expressing YMOR, incubated with 1% DDM to extract membrane proteins, and supernatants from a 100,000 x g spin were passed through a Talon<sup>TM</sup> column. All steps were performed in the presence or absence of 100 nM NTX. Anti-FLAG Western Blot analysis was used to compare the relative amount of YMOR in the detergent-insoluble fraction (P), the detergent-soluble fraction (column load, L), and the column flow through (FT).

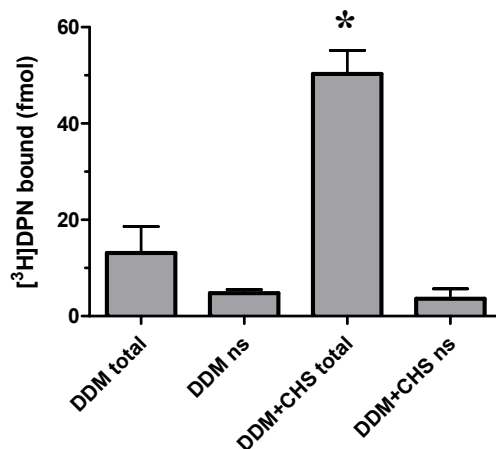


**Figure 2-6.** Inclusion of cholesteryl hemisuccinate (CHS) during n-dodecyl- $\beta$ -D-maltoside (DDM) solubilization stabilizes YMOR. YMOR was solubilized from the plasma membranes of *Sf9* cells with 1% DDM in the presence or absence of 0.01% CHS and then enriched on a Talon<sup>TM</sup> IMAC column in either 0.1% DDM or 0.1% DDM plus 0.01% CHS. [<sup>3</sup>H]DPN binding to these detergent solubilized YMOR samples were then measured in the absence (total) or presence (NS) of 20  $\mu$ M naltrexone. Addition of CHS to solubilized YMOR increased [<sup>3</sup>H]DPN ~3.6-fold, suggesting an improvement in the amount of receptor in an active conformation. Error bars represent the SEM. Experiments were performed in replicate. \*P<0.05, significantly different from DDM total as calculated by a Student's t-test.

The purification strategy for DDM-extracted YMOR involved a series of chromatography steps including metal chelate (Talon<sup>TM</sup>), anion exchange (Source 15Q) and size exclusion (Superdex 200) chromatography columns. Retention of YMOR on the coordinated-cobalt Talon column was initially poor, but increased with the addition of 100 nM NTX (Figure 2-5). The addition of cholesterol (cholesteryl hemisuccinate, CHS, 0.01% w/v) also resulted in an increase in [<sup>3</sup>H]DPN binding to the DDM-solubilized YMOR (Figure 2-6). Peak fractions from each purification step were determined by Coomassie staining, anti-FLAG antibody Western blotting or [<sup>3</sup>H]DPN binding. Fractions displaying the highest [<sup>3</sup>H]DPN binding capacity and appropriate molecular weight on SDS-PAGE were pooled and subjected to the next chromatographic step. After the final Superdex 200 column peak fractions were pooled, concentrated and flash-frozen in liquid N<sub>2</sub>, then stored at -80°C until later use.

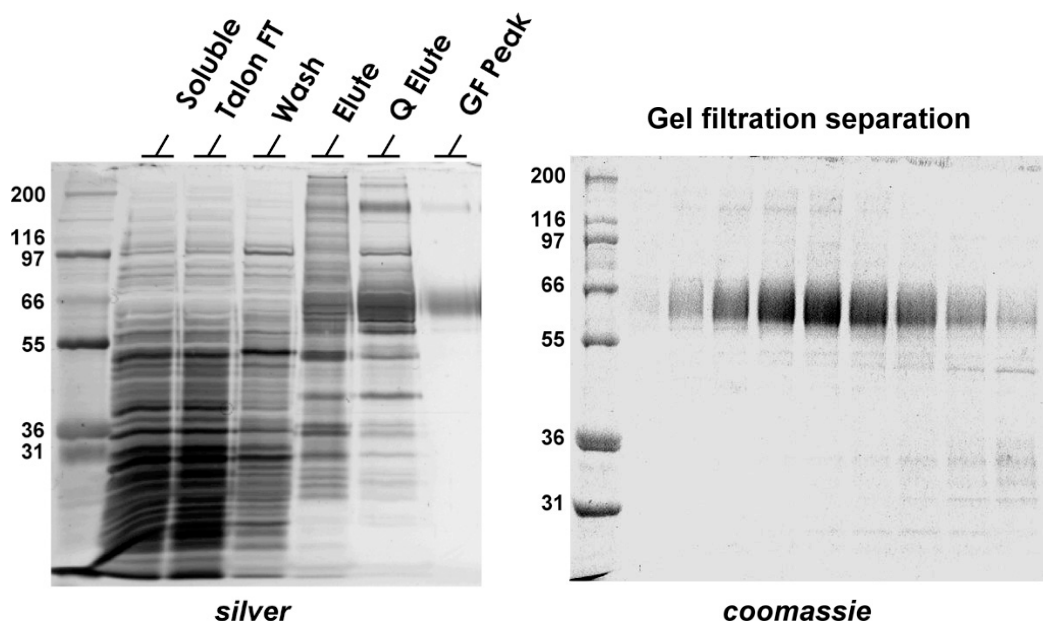


**Figure 2-7.** Purification of YMOR from High Five™ insect cells. **(Left)** YMOR was extracted from membranes in the presence of 100 nM naltrexone with 1% n-dodecyl- $\beta$ -D-maltoside and 0.01% cholesteryl hemisuccinate and enriched on a Talon™ metal affinity column. The Talon pool containing YMOR (predicted 73 kDa MW) was applied to a Source 15Q anion exchange column followed by a size exclusion gel filtration column (Superdex 200). Samples of the purification steps were resolved by SDS-PAGE and silver stained. YMOR was enriched to ~95% purity (GF peak). **(Right)** SDS-PAGE resolution and Coomassie stain of a representative size exclusion chromatography separation of YMOR during the final purification step. MOR has 5 putative *N*-glycosylation sites in its N-terminus (103), and the diffuse staining pattern is indicative of High Five™ cell capacity for incorporation of simple *N*-glycans at these sites in YMOR.

A representative Coomassie stained SDS-PAGE separation of the Superdex 200 YMOR peak and a silver-stained SDS-PAGE separation of each enrichment step are shown in Figure 2-7. YMOR eluted off the SourceQ column between 100 to 150 mM NaCl. YMOR's retention volume on the Superdex 200 column suggested a molecular weight of ~440 kDa. This size is larger than expected for a DDM detergent micelle (~70 kDa) containing YMOR (~73 kDa). It is likely that the detergent-receptor population purified here is composed of more than one receptor per micelle. Importantly, the receptors are resolved to the expected molecular weight on SDS-PAGE. Yields of YMOR were typically ~50  $\mu$ g of >95% pure receptor per liter of insect culture. Purified,



DDM-soluble YMOR bound [<sup>3</sup>H]DPN with decreased affinity ( $K_d \sim 4.1$  nM, Figure 2-8), compared to  $\sim 0.6$  nM in membranes. Typically the purified YMOR sample bound [<sup>3</sup>H]DPN at approximately 15-20% of the predicted binding sites calculated from the molecular mass. This loss of activity may be due to the detrimental freeze/thaw process.

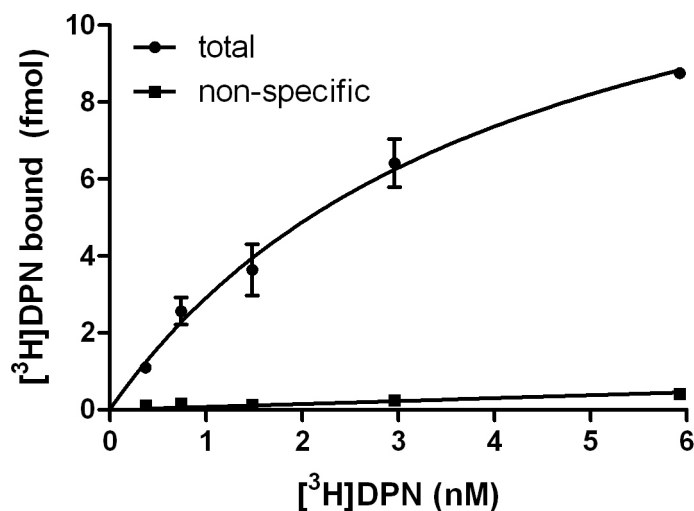


**Figure 2-8.** Detergent solubilization disrupts high affinity [<sup>3</sup>H]DPN binding to YMOR. YMOR was extracted from High Five<sup>TM</sup> cells and purified to  $\sim 95\%$  homogeneity in 0.1% DDM + 0.01% CHS. An estimated 100 fmoles of YMOR (based on a Bradford protein assay) was used in [<sup>3</sup>H]DPN saturation binding experiments. Binding to increasing concentrations of [<sup>3</sup>H]DPN was measured in the absence and presence of 20  $\mu$ M NTX to determine total and non-specific binding. Detergent soluble YMOR bound [<sup>3</sup>H]DPN with a  $K_d$  of 4.14 nM, approximately 10-fold higher than membrane associated YMOR. Data is representative of two three assays performed in duplicate. Error bars represent the SEM.

## Discussion

In order to study the molecular pharmacology of the isolated MOR, we chose to purify this GPCR from insect cells using baculovirus-mediated over-expression, an approach recognized to have the capacity to produce large quantities of protein. This approach has been used by other groups to express MOR, albeit with limited success,

where expression levels were often too low to allow purification (104-106). More importantly, functional assays were either not performed (107) or indicated poor agonist affinities and weak G protein coupling (108). Therefore as we set out to purify active MOR, two critical goals were achieving high expression levels ( $\geq 20$  pmol/mg cellular membrane protein) and illustrating that the receptor was fully functional with regard to G protein coupling.

The general strategy for expression began with creating an N-terminal fusion protein of MOR designed to produce high levels of the receptor at the plasma membrane. FLAG epitope and histidine tags were included for Western Blot visualization and metal chelate column purification steps. A yellow fluorescent protein (YFP) was included in between the His<sub>10</sub> tag and MOR as a means to visualize expression in live cells. This fusion protein, termed YMOR, was expressed in *Sf9* and High Five<sup>TM</sup> insect cells via Baculovirus infection. The cleavable polypeptide signal sequence of influenza hemagglutinin was an important component for increasing MOR insertion into the plasma membrane (109, 110) by driving the large YFP-fusion and N-terminus of MOR to the extracellular side of the plasma membrane.

Maintaining naltrexone concentrations during the infection process further increased YMOR expression levels (Figure 2-3). This strategy was initially taken from insect cell expression of the  $\beta_2$ AR receptor, where the presence of the inverse agonist timolol during expression results in a higher amount of receptor at the plasma membrane (111, 112). As we were unable to find reports of an opioid compound that definitively acted as a strong inverse agonist, the antagonist naltrexone was used as an alternative. Chronic naltrexone has been shown to up-regulate MOR in the brain (113) and 7315c

tumor cells (114), nearly doubling the number of  $\mu$  binding sites without significantly altering affinity. Indeed, we similarly saw a nearly two-fold increase in [ $^3\text{H}$ ]DPN binding sites at High Five<sup>TM</sup> plasma membranes with chronic naltrexone exposure prior to harvesting cells. The mechanism of naltrexone increasing MOR expression *in vivo* and in cell culture is still debated. In the case of inverse agonists increasing expression levels, it is postulated that the ligand decreases basal activity of the receptor, preventing desensitization and internalization. It is possible that the mere binding of a ligand which does not induce activity stabilizes the receptor's conformation, thus decreasing receptor degradation.

The use of cholesteryl hemisuccinate (CHS) was another strategy adopted from the purification of other GPCRs like  $\beta_2\text{AR}$  (115, 116) and the serotonin 5-HT<sub>4(a)</sub> receptor (117). The addition of 0.01% CHS (a concentration based on previous reports) increased the amount of [ $^3\text{H}$ ]DPN binding to DDM-soluble YMOR (Figure 2-6), suggesting that the cholesterol moieties stabilized a receptor conformation that was more active to [ $^3\text{H}$ ]DPN binding. At first this effect appears at odds with prior reports that CHS disrupts MOR function. CHS treatment of rat brain synaptosomal membranes increased microviscosity, and as a result decreased agonist/antagonist discrimination by MOR (118). Addition of CHS to SH-SY5Y and C6 glioma cell membranes disrupted the allosteric effects of sodium and guanine nucleotides on DAMGO binding (52). However, when membrane viscosity was first decreased with egg lecithin (50) or fatty acids (51), CHS addition restored native binding properties. Thus it is apparent that MOR is highly sensitive to the viscosity of surrounding lipids and sterols. It is plausible that detergent solubilization of MOR represents a significant decrease in environmental viscosity, and

the addition of CHS acts to restore some rigidity and conformational activity to the receptor. Indeed, recent reports of GPCR crystal structures have found cholesterol to be involved in stabilization of the receptor (119, 120). In future work it would be interesting to determine if CHS has a similar effect on the binding of agonists to detergent solubilized MOR.

The methodology described here resulted in a highly purified YMOR sample (Figure 2-7). YMOR yields were appreciable at ~30-50  $\mu\text{g}$  (~ 410-690 pmoles) of active receptor per liter of insect cell culture. Importantly, [ $^3\text{H}$ ]DPN binding measurements on column fractions insured that the pooled YMOR was in an active conformation. DDM-soluble YMOR bound [ $^3\text{H}$ ]DPN with lower affinity compared to membrane preparations, which was expected based on previous reports of detergent solubilization altering GPCR ligand binding and G protein coupling, both for rhodopsin (121) and MOR specifically (84, 86, 91). However, our DDM-soluble YMOR still bound [ $^3\text{H}$ ]DPN with an affinity 10-100 fold higher than previously reported receptor purification efforts (84, 86, 91, 96), suggesting an improvement in receptor quality was achieved with this protocol.

Although a high quality purified receptor sample was obtained, there are additional steps that could be taken to improve the purification of YMOR. Importantly, a ligand affinity column could be employed to increase the specific activity of the preparation. Although we postulate that approximately 80% activity of the YMOR is lost during the freeze/thaw process, it is possible that the inactive receptor directly results from the purification process itself. Incorporation of a ligand affinity column step in the purification, such as a 6-succinyl morphine column (91) may result in a YMOR population with an activity much closer to 100%.

The most important aspect of YMOR purification which would benefit from further optimization is the final protein yield. The poor yield of YMOR during the outlined purification process is striking. Starting with an expected  $\sim 370 \mu\text{g/L}$  of insect cell culture (based on  $\sim 20 \text{ pmol/mg}$  expression levels and  $\sim 250 \text{ mg}$  of membrane protein per liter), the end sample of  $\sim 40 \mu\text{g/L}$  represents  $\sim 10\%$  final yield. A likely explanation for the low yield is the extraction step. Figure 2-4 illustrates that a large amount of FLAG immuno-reactivity was not extracted from the membrane. More importantly, as discussed above detergent extraction is known to be detrimental to GPCRs and membrane proteins in general. Indeed, the poor affinity of solubilized YMOR ( $\sim 4.1 \text{ nM}$ ) compared to membrane associated YMOR ( $\sim 0.6 \text{ nM}$ ) reflects the destabilizing effect of detergent solubilization on YMOR. For these reasons further optimization of YMOR extraction is certainly warranted. Novel detergents have recently been marketed which incorporate branching hydrophilic and lipophilic groups, and use of these “tripod amphiphiles” has been shown to improve extraction efficiency of membrane proteins (122). Their use in YMOR purification may greatly aid in increasing YMOR yields.

In addition, Figure 2-4 shows two FLAG-reactive bands at approximately 33-35 kDa. This corresponds with the predicted size of cleavage products containing the Flag-His<sub>10</sub>-YFP tags and a fragment of MOR, indicating that the protease inhibitors used in purification were not completely effective in preventing YMOR proteolysis. These cleavage products were purified away by the final size exclusion chromatography step of the purification. Cleavage of the FLAG and His<sub>10</sub> tags of YMOR will result in an inability to bind the Talon<sup>TM</sup> column, as well as the inability to detect the proteolyzed MOR product via anti-FLAG Western Blot. Indeed, although the addition of NTX and

CHS during Talon™ enrichment improves the retention of full length YMOR, [<sup>3</sup>H]DPN binding (not shown) suggested that the flow through contained a considerable amount of MOR cleavage product, representing up to 50% of the total active receptor. Therefore further optimizations of this purification protocol must determine a spectrum of protease inhibitors which better prevent cleavage to increase protein yields.

Even without these optimizations, the purification protocol outlined here represents a significant advancement in the isolation of MOR for molecular pharmacology studies. While other groups have expressed MOR in insect cells, here we demonstrate allosteric regulation of agonist binding by G<sub>12</sub> heterotrimer for the first time, revealing higher DAMGO binding affinity. MOR expression levels were significantly higher than previous reports, and the detergent-soluble receptor displayed a higher affinity for [<sup>3</sup>H]DPN. In conclusion, YMOR was shown to be fully functional when expressed in High Five™ cells, and the final purification yields are ample for biochemical studies of the isolated receptor in reconstitution systems.

## **Materials and Methods**

### **Materials**

G protein baculoviruses encoding rat G $\alpha_{12}$ , His<sub>6</sub>-G $\beta_1$  and G $\gamma_2$  were provided by Dr. Alfred G. Gilman (University of Texas Southwestern, Dallas, TX). DNA encoding human  $\mu$  opioid receptor was provided by Dr. John R. Traynor (University of Michigan, Ann Arbor, MI). *Spodoptera frugiperda* (Sf9) and *Trichoplusia ni* (High Five™) cells, pFastBac™ Baculovirus expression vectors and Sf900™ serum free medium were from Invitrogen (Carlsbad, CA). InsectExpress™ medium was purchased from Lonza

(Allendale, NJ). N-dodecyl- $\beta$ -D-maltoside was from Dojindo (Rockville, MD). [ $^3$ H]diprenorphine (DPN), [ $^3$ H]DAMGO, and [ $^{35}$ S]GTP $\gamma$ S were obtained from PerkinElmer (Waltham, MA). Ovomuroid Trypsin Inhibitor was purchased from United States Biological (Swampscott, MA). GF/B filters, Source 15Q and Superdex 200 chromatography resins were from GE Healthcare (Piscataway, NJ). Talon<sup>TM</sup> resin was from Clontech (Mountain View, CA). Chromatography columns were run using a BioLogic Duo-Flow Protein Purification System from Bio-Rad. Amicon Ultra centrifugation filters were from Millipore (Billerica, MA). All other chemicals and ligands were from either Sigma-Aldrich (St. Louis, MO) or Fisher Scientific (Pittsburgh, PA).

### **Creation of a yellow fluorescent protein fusion to MOR**

Baculoviruses were created using transfer vectors (pFastBac<sup>TM</sup>, Invitrogen) that encoded an N-terminal cleavable hemagglutinin signal sequence (MKTIIALSYIFCLVF), FLAG epitope (DYKDDDD), histidine<sub>10</sub>-tag, monomeric and enhanced yellow fluorescent protein (Clontech) fusion protein with the human  $\mu$ -opioid receptor (MOR, NM 000914.2). High titer viruses ( $10^7$  to  $10^8$  pfu/mL) were created using the Bac-to-Bac<sup>®</sup> Expression System (Invitrogen) in *Sf9* cell cultures according to the manufacturer's protocol.

### **YMOR receptor fusion protein expression and membrane fraction preparation**

*Sf9* or High Five<sup>TM</sup> cells were infected with FLAG-His<sub>10</sub>-mEYFP-MOR (YMOR) virus at a multiplicity of infection of 0.25 to 1.0 for 48 to 52 hr in the presence of 1  $\mu$ M

naltrexone (NTX). When co-expressing  $G_{i2}$  heterotrimer,  $G\alpha_{i2}$ , His<sub>6</sub>-G $\beta_1$  and G $\gamma_2$  viruses were co-infected with the YMOR virus, all at an MOI of 0.5 to 0.8. Cells were resuspended in Buffer A (50 mM Tris•HCl pH 8.0, 50 mM NaCl, 100 nM NTX and protease inhibitors (3.2  $\mu$ g/mL leupeptin, 3.2  $\mu$ g/mL Ovomuroid Trypsin Inhibitor, 17.5  $\mu$ g/mL phenylmethanesulphonyl fluoride (PMSF), 16  $\mu$ g/mL tosyl-L-lysine-chloromethyl ketone (TLCK), 16  $\mu$ g/mL tosyl-L-phenylalanine chloromethyl ketone (TPCK)) and lysed by nitrogen cavitation. Supernatants from a 500 x g spin were then subjected to 125,000 x g spin for 35 min and pellets containing membrane fractions were resuspended in Buffer A and either stored at -80°C for later Western Blot or binding analysis or further processed to purify receptor. Sample protein concentrations were determined by the method of Bradford (123).

### **Detergent solubilization screen**

Membrane fractions (prepared as above) were diluted to 5 mg/mL in 50 mM Tris•HCl pH 7.7, 50 mM NaCl, 3.2  $\mu$ g/mL leupeptin, 3.2  $\mu$ g/mL trypsin inhibitor, 17.5  $\mu$ g/mL PMSF, 16  $\mu$ g/mL TLCK and 16  $\mu$ g/mL TPCK (1x PIs) and incubated with detergents (listed in Results) at a final concentration of 1% w/v for 1 hr with gentle rotation at 4°C. Samples were subjected to a 100,000 x g spin in an Optima TLX Benchtop Ultracentrifuge (Beckman Coulter). Insoluble pellets were resuspended in a volume of 50 mM Tris•HCl pH 7.7, 50 mM NaCl, 1x PIs equal to that of the removed soluble supernatant fractions. Equal pellet and supernatant volumes were then resolved by sodium dodecyl sulfate polyacrylamide gel electrophoresis (SDS-PAGE) and subjected to Western Blot analysis of relative FLAG epitope levels.



### **Western Blot analysis**

Membrane fraction or soluble protein samples were resolved by SDS-PAGE and transferred to nitrocellulose membranes as previously described (124). Nitrocellulose membranes were initially blocked with a 137 mM NaCl, 10 mM Na<sub>2</sub>HPO<sub>4</sub>, 1.76 mM KH<sub>2</sub>PO<sub>4</sub>, 2.7 mM KCl, 0.01% Tween-20, pH 7.4 (PBS-T), 5% non-fat milk (w/v) solution. The FLAG epitope was visualized with mouse anti-M2 FLAG antibody (Sigma, 1:5,000 dilution in PBS-T) and anti-mouse HRP (Sigma, 1:10,000 dilution in PBS-T + 5% non-fat milk). Antibodies were visualized with enhanced chemiluminescence by incubating nitrocellulose membranes in 100 mM Tris, pH 8.5, 1.25 mM luminol, 0.2 coumaric acid and exposing to Biomax Light Chemiluminescence film (Kodak).

### **Silver nitrate staining**

SDS-PAGE separations of samples were washed two times in 50% MeOH for 15 min. A 0.8% NH<sub>4</sub>OH, 0.084% NaOH solution was titrated to saturation with 2.35 M AgNO<sub>3</sub> immediately before incubating the MeOH washed gels with the silver stain solution for 15 min, followed by two H<sub>2</sub>O washes for 5 min each. The silver stain was developed in a 0.0185% formaldehyde, 0.34 mM sodium citrate solution. Development was stopped with 50% MeOH washes. All glassware was thoroughly washed with 95% EtOH prior to use.

## **YMOR purification**

All purification steps were performed sequentially at 4°C or on ice. Membrane preparations were diluted to 5 mg/mL in Buffer A plus 1% DDM (final w/v) and 0.01% cholesteryl hemisuccinate (CHS) (final w/v) and gently stirred for 1 hr to solubilize YMOR out of the membrane. Detergent extracted YMOR was enriched via Talon<sup>TM</sup> metal affinity chromatography resin (Clontech) in Buffer A plus 0.1% DDM and 0.01% CHS, and eluted with Buffer A plus 0.1% DDM, 0.01% CHS and 150 mM imidazole. Fractions containing YMOR (based on Coomassie staining after resolving on SDS-PAGE) were pooled, diluted 5-fold in Buffer B (20 mM Hepes pH 8.0, 5 mM MgCl<sub>2</sub>, 0.1% DDM, 0.01% CHS, 100 nM NTX, and PMSF-TLCK-TPCK protease inhibitors) and eluted from a 1 mL Source 15Q strong anion-exchange column with a 50-300 mM NaCl linear gradient. Peak fractions were identified by radioligand binding assays using [<sup>3</sup>H]DPN (2-4 nM). Peak fractions were then pooled and concentrated on Amicon Ultra centrifugation filters (10 kDa MW cut-off). As a final purification step this YMOR sample was resolved based on size using a Superdex 200 gel filtration column (GE Healthcare) in Buffer C (20 mM Hepes pH 8.0, 100 mM NaCl, 0.1% DDM, 0.01% CHS, 100 nM NTX and protease inhibitors). [<sup>3</sup>H]DPN binding assays and Coomassie staining after SDS-PAGE were used to identify fractions containing YMOR, which were pooled and concentrated to ~1-2 μM. Glycerol was added to a final concentration of 10% (v/v), samples were flash-frozen in liquid nitrogen and then stored at -80°C until further use.

### **[<sup>3</sup>H]DPN saturation and agonist competition binding assays**

Binding reactions were performed in 200  $\mu$ L volumes. Membrane fractions prepared from *Sf9* or High Five<sup>TM</sup> cells expressing YMOR (0.5 to 5  $\mu$ g total protein, prepared as above) were incubated with [<sup>3</sup>H]DPN (0.25 to 4 nM; 54.9 Ci/mmol) for 1 hr at room temperature in 25 mM Tris•HCl pH 7.7, 136 mM NaCl, 2.7 mM KCl (TBS) buffer. Nonspecific binding was determined in the presence of 20  $\mu$ M NTX. Bound [<sup>3</sup>H]DPN was separated from free by rapid filtration through GF/B filters with three 200 mL washes of ice cold TBS. [<sup>3</sup>H]DPN binding assays on detergent-solubilized YMOR were performed in 100  $\mu$ L of 50 mM Tris•HCl pH 7.7, 136 mM NaCl, 0.1% DDM, 0.01% CHS and separated on Sephadex G-50 gravity flow columns.

Agonist competition assays were performed on 0.5 to 5  $\mu$ g total membrane protein with 0.5 nM [<sup>3</sup>H]DPN and increasing concentrations (1 pM to 1 mM) of the agonist DAMGO in the absence or presence of 10  $\mu$ M GTP $\gamma$ S. Samples were measured for radioactivity on a liquid scintillation counter and the data were fit with one-site saturation, one-site competition or two-site competition binding models using Prism 5.0 (GraphPad, San Diego, CA).

### **[<sup>35</sup>S]GTP $\gamma$ S binding assay**

One hundred  $\mu$ L volume reactions were prepared containing 1-10  $\mu$ g total membrane protein from High Five<sup>TM</sup> cells expressing YMOR and G $\alpha_{i2}$ -His<sub>6</sub>-G $\beta_1$ -G $\gamma_2$  heterotrimer. The binding reaction buffer was composed of 30 mM Tris•HCl pH 7.4, 100 mM NaCl, 5 mM MgCl<sub>2</sub>, 0.1 mM DTT, 10  $\mu$ M GDP, and 0.1 nM [<sup>35</sup>S]GTP $\gamma$ S (1250 Ci/mmol). Samples were incubated with increasing concentrations of DAMGO (1 pM to

1 mM) for 1 hr at room temperature, then rapidly filtered through GF/B filters and washed three times with 2 mL ice cold 30 mM Tris•HCl pH 7.4, 100 mM NaCl, 5 mM MgCl<sub>2</sub>. Samples were measured for radioactivity on a liquid scintillation counter and the data were fit to a log dose-response model using Prism 5.0.

## CHAPTER 3

### RECONSTITUTION OF A $\mu$ -OPIOID RECEPTOR INTO HIGH DENSITY LIPOPROTEIN PARTICLES: THE MONOMER FUNCTIONALLY COUPLES G PROTEINS

#### Introduction

Opioid receptors are members of the G protein-coupled receptor (GPCR) super-family and are clinical target mainstays for inducing analgesia. Three isoforms of opioid receptors,  $\mu$ ,  $\delta$  and  $\kappa$ , have been cloned and are known to couple to  $G_{i/o}$  proteins to regulate adenylyl cyclase and  $K^+/Ca^{2+}$  ion channels (30, 37, 125). An ever growing amount of data suggests that many GPCRs oligomerize (126, 127) and the accumulation of considerable biochemical and biophysical evidence suggests that the  $\mu$ ,  $\delta$ , and  $\kappa$  opioid receptors may function in a fashion that is dependent on their oligomerization. Analysis of receptor over-expression in co-transfected cells suggested the existence of  $\delta$ - $\delta$  homodimers (69) and demonstrated unique pharmacology resulting from  $\mu$ - $\delta$  (71, 72, 128, 129) (71, 72, 128) and  $\delta$ - $\kappa$  heterodimers (70). Bioluminescence resonance energy transfer (BRET) studies have shown that homo- and heterodimers can be formed by all three opioid receptor isoforms (58). In light of these findings, current dogma holds that opioid receptors function as requisite dimers (75).

To better understand the function of isolated GPCRs, our laboratory and others have recently utilized a novel phospholipid bilayer reconstitution method (76-80, 130). In this approach purified GPCRs are reconstituted into the phospholipid bilayer of a high

density lipoprotein (HDL) particle (Figure 3-1). Normally involved in the reverse transport of cholesterol, the unique structural aspects of HDL are exploited in this methodology. HDL particles are composed of a dimer of apolipoproteinA-1 (apoA-1) wrapped around a bilayer of phospholipids. The HDL particles are monodispersed, uniform in size, and their internal diameter of 80 Å preferentially incorporates a GPCR monomer (78, 79). As such, the HDL reconstitution system can be used to investigate the potential requirement of GPCR oligomerization for function. Previous work in our lab has shown that rhodopsin, a class A GPCR previously proposed to function as a dimer (131-133), is fully capable of activating its G protein when reconstituted as a monomer in the HDL lipid bilayer (79). Moreover, agonist binding to a monomeric  $\beta_2$ -adrenergic receptor, another class A GPCR, can be allosterically regulated by G proteins (78). This led us to hypothesize that a monomer of the  $\mu$ -opioid receptor (MOR), a class A GPCR which endogenously binds peptide ligands, is the minimal functional unit required to activate coupled G proteins. We additionally hypothesized that ligand binding to monomeric MOR is allosterically regulated by inhibitory G protein heterotrimer.

To study the function of monomeric MOR a modified version of the receptor was purified to near homogeneity. As described in Chapter 2, a yellow fluorescent protein was fused to the amino-terminus of MOR, and this construct (YMOR) was expressed in insect cells for purification. In this chapter the monomeric reconstitution of purified YMOR into HDL particles is described. This monomeric YMOR sample binds ligands with affinities nearly equivalent to those observed in plasma membrane preparations. Furthermore, monomeric YMOR efficiently stimulates GTP $\gamma$ S binding to G $_{i2}$  heterotrimeric G protein. G protein allosteric regulation of agonist binding to MOR has

been observed in numerous cell based studies (39-42, 134), and using the HDL reconstitution system we show  $G_{i2}$  allosteric regulation of agonist binding occurs at monomeric YMOR. Taken together, these results suggest that oligomerization of MOR is in fact not required for ligand binding and G protein activation.

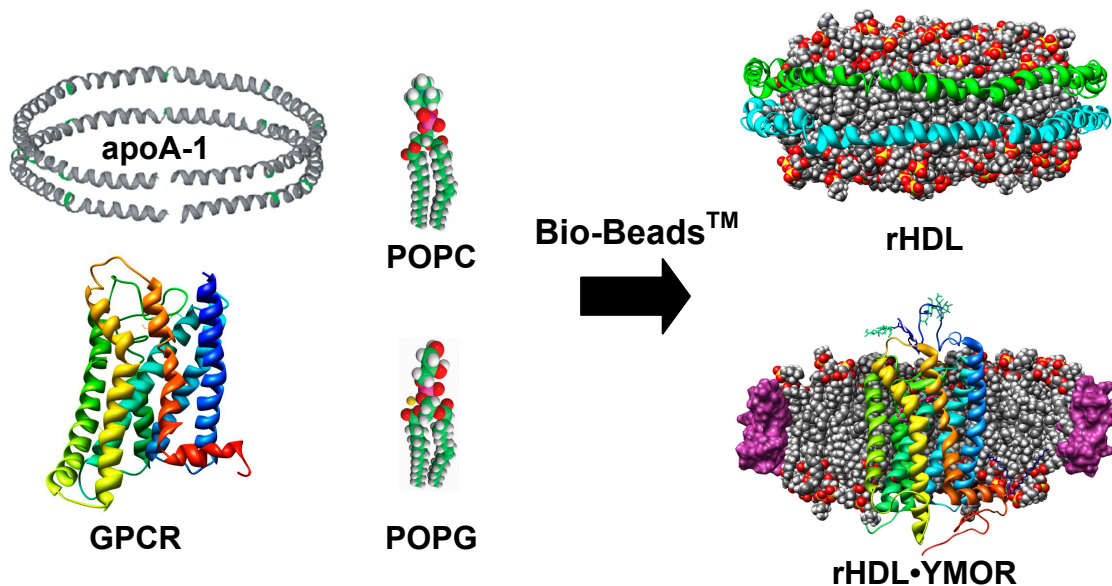


**Figure 3-1.** Schematic overview of GPCR reconstitution into HDL particles. Purified apolipoproteinA-1 is incubated with detergent solubilized 1-Palmitoyl-2-Oleoyl-*sn*-Glycero-3-Phosphocholine (POPC) and 1-Palmitoyl-2-Oleoyl-*sn*-Glycero-3-[Phospho-*rac*-(1-glycerol)] (POPG) and detergent solubilized, purified GPCR. Detergent extraction with Bio-Beads hydrophobic resin (Bio-Rad™) promotes the formation of a lipid bilayer disc, containing the GPCR surrounded by an apoA-1 “belt.” Reconstituted HDL’s inner diameter of ~80 Å sterically favors the incorporation of a GPCR monomer. The apoA-1 and YMOR molar ratios used in this work result in an excess of “empty” rHDL particles compared to rHDL•receptor particles. rHDL is shown in a side view with the apoA-1 dimer in green and blue. rHDL•YMOR is illustrated as a cross-sectional side view with apoA-1 in purple as a space-filling model.

## Results

### Reconstitution of YMOR into High Density Lipoprotein particles

Reconstitution of YMOR into HDL particles was performed with a 500-fold molar excess of apoA-1 to YMOR (250-fold excess of rHDL) to favor reconstitution of a

single YMOR molecule per rHDL particle. Resolution of reconstituted HDL particles containing YMOR (rHDL•YMOR) with size exclusion chromatography (SEC) suggested an apparent Stokes diameter of 10.25 nm based on retention volumes of standard proteins (Figure 3-2a). [<sup>3</sup>H]DPN binding to the SEC fractions confirmed the presence of functional YMOR in particles that eluted slightly earlier than the main UV absorbance peak, indicating the slightly larger Stokes diameter of rHDL•YMOR compared to rHDL. The majority of YFP fluorescence eluted off the SEC column at or near the column's void volume as an aggregated protein species. No [<sup>3</sup>H]DPN binding was detected in these fractions, suggesting that this receptor population was inactive. This aggregated and inactive receptor peak, which accounts for ~75% of the area under the curve, is consistent with the previous observation that ~80% of the purified YMOR is inactive post freeze/thaw and prior to reconstitution into rHDL.

The effectiveness of YMOR reconstitution into HDL is clear when comparing [<sup>3</sup>H]DPN binding between detergent-solubilized receptor and rHDL•YMOR particles. Prior to reconstitution into HDL, DDM-soluble YMOR bound [<sup>3</sup>H]DPN with a  $K_d$  ~4.14 nM whereas reconstituted YMOR bound [<sup>3</sup>H]DPN with a  $K_d$  of ~0.36 nM (Figure 3-2b). This significant disruption of high affinity ligand binding highlights the sensitivity of YMOR to detergents, as discussed in Chapter 2. Replacement of detergents with phospholipids in the form of a bilayer appears to reverse the detergent's deleterious effects and restores YMOR's conformation to one that binds [<sup>3</sup>H]DPN with native, membrane-bound affinity.



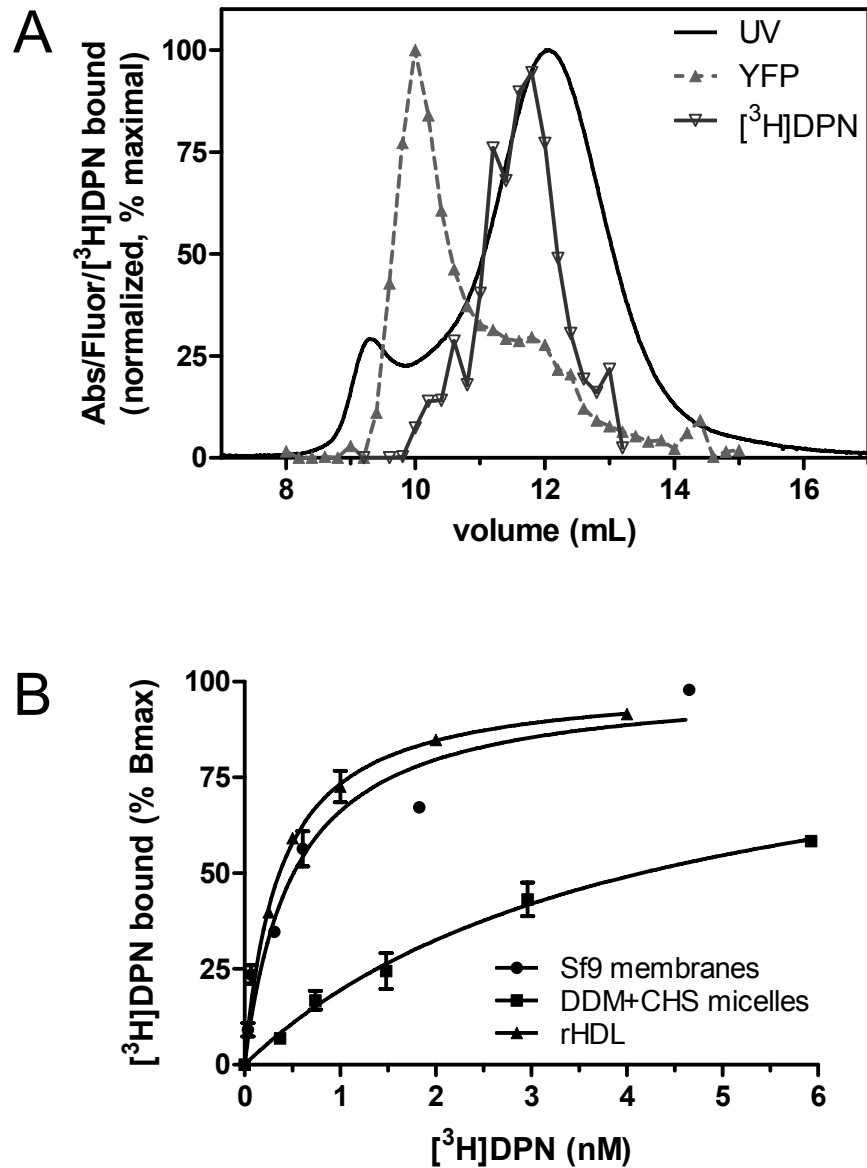


**Figure 3-2.** Reconstitution of Y MOR into HDL particles. **(A)** Purified Y MOR was reconstituted into HDL particles (see Methods) and resolved by size exclusion chromatography (Superdex 200). Fractions were analyzed for total protein content (UV absorbance), active Y MOR ([<sup>3</sup>H]DPN binding), and total Y MOR content (YFP fluorescence). UV absorbance showed a major peak corresponding to rHDL particles (stokes diameter of approximately 10.25 nm). Elution volume of active Y MOR corresponded with the rising slope of the HDL peak. YFP fluorescence eluted as two populations, corresponding to the active Y MOR and a larger Y MOR aggregate which was not incorporated into rHDL particles. This aggregated Y MOR was not active based on [<sup>3</sup>H]DPN binding. **(B)** High affinity [<sup>3</sup>H]DPN binding to Y MOR is disrupted in detergent micelles but restored following reconstitution into rHDL particles. [<sup>3</sup>H]DPN binding to Y MOR in insect cell membranes (●,  $K_d$  of ~0.5 nM), purified in DDM micelles (■,  $K_d$  of ~4.1 nM), and in rHDL particles (▲,  $K_d$  ~0.4 nM). An estimated 2  $\mu$ g of total membrane protein and 5-10 fmol of detergent-soluble or HDL reconstituted Y MOR were used in the saturation assays. Error bars represent the SEM. Data shown is representative of three experiments performed in duplicate. Data was normalized to the  $B_{max}$  calculated by a one-site curve fit (Prism 5.0)

### Lipid composition influences reconstituted YMOR activity

YMOR reconstitutions were initially performed at a 3:2 molar ratio of palmitoyl-oleoyl-phosphocholine (POPC) to palmitoyl-oleoyl-phosphoglycerol (POPG) based on previous reports using  $\beta_2$ AR (78) and rhodopsin (79). Reconstitutions at other ratios were performed and compared by analyzing [ $^3$ H]DPN binding (Figure 3-3). Of the lipid ratios examined, 3:2 POPC:POPG exhibited the highest amount of [ $^3$ H]DPN binding while still maintaining an appropriate  $K_d$  of  $\sim 0.5$  nM (Table 3-1). Further comparisons were made between reconstitutions at 3:2 POPC:POPG versus 1.07:1.5:1 brain lipid extract: POPC:POPG. The addition of polar brain lipid extract (Avanti Lipids, Table 3-2) to the reconstitutions resulted in an approximate doubling of [ $^3$ H]DPN binding (Figure 3-4). As such, most of the YMOR reconstitutions were performed with brain lipid extract.

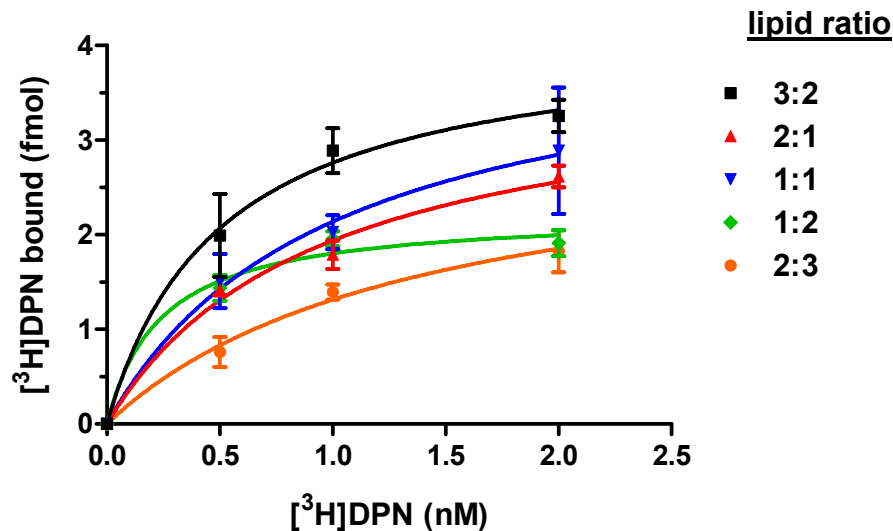


**Figure 3-3.** The ratio of POPC to POPG in rHDL particles influences the binding properties of incorporated YMOR. An estimated 1.7 pmol of YMOR was added to 100  $\mu$ M apoA-1 and a 7 mM lipid mixture of POPC and POPG at the indicated ratios of POPC:POPG, and rHDL particle formation was promoted with the addition of Bio-Beads<sup>TM</sup>. The relative levels of YMOR incorporation ( $B_{max}$ ) and ligand affinity were then determined by measuring [ $^3$ H]DPN binding to reconstitution samples. Lipid ratios are listed as POPC:POPG. A ratio of 3:2 POPC:POPG supported the highest maximal [ $^3$ H]DPN binding while maintaining high affinity for [ $^3$ H]DPN ( $K_d = 0.5$  nM).

**Table 3-1**  
**[<sup>3</sup>H]DPN binding parameters of YMOR reconstituted with varying lipid ratios**

<b>Lipid ratio<sup>a</sup></b>	<b>B<sub>max</sub> (fmol)</b>	<b>K<sub>d</sub> (nM)</b>
3:2	4.15	0.50
2:1	3.76	0.94
1:1	4.26	0.99
1:2	2.23	0.24
2:3	3.15	1.39

<sup>a</sup> Lipid ratios are listed as POPC:POPG.

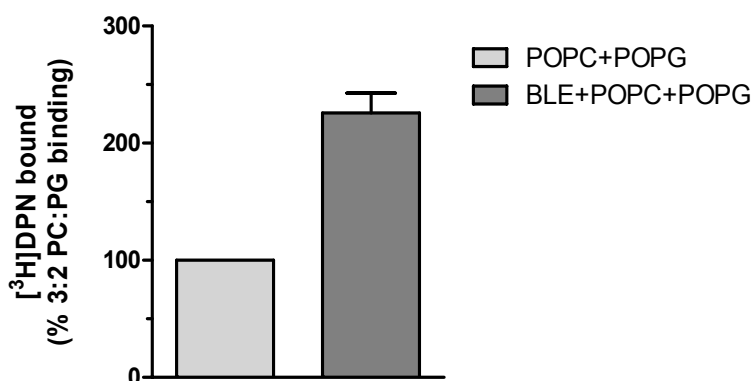


**Figure 3-4.** The presence of brain lipid extract during YMOR reconstitution into HDL increases [<sup>3</sup>H]DPN binding levels. An estimated 20 fmoles of purified YMOR was reconstituted into HDL particles using either a lipid mixture of POPC and POPG at a 3:2 molar ratio or a mixture of polar brain lipid extract (BLE), POPC, and POPG at a 2.14:3:2 molar ratio. Equivalent volumes of the resulting rHDL•YMOR particles were then measured for activity by comparing binding of 4 nM [<sup>3</sup>H]DPN. Binding assays were performed in replicate.

**Table 3-2**  
**Components of porcine polar lipid brain extract<sup>a</sup>**

<b>Lipid</b>	<b>Percent/Wt.</b>
Phosphatidylethanolamine	33.1
Phosphatidylserine	18.5
Phosphatidylcholine	12.6
Phosphatidic acid	0.8
Phosphatidylinositol	4.1
Other (undetermined)	30.9

<sup>a</sup> Adapted from Avanti Lipids ([www.avantilipids.com](http://www.avantilipids.com)).

## **YMOR is monomeric when incorporated into HDL**

Further analysis of reconstituted YMOR required a determination of the number of YMOR molecules present in each rHDL particle. To do so, we assessed the degree of receptor co-localization between Cy3- and Cy5-labeled YMOR using single particle imaging. Ideally the fluorescence of the YFP moiety would be used for these studies; however the quantum yield of this fluorophore proved insufficient for imaging. Purified YMOR was covalently labeled with Cy3- or Cy5-reactive fluorescent dyes and reconstituted into HDL using recombinant  $\Delta(1-43)$ -His<sub>6</sub>-apoA-1 which was biotinylated (Figure 3-5). This biotin-rHDL•Cy-YMOR complex was then incubated on a streptavidin-coated microfluidic slide and excited with 532 and 638 nm lasers. Fluorescence emission was detected using prism-based single molecule total internal reflection fluorescence (SM-TIRF). Reconstituted Cy3-YMOR and Cy5-YMOR were visualized as mono-disperse fluorescent foci (Figure 3-6 a and b). A false-positive co-localization signal of 2.2% and 2.8% was observed for the Cy3-YMOR and Cy5-YMOR samples, respectively (Figure 3-6e). When Cy3-YMOR and Cy5-YMOR were mixed prior to reconstitution (rHDL•(Cy3-YMOR+Cy5-YMOR)), a low level of co-localization of the two fluorophores (3.4%) was observed (Figure 3-6 c and e). Since our method does not allow for differentiation between YMOR labeled with multiple Cy probes of the same fluorophore versus co-localization of multiple YMORs labeled with the same Cy probe (i.e. a Cy3-YMOR•Cy3-YMOR homodimer), we may underestimate co-localization by as much two-fold. Thus we estimate an upper limit for co-localization, i.e. incorporation of two or more YMORs into a single HDL particle, of ~1.8% (maximal co-localization minus false-positive co-localization:  $3.4\% \times 2 - (2.2\% + 2.8\%)$ ). As a co-localization

positive control YMOR was co-labeled with both Cy3 and Cy5 dyes prior to reconstitution (rHDL•Cy3-Cy5-YMOR). The labeling reaction was performed under sub-optimal conditions (lower pH and temperature) to accommodate receptor stability, which is likely the cause for low amounts of co-labeling (~25%). Even so, these results suggest that HDL reconstitution resulted in a sample almost exclusively containing monomeric YMOR. Therefore the ligand binding and G protein coupling characteristics of the HDL reconstituted YMOR are indicative of the properties of a monomeric receptor.

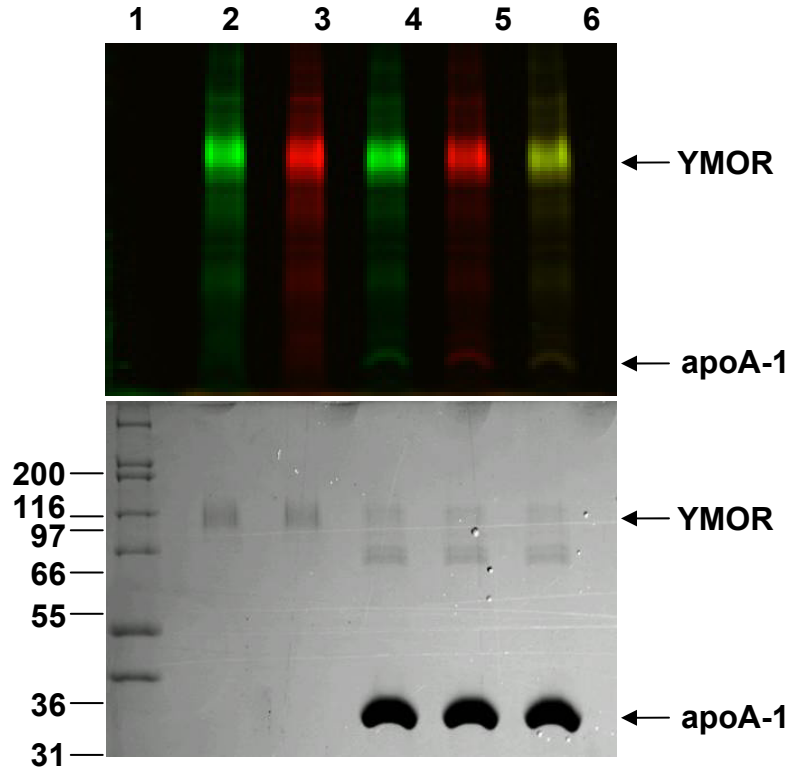


**Figure 3-5.** HDL reconstitution of Cy3- and Cy5-labeled YMOR. Purified YMOR was labeled with Cy3 and Cy5 fluorescent dyes for final dye to protein ratios of 3.8:1 Cy3:YMOR (Lane 2) and 3.7:1 Cy5:YMOR (Lane 3). Labeled YMOR was then reconstituted into biotinylated-rHDL particles, either as Cy3-YMOR (Lane 4) or Cy5-YMOR (Lane 5), or a 1:1 mixture of Cy3-YMOR and Cy5-YMOR (Lane 6). SDS-PAGE resolution of the samples was analyzed for fluorescence (upper image) followed by Coomassie staining for protein (lower image). False-color imaging showed Cy3 (green) and Cy5 (red) labeling of purified YMOR. The reconstitution of a 1:1 mixture of Cy3-YMOR and Cy5-YMOR was apparent as a yellow signal. Labeling of apoA-1 was observed, but is nearly insignificant compared to the total amount of apoA-1 present based on Coomassie staining. Two contaminating proteins from the apoA-1 purification are observed at ~55 kDa in the reconstitution samples (see Appendix B, Figure B-1).

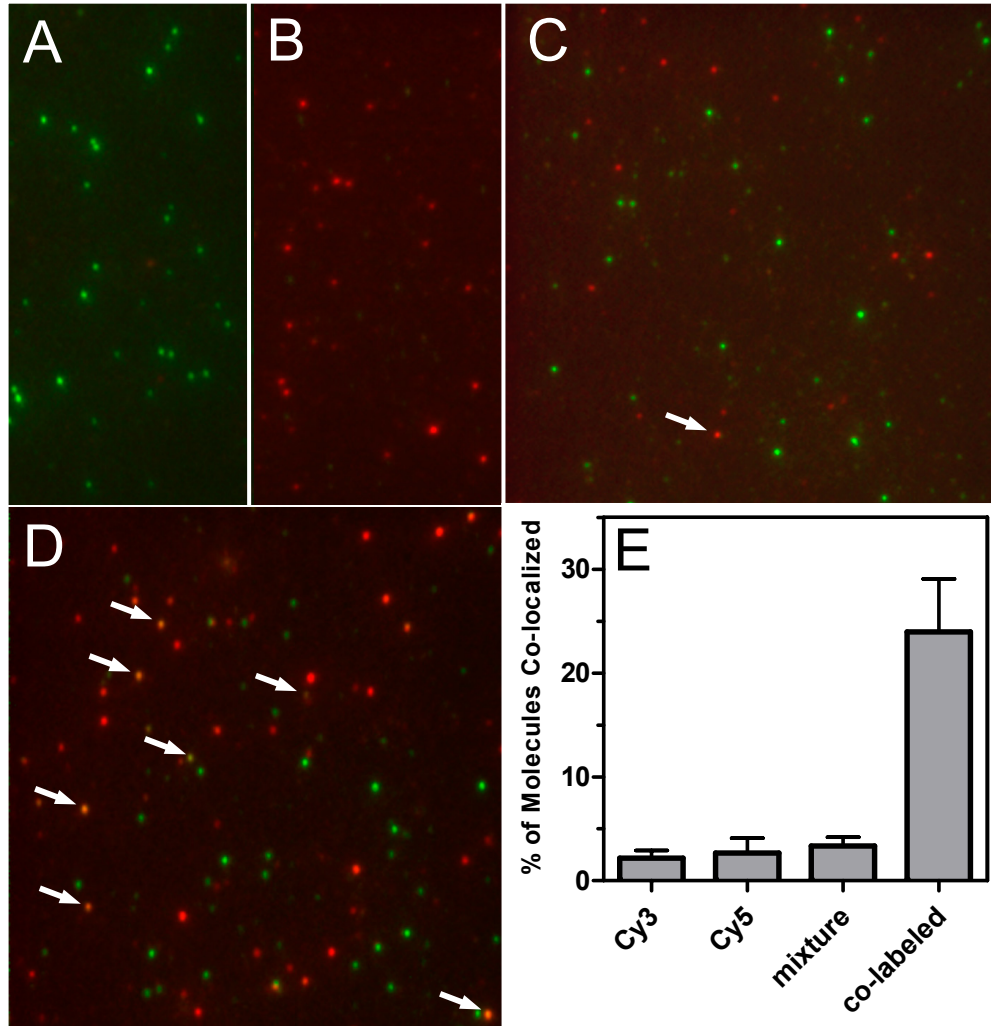


**Figure 3-6.** YMOR is monomeric when reconstituted into HDL particles. Purified YMOR was labeled with Cy3 or Cy5 fluorescent dyes and reconstituted separately or together into biotin-labeled HDL. Particles were imaged using single molecule total internal reflection fluorescence microscopy on quartz slides coated with streptavidin. Representative overlay images of reconstituted rHDL•Cy3-YMOR (A), rHDL•Cy5-YMOR (B), rHDL•(Cy3-YMOR + Cy5-YMOR) (C), and rHDL•Cy3-Cy5-YMOR (D) are shown. Arrows indicate foci of co-localized Cy3 and Cy5 fluorescence. Quantification of Cy3 and Cy5 colocalization (E) showed that when both Cy3-YMOR and Cy5-YMOR were mixed together prior to reconstitution (mixture, 4c), only approximately 3.4% of HDL particles contained two labeled receptors. This amount of co-localization was not significantly higher than that seen for Cy3-YMOR (2.2%) or Cy5-YMOR (2.8%). YMOR co-labeled with both Cy3 and Cy5 was also imaged as a positive control for co-localization. Approximately 24% of rHDL•Cy3-Cy5-YMOR particles (co-labeled, D) exhibited co-localization, indicating that all of the receptors did not receive a secondary label. Arrows indicate co-localized Cy3 and Cy5 signals. Error bars represent the SEM. A minimum of four slide regions and 200 fluorescent spots were counted for each sample.

## Monomeric YMOR binds antagonists with appropriate affinities

Reconstituted and monomeric YMOR in HDL binds antagonists with affinities similar to those observed in the plasma membrane. The non-specific antagonists naloxone and naltrexone, and the  $\mu$ -specific peptide CTAP (D-Phe-Cys-Tyr-D-Trp-Arg-Thr-Pen-Thr-NH<sub>2</sub>) compete [<sup>3</sup>H]DPN binding in similar fashion in High Five<sup>TM</sup> cell membrane preparations or in reconstituted HDL particles (Figure 3-7). Therefore reconstitution into HDL allows YMOR to adopt a conformation that appears identical to receptor in plasma membranes in terms of antagonist binding. Notably, while the affinity of CTAP is equivalent in membranes and rHDL, it is considerably lower than affinities observed in other mammalian cell preparations ( $K_i \sim 1$  nM). This altered affinity appears to be related to both the concentration of Na<sup>+</sup> in the assay and the absence of G protein coupling. A discussion of these findings is presented in Appendix B, Figure B-5.

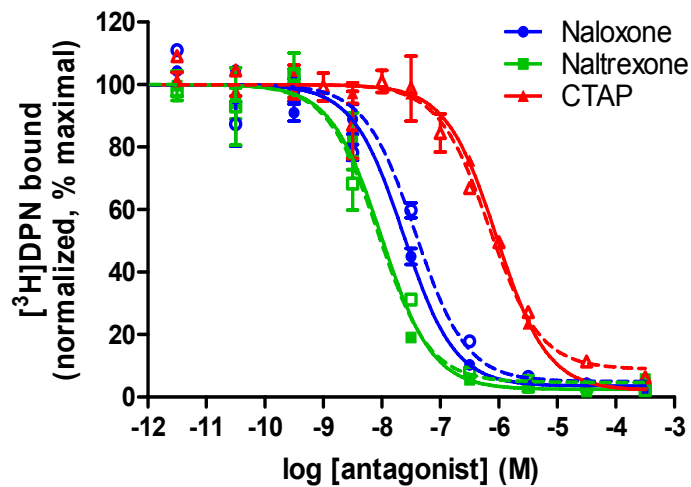


**Figure 3-7.** Opioid antagonists bind YMOR in rHDL with affinities equivalent to those observed for membrane preparations. Competition binding assays were performed in TBS using plasma membranes preparations of High Five<sup>TM</sup> cells expressing YMOR (dotted lines, open symbols) or rHDL•YMOR (solid lines, closed symbols). Increasing concentrations of naloxone, naltrexone, or CTAP competed the binding of 1 or 0.5 nM [<sup>3</sup>H]DPN in the rHDL system or in membrane preparations, respectively. Observed binding constants were: Naloxone (●)  $K_{i_{mem}} \sim 19$  nM,  $K_{i_{rHDL}} \sim 7.8$  nM; Naltrexone (■)  $K_{i_{mem}} \sim 4.3$  nM,  $K_{i_{rHDL}} \sim 3.3$  nM; CTAP (▲)  $K_{i_{mem}} \sim 340$  nM,  $K_{i_{rHDL}} \sim 307$  nM. Error bars represent the SEM. Competitions are representative of at least two experiments performed in replicate.

## Monomeric YMOR functionally couples to G proteins

We next analyzed the ability of monomeric YMOR in rHDL to functionally couple to heterotrimeric G protein. Functional measurements included allosteric regulation of agonist binding (Figure 3-8) and agonist-mediated stimulation of [<sup>35</sup>S]GTPγS binding (Figure 3-9). Anti-FLAG column-purification of rHDL•YMOR was performed to remove “empty” HDL particles and purified G<sub>i2</sub> heterotrimer was added at a 10:1 G<sub>i2</sub>:rHDL•YMOR molar ratio. The concentration of purified G protein was determined by [<sup>35</sup>S]GTPγS binding assays and receptor concentration was measured with [<sup>3</sup>H]DPN saturation assays in rHDL•YMOR samples. G<sub>i2</sub> addition results in high affinity agonist binding. Morphine competed [<sup>3</sup>H]DPN binding with a K<sub>ihi</sub> of ~1.6 nM and a K<sub>ilo</sub> of ~320 nM (Figure 3-8a) while DAMGO inhibited with a K<sub>ihi</sub> ~ 9.6 nM and a K<sub>ilo</sub> ~ 2 μM (Figure 3-8b). As in membranes the addition of 10 μM GTPγS to the monomeric rHDL•YMOR+G<sub>i2</sub> uncouples the G protein and results in a single site, low affinity agonist competition curve (morphine K<sub>iGTPγS</sub> ~ 1 μM; DAMGO K<sub>iGTPγS</sub> ~ 960 nM).

Just as YMOR membrane preparations displayed DAMGO-induced [<sup>35</sup>S]GTPγS binding to Gα<sub>i2</sub>, monomeric YMOR in rHDL particles showed strong DAMGO stimulation of nucleotide exchange (~4.7-fold stimulation with an EC<sub>50</sub> of 31 ± 2.2 nM, Figure 3-9a). A fluorescently-labeled agonist, [Lys<sup>7</sup>, Cys<sup>8</sup>]dermorphin-Cy3 was also tested and showed concentration-dependent stimulation of [<sup>35</sup>S]GTPγS binding to Gα<sub>i2</sub> by monomeric YMOR (EC<sub>50</sub> of 32 ± 9.1 nM, Figure 3-7b).



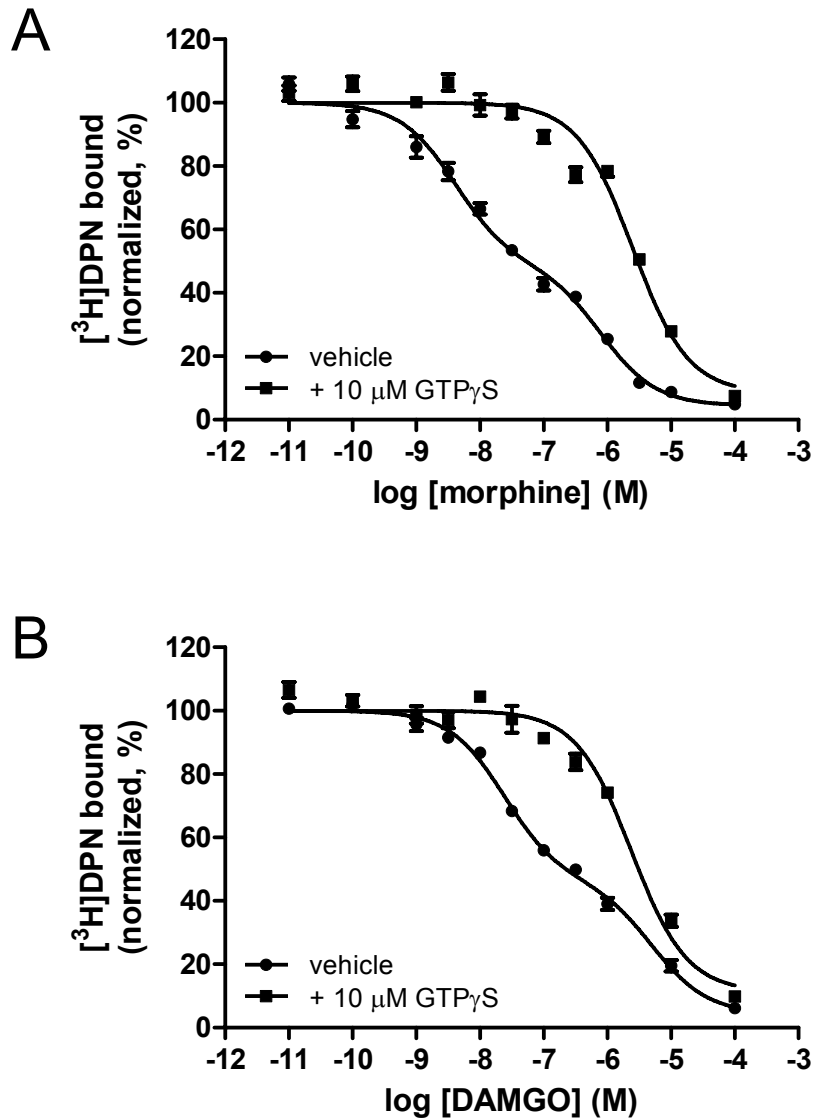


**Figure 3-8.** Binding of agonists to rHDL•YMOR is allosterically regulated by G proteins. Purified G<sub>12</sub> heterotrimer was added to rHDL•YMOR at a molar ratio of 10:1, G protein to receptor. **(A)** Morphine bound rHDL•YMOR+G<sub>12</sub> with high affinity, competing the binding of 0.75 nM [<sup>3</sup>H]DPN in a biphasic manner (K<sub>ihi</sub> ~ 1.6 nM, K<sub>i<sub>lo</sub></sub> ~ 320 nM; fraction<sub>hi</sub> = 0.53). High affinity morphine binding was lost with the addition of 10 μM GTP $\gamma$ S (one-site binding K<sub>i</sub> ~ 1 μM; two-site binding K<sub>ihi</sub> ~ 40 nM, K<sub>i<sub>lo</sub></sub> ~ 2.2 μM; one-site binding shown). **(B)** DAMGO displayed similar G protein regulated binding characteristics (K<sub>ihi</sub> ~ 9.6 nM, K<sub>i<sub>lo</sub></sub> ~ 2 μM; fraction<sub>hi</sub> = 0.56). Addition of 10 μM GTP $\gamma$ S eliminated high affinity binding (one-site binding K<sub>i</sub> ~ 960 nM; two-site binding K<sub>ihi</sub> ~ 17 nM, K<sub>i<sub>lo</sub></sub> ~ 1.9 μM; one-site binding shown). Error bars represent the SEM. Graphs are representative of three experiments performed in duplicate. Data are normalized to the curve fit maximum.

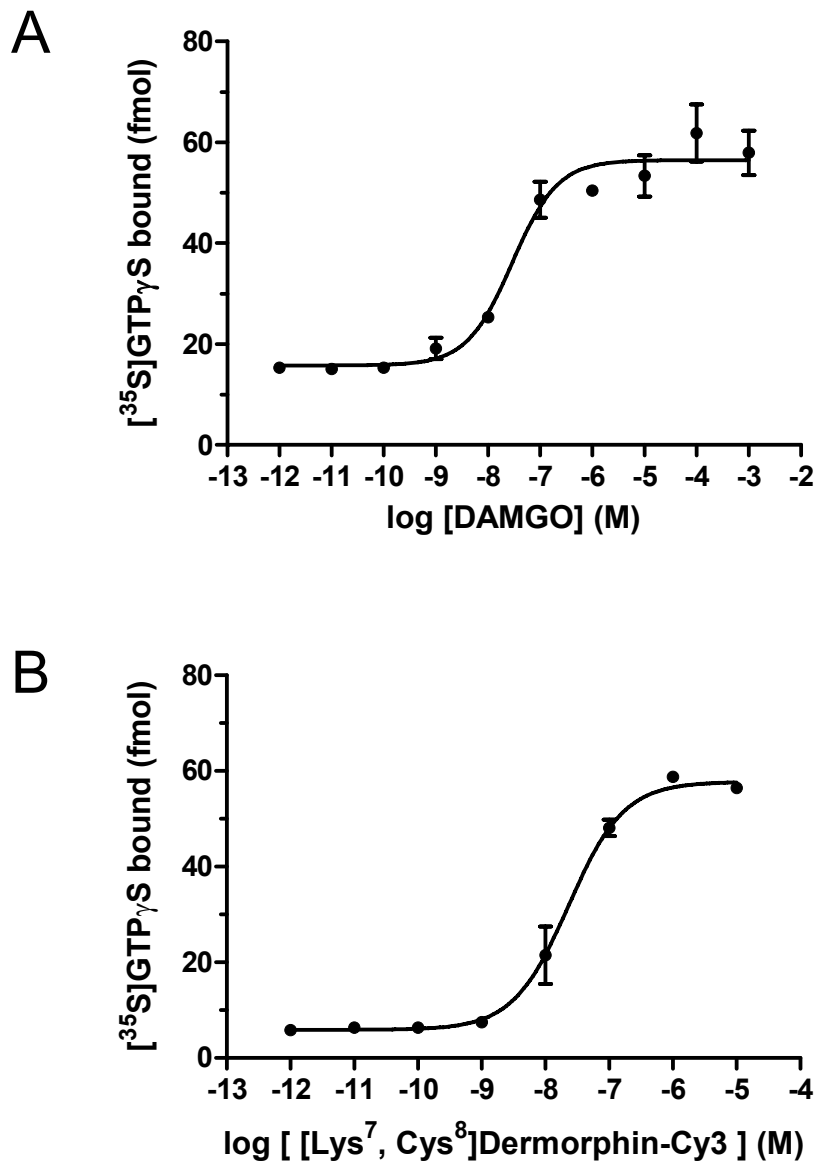


**Figure 3-9.** HDL reconstituted YMOR activates  $G_{i2}$  in response to agonist binding. YMOR (50 fmoles) and associated  $G_{i2}$  heterotrimer were incubated with 100 nM [ $^{35}$ S]GTP $\gamma$ S in the presence of increasing concentrations of the  $\mu$ -opioid specific agonists. **(A)** DAMGO activated  $G_{i2}$  with an  $EC_{50}$  of 29.1 nM, stimulating  $\sim 40$  fmoles of [ $^{35}$ S]GTP $\gamma$ S binding, suggesting stimulation of  $\sim 40$  fmoles of  $G\alpha_{i2}$  and indicating approximately 80% of YMOR is coupled to G protein. **(B)** [Lys<sup>7</sup>, Cys<sup>8</sup>]dermorphin-Cy3 activated  $G_{i2}$  with an  $EC_{50}$  of 23 nM and a  $B_{max}$  of 51.8 fmoles. Error bars represent the SEM. Data are representative of at least two experiments performed in duplicate.

## Discussion

Intense research over the past decade has focused on the existence and functional consequences of GPCR oligomerization. Recently, our lab and others have taken advantage of a unique phospholipid bilayer platform in the form of high density lipoprotein (HDL) particles to reconstitute two prototypical GPCRs: rhodopsin (76, 79, 80) and  $\beta_2$ AR (77, 78). This system was used to demonstrate the functional coupling of the monomeric receptors to their respective G proteins (78, 79), and illustrate that dimerization is not required for functional G protein coupling in the prototypical class A GPCRs rhodopsin and  $\beta_2$ AR.

These findings stand at odds with current opinions of opioid receptor function. Many biochemical studies have suggested that all three isoforms of opioid receptors form homo- and heterodimers (58, 69-72, 128, 129). In light of the fact that only three isoforms were identified based on molecular cloning, the notion of opioid receptor oligomerization was an appealing explanation for the multiple receptor sub-types predicted by ligand binding pharmacology (135-137). This in turn has led to the idea that oligomerization is required for opioid receptor ligand binding and G protein activation. Indeed, specific targeting of opioid receptor dimers has been suggested as a new therapeutic goal (75).

Considering these opposing views of general class A GPCR function and specific opioid GPCR function, we rationalized that it was vital to determine whether the monomeric form of the MOR behaves in a pharmacologically similar manner as the native, membrane-bound form. Probing the function of monomeric MOR required HDL particle reconstitution, as this approach is highly effective in facilitating the isolation of

monomeric GPCRs compared to the more traditional method of phospholipid vesicle reconstitution, which allows uncontrolled receptor oligomerization (138, 139). In addition, studies of detergent-soluble MOR and inhibitory G proteins reconstituted into phospholipid vesicles exhibited agonist affinities and nucleotide binding kinetics which were significantly reduced compared to membrane preparations (140-142), suggesting a disruption in MOR function. For these reasons reconstitution into phospholipid vesicles would have been inappropriate for testing our hypotheses concerning the monomer.

In light of previous success in our laboratory with HDL particle reconstitution of  $\beta_2$ AR, the YMOR was initially reconstituted under identical conditions. Specifically, a 3:2 molar ratio of POPC:POPG was used to mimic plasma membrane phospholipids. However it was important to ascertain if these particular conditions were ideal for the incorporation and function of YMOR. The importance of lipid composition on YMOR incorporation and function were revealed by the influence of polar brain lipid extracts. The brain lipid extract contains a mixture of different phospholipids, and we hypothesized that reconstitution of YMOR into lipid conditions more indicative of a natural brain composition would better support opioid receptor function. This strategy did indeed increase the amount of YMOR [ $^3$ H]DPN binding, suggesting a higher amount of YMOR incorporated in an active conformation. These findings echo those reported for lipid effects on partially purified DOR preparations, where reconstitution of the receptor into phospholipid vesicles composed of brain lipid extract exhibited nearly four-fold increase in ligand binding compared to phosphatidylcholine and phosphatidylglycerol vesicles (143). We did not make an effort to determine the critical lipid component of the brain extract responsible for this increase in binding, but future work should address this

matter as it would be desirable to have a reconstitution system in which the lipid component is clearly defined.

In this study we demonstrate that monomeric MOR couples to heterotrimeric G proteins and stimulates [<sup>35</sup>S]GTPγS binding to the Gα subunit. We also illustrate that the inhibitory G protein Gα<sub>i</sub>βγ can allosterically regulate agonist binding to monomeric MOR. Furthermore, agonist binding and G protein activation by the monomeric receptor displayed potencies identical to those seen in plasma membrane preparations. Therefore we have demonstrated that monomeric MOR is the minimal functional unit, illustrating that the opioid GPCR does not require dimerization to bind ligands and signal to G proteins. However, these data by no means refute the existence of opioid receptor dimerization in cells. It remains possible that homo- and heterodimerization creates unique ligand binding entities that may be subject to differential regulation, desensitization, and internalization. In fact, recent reports have suggested that μ-δ heterodimerization results in a preference for arrestin mediated signal transduction (74) and may play a role in enhancing morphine analgesia (144). One of our ultimate goals is to isolate various oligomeric states of opioid receptors and other GPCRs in rHDL particles, and compare their activities towards ligands and signaling partners directly.

A major technical obstacle is the formation of ‘anti-parallel’ receptor dimers, where the amino termini for the reconstituted GPCRs in the oligomer are on opposite sides of the phospholipid bilayer. Indeed, reconstitution of two GPCRs in a single rHDL particle has been previously demonstrated for rhodopsin (77, 80), but a detailed analysis by nano-gold labeling and single particle electron microscopy of the reconstituted ‘dimers’ reveals that a significant fraction were anti-parallel (80). It is plausible, or even

likely, that an anti-parallel GPCR dimer will result in suboptimal or disrupted G protein coupling. Therefore the development of approaches to insure parallel GPCR dimer incorporation into rHDL particles is critical to confidently study the functional relevance of opioid receptor dimerization.

## **Materials and Methods**

### **Materials**

G protein baculoviruses encoding rat  $G\alpha_{i2}$ , His<sub>6</sub>-G $\beta_1$  and G $\gamma_2$  were provided by Dr. Alfred G. Gilman (University of Texas Southwestern, Dallas, TX). Expired serum was generously provided by Dr. Bert La Du (University of Michigan, Ann Arbor, MI). All lipids were from Avanti Polar Lipids (Alabaster, AL). [<sup>3</sup>H]diprenorphine (DPN) and [<sup>35</sup>S]GTP $\gamma$ S were obtained from PerkinElmer (Waltham, MA). EZ-Link<sup>TM</sup> NHS-Biotin reagent was from Pierce (Rockford, IL). BA85 filters, Cy3 and Cy5 NHS-ester mono-reactive dyes were from GE Healthcare (Piscataway, NJ). Bio-Beads<sup>TM</sup> SM-2 absorbant resin was from Bio-Rad (Hercules, CA). Chromatography columns were run using a BioLogic Duo-Flow Protein Purification System from Bio-Rad. Amicon Ultra centrifugation filters were from Millipore (Billerica, MA). All other chemicals and ligands were from either Sigma-Aldrich (St. Louis, MO) or Fisher Scientific (Pittsburgh, PA).

### **ApolipoproteinA-1 purification**

Wild type human apoA-1 was purified from expired serum as previously described (78). A recombinant apoA-1 with an N-terminal 43 amino acid deletion and a

histidine tag ( $\Delta(1-43)$ -His<sub>6</sub>-apoA-1) was expressed using a pET15b vector to transform competent *Escherichia coli* cells (BL21). Cells were resuspended and lysed by gentle vortexing in 10 mM Tris•HCl pH 8.0, 100 mM NaH<sub>2</sub>PO<sub>4</sub>, 6 M guanidine hydrochloride (GuHCl), 1% Triton X-100. Lysate was fractionated by centrifugation at 10,000 g and the supernatant was loaded onto a Ni-NTA column by gravity flow. The column was washed with 10 mM Tris•HCl pH 8.0, 100 mM NaH<sub>2</sub>PO<sub>4</sub>, 6 M GuHCl, 1% Triton X-100 and then with 50 mM NaH<sub>2</sub>PO<sub>4</sub> pH 8.0, 300 mM NaCl, 1% Triton X-100. Bound  $\Delta(1-43)$ -His<sub>6</sub>-apoA-1 was eluted with 50 mM NaH<sub>2</sub>PO<sub>4</sub> pH 8.0, 300 mM NaCl, 250 mM imidazole, 1% Triton X-100. Peak fractions were further purified on a Superdex 75 gel filtration chromatography column in 20 mM Hepes pH 8.0, 100 mM NaCl, 1 mM EDTA, 20 mM Na•cholate. Pooled  $\Delta(1-43)$ -His<sub>6</sub>-apoA-1 was then dialyzed against 20 mM Hepes pH 8.0, 100 mM NaCl, 1 mM EDTA, 5 mM Na•cholate. Analysis of the final sample purity is shown in Appendix B, Figure B-1. Purified  $\Delta(1-43)$ -His<sub>6</sub>-apoA-1 was concentrated to ~10 mg/mL and stored at -80°C until use.

### **In vitro HDL reconstitution**

Reconstituted HDL particles (containing ‘wild-type’ apoA-1 from serum or recombinant  $\Delta(1-43)$ -His<sub>6</sub>-apoA-1 from *E. coli*) were prepared according to previously reported protocols (78, 145). Briefly, 21 mM Na•cholate, 7 mM lipids (1-palmitoyl-2-oleoyl-*sn*-glycero-3-phosphocholine (POPC) and 1-palmitoyl-2-oleoyl-*sn*-glycero-3-[phospho-*rac*-(1-glycerol)] (POPG) at a molar ratio of 3:2), purified YMOR (DDM-solubilized) and 100  $\mu$ M purified apoA-1 were solubilized in 20 mM Hepes pH 8.0, 100 mM NaCl, 1 mM EDTA, 50 mM Na•cholate. The final concentration of YMOR varied

from 0.2 to 0.4  $\mu\text{M}$ , but the purified YMOR sample always comprised 20% of the total reconstitution volume. In some reconstitutions the lipid component was modified such that porcine polar brain lipid extract (Avanti Polar Lipids) was used in addition to POPC and POPG for a final concentration of 7 mM lipids at a molar ratio of 1.07:1.5:1 brain lipid:POPC:POPG. Following incubation on ice (1.5 to 2 hr), samples were added to Bio-Beads<sup>TM</sup> (Bio-Rad, 0.05 mg/mL of reconstitution volume) to remove detergent and to form HDL particles. Particles containing YMOR were purified via M1 anti-FLAG immunoaffinity chromatography resin (Sigma), eluted with 1 mM EDTA plus 200  $\mu\text{g/mL}$  FLAG peptide. YMOR reconstituted into HDL was stored on ice until further use. Reconstituted particles were analyzed on a Superdex 200 gel filtration column which was calibrated with thyroglobulin (669 kDa, Stokes diameter (Sd) = 17.2 nm), apoferritin (432 kDa, Sd = 12.2 nm), alcohol dehydrogenase (150 kDa, Sd = 9.1 nm), BSA (66 kDa, Sd = 12.2 nm), and carbonic anhydrase (29 kDa, Sd = 4 nm).

### **Single molecule imaging of reconstituted Cy3- and Cy5-YMOR**

Purified YMOR (~200 picomoles) was incubated with NHS-ester Cy3 or Cy5 mono-reactive dye (GE Healthcare) in 20 mM HEPES pH 8.0, 100 mM NaCl, 5 mM  $\text{MgCl}_2$ , 6 mM EDTA, 0.1% DDM, 0.01% CHS, 100 nM NTX for 30 min at 25°C and then 1 hr at 4°C. Conjugation reactions were quenched by the addition of Tris•HCl, pH 7.7 buffer (10 mM final). Cy-labeled YMOR was then separated from free dye using a 12 cm Sephadex G-50 column. The final dye to protein molar ratio was 3.8:1 for Cy3-YMOR and 3.7:1 for Cy5-YMOR as measured on a NanoDrop ND-1000 Spectrophotometer (280 nm absorbance for total protein, 550 nm for Cy3 and 650 nm for



Cy5). A separate aliquot of YMOR was co-labeled with both Cy3 and Cy5 for final molar ratios of 2:1 Cy3:YMOR and 1.8:1 Cy5:YMOR. HDL reconstitutions of Cy3-YMOR alone, Cy5-YMOR alone, a mixture of Cy3- and Cy5-YMOR, and Cy3-Cy5-YMOR were then performed. Reconstitutions were performed as previously described, using  $\Delta(1-43)$ -His<sub>6</sub>-apoA-1 which had been biotinylated at a 4:1 molar ratio using EZ-Link NHS-Biotin according to the manufacturer's protocol (Pierce). Cy3- and Cy5-labeling of YMOR was confirmed by analyzing SDS-PAGE sample separations on a Typhoon 9200 Imager (GE Healthcare, 532/638 nm excitation, 580/680 nm emission).

Reconstituted samples were diluted 5,000-fold in 25 mM Tris•HCl, pH 7.7 and immediately injected into a microfluidic channel on a quartz slide, previously coated with biotinylated-PEG and treated with 0.2 mg/mL streptavidin to generate a surface density of  $\sim 0.05$  molecules per  $\mu\text{m}^2$ . An oxygen scavenging system (OSS) of 10 mM trolox, 100 mM protocatechuic acid and 1  $\mu\text{M}$  protocatechuate-3,4-dioxygenase was included in the sample dilution (146). Following a 10 min incubation to allow binding of the biotin-HDL•Cy-YMOR complex to the streptavidin coated slide, the channel was washed with ice cold 25 mM Tris•HCl pH 7.7 containing the OSS. An Olympus IX71 inverted microscope configured for prism-based total internal reflection fluorescence (TIRF) and coupled to an intensified CCD camera was used to image Cy3 and Cy5 fluorophores (CrystaLaser - 532 nm, Coherent CUBE laser - 638 nm, Chroma bandpass filters HQ580/60 and HQ710/130 nm). Fluorophore intensity time traces were collected for 30 to 100 s at 10 frames per s. Time traces were analyzed for photobleaching with in-house software (MatLab 7.0).

### **FLAG affinity column purification of rHDL•YMOR**

All steps were carried out at 4°C or on ice. Calcium chloride was added to reconstituted HDL•YMOR samples for a final concentration of 3 mM. A M1 FLAG affinity resin (Sigma) gravity flow column was equilibrated in 20 mM Hepes, pH 7.4, 100 mM NaCl, 1 mM CaCl<sub>2</sub>, 0.1% BSA, and the rHDL•YMOR sample was passed through the column 8 times to achieve maximal binding. The resin was washed with 10 column volumes of the same equilibration buffer and samples were eluted with 7 ½ column volumes of 20 mM Hepes, pH 7.4, 100 mM NaCl, 1 mM EDTA, 0.1% BSA, 200 µg/mL FLAG peptide (Sigma). Elution fractions were pooled based on [<sup>3</sup>H]DPN binding.

### **G protein addition to rHDL-YMOR particles**

G<sub>i2</sub> heterotrimer (Gα<sub>i2</sub>-His<sub>6</sub>Gβ<sub>1</sub>-Gγ<sub>2</sub>) was expressed in *Sf9* cells and purified as previously described (147) (Appendix B, Figure B-2). Importantly, the Gα<sub>i2</sub> construct is subject to myristoylation during production in *Sf9* cells. The concentration of active G protein was determined by filter binding of 20 µM [<sup>35</sup>S]GTPγS (12.5 Ci/mmmole) in 30 mM Na•Hepes, pH 8.0, 100 mM NaCl, 50 mM MgCl<sub>2</sub>, 1 mM EDTA, 0.05% C<sub>12</sub>E<sub>10</sub>, and 1 mM DTT after 1 hr incubation at room temperature. Purified G protein heterotrimer (in 0.7% CHAPS) was added to preformed, FLAG-purified rHDL•YMOR particles at a molar ratio of 1:10 receptor to G protein, in volumes such that the final CHAPS concentration was well below its critical micelle concentration. Reconstituted receptor and G protein samples were then incubated in Bio-Beads™ for 30-45 min at 4°C to remove residual detergent.

### **[<sup>3</sup>H]DPN saturation and agonist competition binding assays**

Binding reactions were performed in 100  $\mu$ L volumes. Reconstituted YMOR samples were diluted 20 to 100-fold in 20 mM Hepes pH 8, 100 mM NaCl, 1 mM EDTA, 0.1% BSA and then incubated with [<sup>3</sup>H]DPN (0.25 to 4 nM) for 1 hr at room temperature in 25 mM Tris pH 7.7, 136 mM NaCl, 2.7 mM KCl, 0.1% BSA. Nonspecific binding was determined in the presence of 20  $\mu$ M NTX. Bound [<sup>3</sup>H]DPN was separated from free by on Sephadex G-50 Fine (GE Healthcare) gravity-flow columns. Agonist competition assays in HDL particles were performed in 25 mM Tris•HCl pH 7.7, 7 mM NaCl, 0.1% BSA. For agonist competition assays receptor samples were incubated with 0.5 to 1 nM [<sup>3</sup>H]DPN and increasing concentrations of agonist (1 pM to 1 mM) in the absence or presence of 10  $\mu$ M GTP $\gamma$ S. Samples were measured for radioactivity on a liquid scintillation counter and the data were fit with one-site saturation, one-site competition or two-site competition binding models using Prism 5.0 (GraphPad, San Diego, CA).

### **rHDL•YMOR+G<sub>i2</sub> [<sup>35</sup>S]GTP $\gamma$ S binding assay**

One hundred  $\mu$ L volume reactions were prepared containing ~50-60 fmoles of YMOR incorporated into rHDL particles in 30 mM Tris•HCl, pH 7.4, 100 mM NaCl, 5 mM MgCl<sub>2</sub>, 0.1 mM DTT, 1  $\mu$ M GDP, 0.1% BSA, and 10 nM [<sup>35</sup>S]GTP $\gamma$ S (12.5 Ci/mmol). YMOR samples were incubated with increasing concentrations of agonists (1 pM to 1 mM) for 1 hr at room temperature, then rapidly filtered through BA85 filters and washed three times with 2 mL ice cold 30 mM Tris•HCl, pH 7.4, 100 mM NaCl, 5 mM MgCl<sub>2</sub>. Samples were measured for radioactivity on a liquid scintillation counter and the data were fit with a log dose-response model using Prism 5.0.

## CHAPTER 4

### INVESTIGATING DIFFERENTIAL G PROTEIN ACTIVATION AND AGONIST BINDING TO MONOMERIC $\mu$ -OPIOID RECEPTOR

#### **Introduction**

In Chapter 3 the functionality of a monomeric modified  $\mu$ -opioid receptor, YMOR, to couple  $G_{12}$  heterotrimeric G proteins was established. The nature of monomeric YMOR as the minimal functional unit was demonstrated by stimulation of nucleotide binding to  $G\alpha_{12}$  in response to agonists, as well as illustrating allosteric regulation of agonist binding by  $G_{12}$ . These findings are highly relevant to the field of opioid receptor pharmacology, as current opinion holds that opioid receptor dimerization is ubiquitous and a potential target for rational design of therapeutics (75, 148).

Many compelling biochemical investigations have suggested the importance of opioid receptor oligomerization (13, 129), and therefore this phenomenon should in theory serve an important function in the opioid receptor system. One appealing hypothesis is that opioid GPCR oligomerization generates unique ligand binding and/or G protein coupling interfaces. Receptor oligomerization may begin to explain the pharmacological observation of multiple receptor subtypes (64, 82, 83, 129) which are at odds with the fact that only three receptor isoforms have been cloned. It is possible that certain opioid agonists bind receptor dimers differently than monomers and induce

different kinds of conformational changes in the receptor helices. This in turn may result in differential G protein activation and serve as the underlying mechanism distinguishing full and partial agonists. Conversely, an alternate hypothesis is that receptor dimerization is required for the differential activation of G proteins by agonists because G protein heterotrimers interact with GPCR homo- and heterodimers differently than monomers, resulting in altered coupling and activation.

The work presented in this chapter investigates the capacity of alkaloid and peptide agonists to differentially stimulate multiple  $G\alpha_i$  and  $G\alpha_o$  subunits of G protein heterotrimers coupled to monomeric YMOR. Differential stimulation is defined as differences in agonist potency and efficacy in stimulating [ $^{35}$ S]GTP $\gamma$ S binding to  $G\alpha$  subunits. In low GDP concentrations, rank-order potency and efficacy profiles for the agonists DAMGO and morphine can be seen with  $G\alpha_{i2}$ ,  $G\alpha_{i3}$  and  $G\alpha_{oA}$ . This apparent rank-order is less defined when the nucleotide concentration is increased. In addition, equivalent allosteric regulation of agonist binding to YMOR by both  $G_{i2}$  and  $G_{oA}$  isoforms is demonstrated. Taken together these results suggest that monomeric  $\mu$ -opioid receptor may be capable of differential G protein activation.

## Results

### **DAMGO and morphine differentially activate $G\alpha_{i3}$ coupled to monomeric YMOR**

To begin investigating the differential activation of a particular G protein by agonists, the potency and efficacy of DAMGO and morphine at promoting [ $^{35}$ S]GTP $\gamma$ S binding to  $G\alpha_{i3}$  were analyzed (Figure 4-1). Reconstituted HDL•YMOR plus  $G_{i3}$  heterotrimer samples were prepared such that the final concentration of GDP was 1  $\mu$ M.

Receptor-G protein samples were then diluted 100-fold in the final assay, such that if no GDP was added to the reaction the final concentration was 10 nM and the final receptor concentration was 0.5-1 nM. Under these conditions (10 nM GDP) DAMGO and morphine had nearly equivalent potencies of 47.9 and 50.7 nM, respectively, for stimulating  $G\alpha_{i3}$  (Figure 4-1). Morphine, however, elicited a lower maximal level of [ $^{35}$ S]GTP $\gamma$ S binding, ~70% of the DAMGO response. This difference in efficacy is similar to results in mammalian cell systems, where DAMGO is considered the prototypical full agonist at MOR, while morphine has partial agonist properties (99, 100).

#### **DAMGO can differentially activate $G\alpha_{i2}$ , $G\alpha_{i3}$ and $G\alpha_{oA}$ coupled to monomeric YMOR**

DAMGO potency for stimulating [ $^{35}$ S]GTP $\gamma$ S binding was then compared between rHDL•YMOR coupled to  $G_{i2}$ ,  $G_{i3}$  and  $G_{oA}$  heterotrimers (Table 4-1). An apparent rank-order potency profile of  $G\alpha_{i2} > G\alpha_{i3} > G\alpha_{oA}$  for DAMGO acting at monomeric YMOR was observed. Furthermore, an apparent rank-order for maximal stimulation (agonist efficacy) of  $G\alpha_{i3} \geq G\alpha_{i2} > G\alpha_{oA}$  was observed for DAMGO. Importantly, these rank-order profiles were observed when the assay was performed at a final GDP concentration of 1  $\mu$ M; the GDP concentration was increased from 10 nM to reduce basal [ $^{35}$ S]GTP $\gamma$ S binding. Manipulation of the GDP concentration strongly affected the potency of DAMGO for stimulating nucleotide exchange at  $G\alpha$  (Table 4-1). This nucleotide effect on potency is likely related to the concentrations of GDP, [ $^{35}$ S]GTP $\gamma$ S, and G protein in the assay. Although purified heterotrimers were added to rHDL•YMOR at a 10:1 G protein to receptor molar ratio, we estimate up to 95% of the G

protein precipitates out during the detergent removal process (Appendix B Figure B-3 and Whorton *et al.* 2007 (78)). Therefore it is possible that the final reconstituted G protein to YMOR ratio was as low as 0.5:1, which was readily observed in agonist competition assays (Chapter 3). This would correspond to an average heterotrimer concentration in the [<sup>35</sup>S]GTPγS binding assays of 0.4 nM. Increasing the GDP concentration from 10 nM to 1 μM while maintaining the same concentration of [<sup>35</sup>S]GTPγS, as was done here, would likely alter concentration of agonist needed to elicit nucleotide exchange. Indeed, similar effects have been previously observed for DAMGO stimulation of MOR in rat thalamic membrane preparations (149).

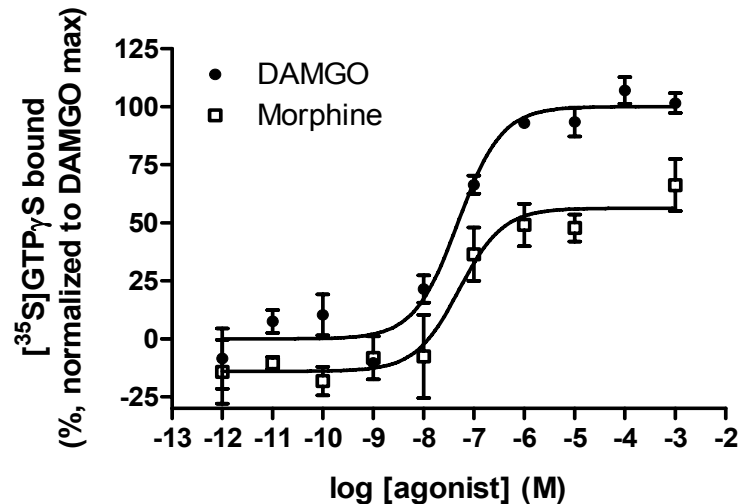


**Figure 4-1.** Morphine is less efficacious than DAMGO towards activation of  $G\alpha_{i3}$  coupled to monomeric YMOR. Stimulation of [<sup>35</sup>S]GTPγS binding to  $G\alpha_{i3}$  coupled rHDL•YMOR in response to increasing concentrations of DAMGO and morphine was determined. Experiments were performed at 0.01 μM GDP. DAMGO exhibited ~1.8-fold stimulation over basal;  $EC_{50} = 47.9$  nM. Morphine exhibited ~1.6-fold stimulation over basal;  $EC_{50} = 50.7$  nM. Morphine treatment resulted ~70% of the [<sup>35</sup>S]GTPγS binding over basal levels that DAMGO treatment stimulated. Data are normalized to the maximal stimulation curve fit value observed for DAMGO. Error bars represent the SEM of experiments performed in duplicate.

**Table 4-1**  
**DAMGO stimulation of [<sup>35</sup>S]GTPγS binding to**  
**G protein heterotrimers coupled to rHDL•YMOR**

	<b>G<sub>i2</sub></b>		<b>G<sub>i3</sub></b>		<b>G<sub>oA</sub></b>	
	<u>GDP<sup>a</sup></u>		<u>GDP</u>		<u>GDP</u>	
	1	10	0.01	1	1	10
EC <sub>50</sub> <sup>b</sup>	30.7 ± 1.6 <sup>d</sup>	173.1 ± 14.6	30.9 ± 8.5 <sup>e</sup>	242.4 ± 20.8	1320 <sup>f</sup>	205.9 ± 6.4
Stim <sup>c</sup>	4.7 ± 1.1	5.9 ± 0.3	1.74 ± 0.1 <sup>e</sup>	6.9 ± 0.1	1.38 <sup>f</sup>	2.7 ± 0.1

<sup>a</sup> GDP values listed in micromolar

<sup>b</sup> EC<sub>50</sub> values reported in nanomolar

<sup>c</sup> Stimulation reported as fold over basal

<sup>d</sup> Values reported as ± the SEM of at least two independent experiments performed in duplicate  
 Values determined based on n=2, except for <sup>e</sup> (n=3) and <sup>f</sup> (n=1)

### **Gα<sub>oA</sub> exhibits higher basal nucleotide binding compared to Gα<sub>i2</sub>**

Comparison of nucleotide binding between Gα<sub>i2</sub> and Gα<sub>oA</sub> under 1 μM GDP conditions revealed that the basal level of Gα<sub>oA</sub> [<sup>35</sup>S]GTPγS binding (~70% of the maximal) was significantly higher than that for Gα<sub>i2</sub> (~28% of the maximal) (Figure 4-2). This basal activity reflects Gα rather than YMOR activity, as the difference between Gα<sub>oA</sub> and Gα<sub>i2</sub> is observed under identical receptor conditions and low agonist concentrations. In an effort to reduce the basal level of nucleotide binding by Gα<sub>oA</sub> and increase detectable DAMGO stimulation the final GDP concentration was increased to 10 μM. This modification effectively decreased basal [<sup>35</sup>S]GTPγS binding to ~36% of the maximal levels. Increasing the GDP concentration also decreased basal Gα<sub>i2</sub> nucleotide binding to ~16% maximal. To effectively compare stimulation of G protein alpha subunits coupled to monomeric YMOR, assay conditions which allowed for a strong stimulation over basal were required. Therefore the next set of experiments comparing agonist potency and efficacy at G<sub>i2</sub> and G<sub>oA</sub> were performed at 10 μM GDP.



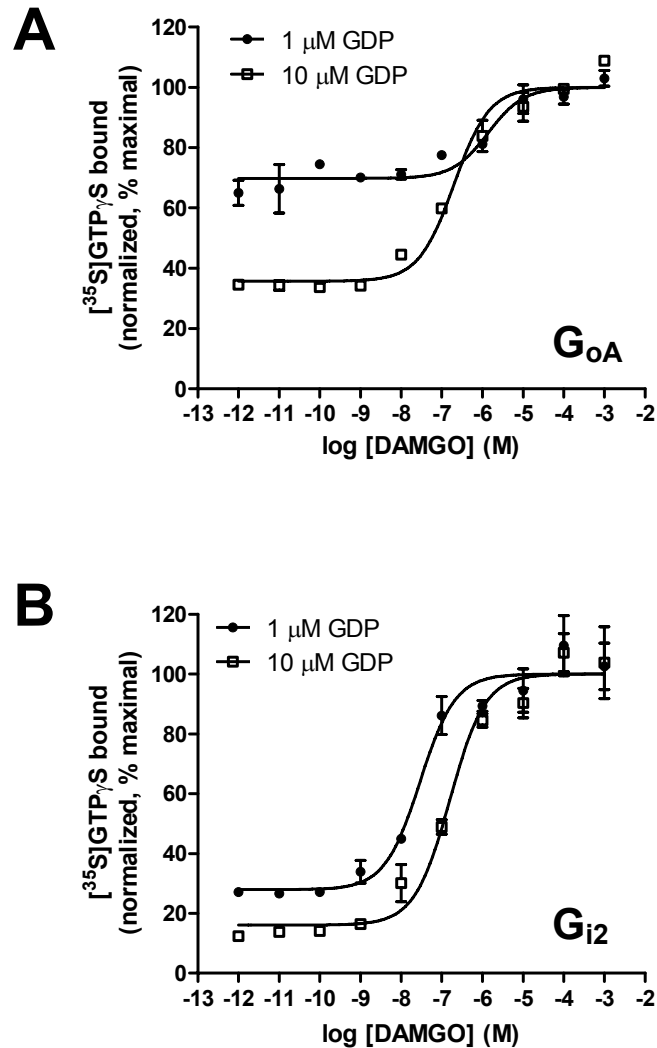


**Figure 4-2.**  $G_{\alpha oA}$  exhibits higher basal nucleotide binding than  $G_{\alpha i2}$  when coupled to rHDL•YMOR. Dose-response curves for DAMGO stimulation of  $[^{35}\text{S}]\text{GTP}\gamma\text{S}$  binding to  $G_{\alpha oA}$  (**A**) or  $G_{\alpha i2}$  (**B**) coupled to rHDL•YMOR (as heterotrimer) were determined in 30 mM Tris•HCl, pH 7.4, 100 mM NaCl, 5 mM  $\text{MgCl}_2$ , 0.1% BSA and 1 or 10  $\mu\text{M}$  GDP. Bound  $[^{35}\text{S}]\text{GTP}\gamma\text{S}$  is normalized to the curve fit maximal binding level. (**A**) DAMGO stimulated  $[^{35}\text{S}]\text{GTP}\gamma\text{S}$  binding to  $G_{\alpha oA}$  with an  $\text{EC}_{50}$  of 1.32  $\mu\text{M}$  and 199.7 nM at 1  $\mu\text{M}$  GDP and 10  $\mu\text{M}$  GDP, respectively. Basal binding levels were 70% and 36% of the maximum at 1  $\mu\text{M}$  GDP and 10  $\mu\text{M}$  GDP, respectively. (**B**) DAMGO stimulated  $[^{35}\text{S}]\text{GTP}\gamma\text{S}$  binding to  $G_{\alpha i2}$  with an  $\text{EC}_{50}$  of 29.1 nM and 158.8 nM at 1  $\mu\text{M}$  GDP and 10  $\mu\text{M}$  GDP, respectively. Basal binding levels were 28% and 16% of the maximum at 1  $\mu\text{M}$  GDP and 10  $\mu\text{M}$  GDP, respectively. Error bars represent the SEM of experiments performed in duplicate.

### **DAMGO and morphine appear equipotent at activating $G\alpha_{i2}$ coupled to monomeric YMOR**

The ability of  $G_{i2}$  to be differentially activated by agonists was investigated with agonist dose-response [ $^{35}\text{S}$ ]GTP $\gamma$ S binding assays comparing DAMGO and morphine activation (Figure 4-3). In assays conducted at 10  $\mu\text{M}$  GDP, the two agonists exhibited nearly equivalent potency for stimulating [ $^{35}\text{S}$ ]GTP $\gamma$ S binding (DAMGO  $\text{EC}_{50} = 170 \pm 15$  nM; morphine  $\text{EC}_{50} = 120 \pm 16$  nM). The agonists also appeared to be equally efficacious under these conditions with maximal stimulations of 66.6 and 64.1 fmoles of bound [ $^{35}\text{S}$ ]GTP $\gamma$ S for DAMGO and morphine, respectively. Basal binding levels were approximately 11 fmoles of [ $^{35}\text{S}$ ]GTP $\gamma$ S binding, indicating approximately 55 fmoles of  $G\alpha_{i2}$  was stimulated. An estimated 80 fmoles of YMOR were present in the binding reaction, suggesting that at least 68% of receptors were actively coupled to G protein heterotrimer.

### **Morphine appears equipotent at activating $G\alpha_{i2}$ and $G\alpha_{oA}$ coupled to monomeric YMOR**

To investigate the potential of a single agonist to differentially activate G protein isoforms, morphine dose-response assays were compared between samples of rHDL•YMOR coupled to either  $G\alpha_{i2}$  (Figure 4-3) or  $G\alpha_{oA}$  (Figure 4-4). Morphine stimulate approximately 60 fmoles of [ $^{35}\text{S}$ ]GTP $\gamma$ S binding at  $G\alpha_{oA}$  with an  $\text{EC}_{50}$  of  $107 \pm 1.5$  nM. Comparing these data to those for  $G\alpha_{i2}$  described above, morphine appears to be equipotent at activating  $G\alpha_{i2}$  and  $G\alpha_{oA}$  coupled monomeric YMOR in the presence of 10  $\mu\text{M}$  GDP. The fact that a maximum of  $\sim 80$  fmoles of [ $^{35}\text{S}$ ]GTP $\gamma$ S binding was observed

raises the possibility that more than one  $G_{\alpha A}$  heterotrimer was incorporated into some of the rHDL•YMOR particles, though only one heterotrimer should couple to the receptor at a time.

### Naloxone does not significantly alter basal activity of $G_{\alpha_{i2}}$ or $G_{\alpha_{oA}}$

Recent investigations using the non-selective opioid ligand naloxone have suggested that while traditionally defined as an antagonist, naloxone may exhibit characteristics of inverse agonism. Therefore the ability of naloxone to decrease basal levels of [ $^{35}$ S]GTP $\gamma$ S binding was determined with rHDL•YMOR coupled to  $G_{i2}$  and  $G_{\alpha A}$  (Figures 4-3 and 4-4). In assays performed at 10  $\mu$ M GDP, naloxone showed no significant effect on [ $^{35}$ S]GTP $\gamma$ S binding at either  $G_{\alpha_{i2}}$  or  $G_{\alpha_{oA}}$ .

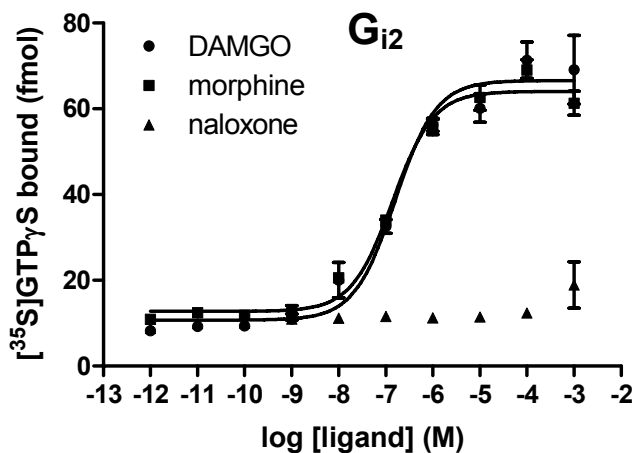


**Figure 4-3.** Ligand dose-responses for [ $^{35}$ S]GTP $\gamma$ S binding to  $G_{i2}$  coupled monomeric YMOR. Reconstituted HDL•YMOR was coupled to  $G_{i2}$  at a 10:1 molar ratio. An estimated 80 fmoles of receptor was incubated with 100 nM [ $^{35}$ S]GTP $\gamma$ S in Tris•HCl, pH 7.4, 100 mM NaCl, 5 mM MgCl<sub>2</sub>, 10  $\mu$ M GDP for 1 hr. DAMGO stimulated [ $^{35}$ S]GTP $\gamma$ S binding ~6-fold over basal with an EC<sub>50</sub> of 158 nM. Morphine exhibited an EC<sub>50</sub> of 139 nM with ~5-fold stimulation over basal [ $^{35}$ S]GTP $\gamma$ S binding. Maximal bound [ $^{35}$ S]GTP $\gamma$ S levels were ~66 fmoles for DAMGO and ~64 fmoles for morphine, indicating that approximately 68% of the YMOR was actively coupled to G protein. Naloxone exhibited no significant change in basal [ $^{35}$ S]GTP $\gamma$ S binding levels. Data are representative of two experiments performed in duplicate. Error bars represent the SEM.

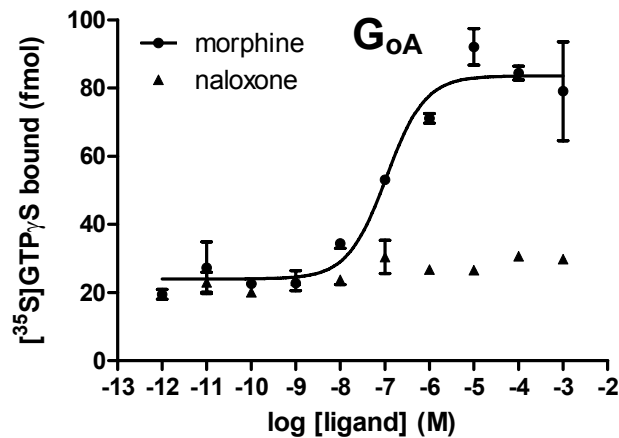


**Figure 4-4.** Ligand dose-responses for [<sup>35</sup>S]GTP<sub>γ</sub>S binding to G<sub>α<sub>oA</sub></sub> coupled monomeric YMOR. An estimated 60 fmoles of rHDL•YMOR was coupled to G<sub>α<sub>oA</sub></sub> at a 10:1 molar ratio and incubated with 100 nM [<sup>35</sup>S]GTP<sub>γ</sub>S in Tris•HCl, pH 7.4, 100 mM NaCl, 5 mM MgCl<sub>2</sub>, 10 μM GDP for 1 hr. Morphine exhibited an EC<sub>50</sub> of 107.5 ± 1.5 nM with ~3.5-fold stimulation over basal [<sup>35</sup>S]GTP<sub>γ</sub>S binding. Naloxone exhibited no significant change in basal [<sup>35</sup>S]GTP<sub>γ</sub>S binding levels. Error bars represent the SEM of three experiments performed in duplicate.

### **G<sub>i2</sub> and G<sub>oA</sub> heterotrimers regulate high affinity morphine binding to monomeric YMOR**

The capacity of G<sub>i2</sub> and G<sub>oA</sub> to differentially affect agonist binding to monomeric YMOR was next determined by measuring allosteric regulation of morphine binding in agonist competition binding assays. Both G<sub>i2</sub> and G<sub>oA</sub> were able to allosterically regulate high affinity morphine binding to monomeric YMOR (Figure 4-5). High affinity morphine binding was nearly equivalent whether YMOR was coupled to G<sub>i2</sub> (K<sub>ihi</sub> ~0.53 nM) or G<sub>oA</sub> (K<sub>ihi</sub> ~1.0 nM). As expected, uncoupling G<sub>i2</sub> and G<sub>oA</sub> with the addition of 10 μM GTP<sub>γ</sub>S resulted in similar low binding affinities (G<sub>i2</sub> GTP<sub>γ</sub>S K<sub>i</sub> ~322 nM; G<sub>oA</sub> GTP<sub>γ</sub>S K<sub>i</sub> ~ 766 nM). Notably, GTP<sub>γ</sub>S treatment increased the amount of [<sup>3</sup>H]DPN binding to rHDL•YMOR+G<sub>oA</sub> 1.4-fold over the vehicle condition at low morphine concentrations. This GTP<sub>γ</sub>S effect of increasing [<sup>3</sup>H]DPN binding was not observed for YMOR coupled to G<sub>i2</sub>.

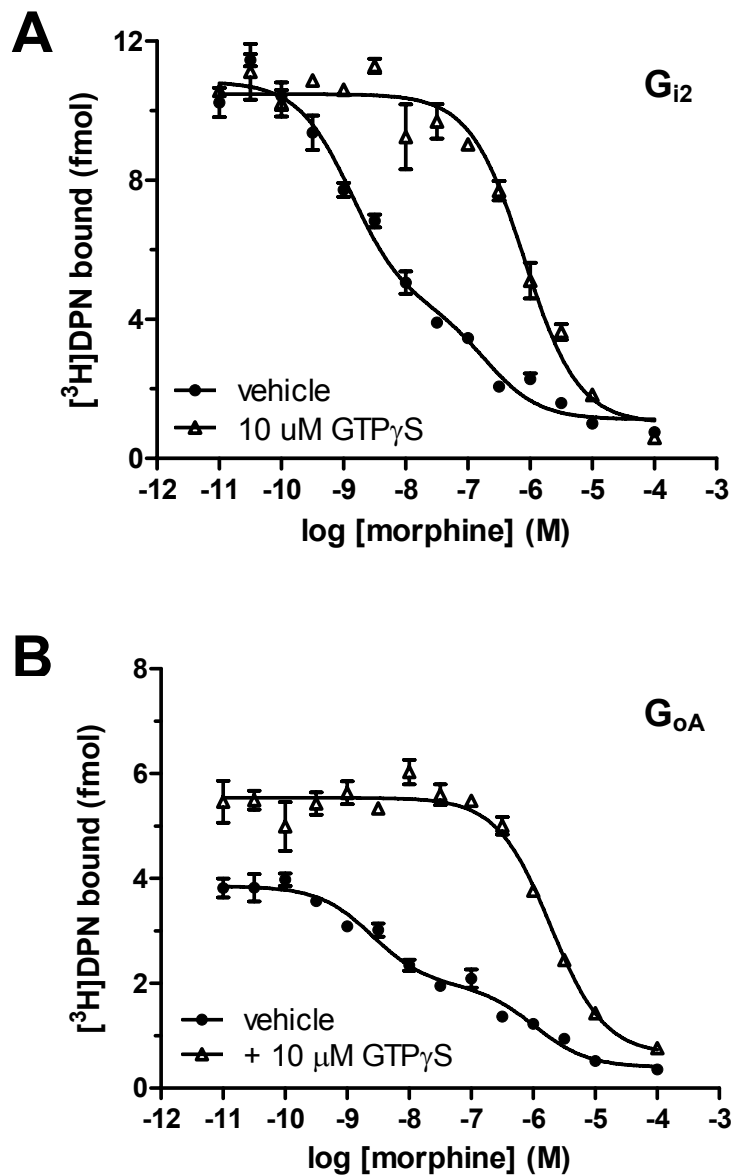


**Figure 4-5.** Allosteric regulation of morphine binding to monomeric YMOR by  $G_{i2}$  and  $G_{oA}$ . Purified  $G_{i2}$  (A) and or  $G_{oA}$  (B) heterotrimer was added to reconstituted HDLYMOR samples at a 10:1 G protein:YMOR molar ratio. Binding of 0.75 nM  $[\text{}^3\text{H}]\text{DPN}$  was determined at 7 mM NaCl in the presence of increasing concentrations of morphine, in the absence or presence of 10  $\mu\text{M}$   $\text{GTP}\gamma\text{S}$ . (A)  $K_{i_{hi}} \sim 0.5$  nM;  $K_{i_{lo}} \sim 80$  nM;  $K_{i_{\text{GTP}\gamma\text{S}}} \sim 320$  nM; high state = 66%. (B)  $K_{i_{hi}} \sim 1.0$  nM;  $K_{i_{lo}} \sim 420$  nM;  $K_{i_{\text{GTP}\gamma\text{S}}} \sim 760$  nM; high state = 55%. Data are representative of three independent experiments performed in duplicate. Error bars represent the SEM of replicate measurements.

## Discussion

Following the demonstration that MOR can activate both  $G_i$  and  $G_o$  heterotrimeric G proteins, extensive research has focused on determining if the receptor preferentially couples to a specific  $G\alpha$  isoform (35). Studies have illustrated both the ability of a particular  $G\alpha$  isoform to be differentially stimulated by multiple agonists (99-101, 150), and the potential for a particular agonist to differentially stimulate multiple  $G\alpha$  isoforms (101, 150-153). DAMGO has been found to elicit differential G protein activation based on potency profiles including  $G\alpha_{i3} > G\alpha_{o2} > G\alpha_{i2}$  (151);  $G\alpha_{i3} \geq G\alpha_{oA} \approx G\alpha_{i1} \geq G\alpha_{i2}$  (101); and  $G\alpha_o \approx G\alpha_{i2} > G\alpha_{i1} \approx G\alpha_{i3}$  when measuring adenylyl cyclase inhibition (150). An activation profile of  $G\alpha_{o1} \approx G\alpha_{i2}$  for DAMGO compared to  $G\alpha_{i2} > G\alpha_{o1}$  for morphine illustrates the potential for selective G protein activation by different agonists (154). Studies using fusion proteins between MOR and G proteins suggested that the receptor activated  $G\alpha_{i1} > G\alpha_{i2}$  in response to DAMGO (106). These investigations were performed using plasma membrane preparations from human embryonic kidney, C<sub>6</sub> glioma, or SH-SY5Y neuroblastoma cell lines and differences in these cell lines could conceivably account for these varied responses. Considering researchers have used cell culture over-expression systems to allow for putative opioid receptor oligomerization, an oligomeric state of MOR would similarly be presumed in these studies. However, the exact nature of the receptor complex at the plasma membrane is ultimately unknown.

While we have demonstrated that a MOR monomer efficiently couples to G proteins, it is possible that differential agonist potencies and  $G\alpha$  activations required MOR oligomerization. Receptor dimerization may alter an agonist's ability to activate the complex. Conversely it may alter the capacity of the receptor complex to activate coupled

G protein. Therefore we determined the ability of the alkaloid morphine and peptide mimic DAMGO to stimulate [<sup>35</sup>S]GTPγS binding to Gα<sub>i2</sub>, Gα<sub>i3</sub>, and Gα<sub>oA</sub> at monomeric YMOR. The potency of the agonists for promoting nucleotide exchange at Gα subunits was strongly dependent upon GDP concentrations. When the GDP concentration was 1 μM, DAMGO stimulated [<sup>35</sup>S]GTPγS binding with a rank-order of Gα<sub>i2</sub> > Gα<sub>i3</sub> > Gα<sub>oA</sub>. Morphine exhibited a similar rank-order, stimulating Gα<sub>i2</sub> with higher potency than Gα<sub>i3</sub>. Typical GDP concentrations in cells have been found to anywhere from ~3-50 μM (155-157), and most cell based [<sup>35</sup>S]GTPγS binding assays on opioid receptors have been performed at 10 or 100 μM GDP. When HDL assays were performed at 10 μM GDP the apparent differences in the activation of Gα<sub>i2</sub> and Gα<sub>oA</sub> were ablated. This may imply that a MOR monomer is incapable of differential G protein activation at physiologically relevant nucleotide concentrations. However, one must consider the G protein and GDP conditions in these comparisons. The concentration of G protein in our assays is estimated to be 0.1 to 0.8 nM, such that 1 μM GDP would likely result in all G proteins being bound to nucleotide prior to stimulation. It is difficult to know the proportion of G proteins bound to nucleotide in cell membrane assays; however at concentrations of 10-100 μM GDP it is likely that G proteins will be saturated with nucleotide. Therefore it is likely that both the HDL and membrane assays would have similar conditions of G protein bound to nucleotide. Thus, the relatively lower GDP concentrations needed to see differential activation by the monomer may still be physiologically relevant.

The reconstituted HDL approach also provided a means to probe basal activity of monomeric YMOR. While basal signaling activity of MOR has been observed by others (158, 159), our [<sup>35</sup>S]GTPγS binding data further suggests that G<sub>o</sub> itself exhibits a higher

basal activity than  $G_{i2}$ . As such, rHDL•YMOR+ $G_0$  can be used as a platform to investigate potential inverse agonists. This approach may prove very useful, as some key recent findings have sparked interest in MOR inverse agonists. First,  $G_0$  appears to be preferentially stimulated under conditions of constitutive MOR activity, as measured by azidoanilido- $[\alpha^{32}\text{-P}]\text{GTP}$  labeling (160). Second, naloxone activity is altered during constitutive MOR activation with agonists, in which it behaves as an inverse agonist rather than a neutral antagonist (158, 161, 162). Finally basal activity of MOR is coming under increased scrutiny as these alterations in G protein partners with chronic opioid exposure suggest a cellular mechanism for the development of dependence (58, 163). In light of these findings, we hypothesized that the pharmacological profile of naloxone is dependent upon which G protein isoform is coupled to MOR. When YMOR is coupled to  $G_i$ , naloxone would behave as a neutral antagonist due to the low basal activity of  $G\alpha_{i2}$ . The higher basal activity of YMOR- $G_0$  coupling, however, would reveal inverse agonist activity of naloxone. When this hypothesis was tested, however, naloxone failed to show inverse agonist activity at YMOR coupled to  $G_0$  or  $G_{i2}$ . These results suggest that the inverse agonist activity of naloxone at MOR is not merely indicative of which G protein it is coupled to, and may suggest alterations in other MOR signaling complex components at the whole cell level occur during chronic stimulation.

Allosteric regulation of agonist binding to monomeric YMOR by  $G_{i2}$  was demonstrated previously, and here we show that this is also true for  $G_{0A}$ . Interestingly, the agonist competition assays revealed different levels of  $[\text{}^3\text{H}]\text{DPN}$  binding to YMOR coupled to  $G_{i2}$  versus  $G_{0A}$ , following  $\text{GTP}\gamma\text{S}$  treatment (Figure 4-5). This phenomenon of altered antagonist binding to GPCRs by nucleotide treatment has been known for years



(164), however an understanding of the underlying mechanism has eluded researchers. Recent studies in our laboratory have seen similar results with antagonist binding to the  $\beta_2$ AR coupled to  $G_s$  in HDL particles (Gisselle Vélez Ruiz, personal communication). While this work with YMOR does not directly suggest a mechanism, additional preliminary investigations with the  $\beta_2$ AR- $G_s$  complex have lead us to hypothesize that the nucleotide state of the G protein coupled to a GPCR influences antagonist binding. Although much further work needs to be done regarding this phenomenon, the fact that it is observed in the HDL reconstitution system suggests that it is not the result of allosteric regulation between multiple receptors in an oligomer, but rather is related to direct allosteric regulation of ligand binding by coupled G proteins.

In conclusion, this work illustrates that monomeric MOR is capable of differential G protein activation. Considering the high sensitivity of  $G\alpha$  stimulation to nucleotide concentration further investigation of these phenomena is ultimately warranted, especially experiments investigating additional MOR alkaloid and peptide agonists. In particular, experiments looking at endogenous opioid peptides will contribute to our understanding of MOR function in response to its physiological ligands. This work has underscored the exquisite sensitivity of G protein coupling and activation to nucleotide concentrations. The rHDL particle methodology will continue to prove highly useful in these future characterizations of MOR ligand binding and G protein coupling, as it allows for fine control over receptor, G protein, and nucleotide variables.

## Materials and Methods

### Materials

All reagents and materials were obtained as previously described.

### In vitro reconstitution of HDL particles

High density lipoprotein particles containing monomeric YMOR were prepared as described in Chapter 3.  $G_{i2}$ ,  $G_{i3}$ , and  $G_{oA}$  heterotrimeric G proteins were purified according to Kozasa (147). An analysis of the heterotrimer purity is shown in Appendix B, Figure B-2. Heterotrimers were added to FLAG affinity column enriched rHDL•YMOR particles as described in Chapter 3 at a G protein to YMOR ratio of either 10:1.

### rHDL•YMOR+G protein [ $^{35}$ S]GTP $\gamma$ S binding assay

One hundred  $\mu$ L volume reactions were prepared containing ~50-80 fmoles of YMOR incorporated into rHDL particles in 30 mM Tris•HCl pH 7.4, 100 mM NaCl, 5 mM MgCl<sub>2</sub>, 0.1 mM DTT, 0.1% BSA, and 10 nM isotopically diluted [ $^{35}$ S]GTP $\gamma$ S (12.5 Ci/mmol). The concentration of GDP was 0.01, 1, or 10  $\mu$ M. YMOR samples were incubated with increasing concentrations of agonists (1 pM to 1 mM) for 1 hr at room temperature, then rapidly filtered through nitrocellulose BA85 filters and washed three times with 2 mL ice cold 30 mM Tris•HCl pH 7.4, 100 mM NaCl, 5 mM MgCl<sub>2</sub>. Samples were measured for radioactivity on a liquid scintillation counter and the data were fit with a log dose-response model using Prism 5.0 (GraphPad, San Diego, CA).

### **[<sup>3</sup>H]DPN agonist competition binding assays**

Agonist competition assays in rHDL particles were performed in 25 mM Tris•HCl pH 7.7, 7 mM NaCl, 0.1% BSA, 10 μM DTT. Receptor samples were incubated with 0.5 to 1 nM [<sup>3</sup>H]DPN and increasing concentrations of agonist (1 pM to 1 mM) in the absence or presence of 10 μM GTPγS. Bound [<sup>3</sup>H]DPN was separated from free radioligand by on Sephadex G-50 Fine (GE Healthcare) gravity-flow columns. Samples were measured for radioactivity on a liquid scintillation counter and the data were fit with one-site saturation, one-site competition or two-site competition binding models using Prism 5.0.

## CHAPTER 5

### CONCLUSIONS

#### **Summary**

Over the past decade dimerization of G protein-coupled receptors (GPCRs) has increasingly been purported as a fundamental aspect to receptor organization in vivo. Within the field of opioid receptor research, the prevalent thought is that receptors function as requisite homo- and heterodimers to generate signaling units capable of coupling to multiple G protein isoforms and activating them in a differential manner in response to many different small alkaloid and peptide ligands (13, 75, 165). In work that challenges the notion that GPCR function requires dimerization, our laboratory has used a reconstitution approach to illustrate that prototypical class A GPCR monomers can functionally couple G proteins (78, 79). This thesis therefore asked if the  $\mu$ -opioid receptor (MOR) could function as a monomer. Beyond functional coupling to a particular G protein, we hypothesized that monomeric MOR could differentially activate multiple G protein isoforms. We further hypothesized that agonist binding to monomeric MOR would be subject to allosteric regulation by multiple G protein isoforms.

Studying monomeric MOR necessitated use of the reconstituted HDL particle system, which in turn required the development of novel expression and purification schemes to generate active receptor in high enough yields for biochemical manipulation

and characterization. For these studies a MOR fused to YFP at the N-terminus (YMOR) was used. High affinity agonist binding, which was stabilized by G<sub>i</sub> and G<sub>o</sub> heterotrimers, and stimulation of nucleotide exchange at the G $\alpha$  subunits demonstrated that a monomeric YMOR functions in an identical fashion to putative homodimers in plasma membrane preparations. The capacity of a single agonist to differentially activate G proteins via monomeric YMOR was also observed. Furthermore, different levels of activation of a particular G protein isoform were induced by alkaloid and peptide agonist binding to monomeric YMOR. In conclusion, this thesis has illustrated that efficient G protein signaling, which results in ion channel regulation and adenylyl cyclase inhibition, does not require opioid receptor oligomerization.

### **A potential role for opioid receptor oligomerization**

The findings presented here then beg the question, what is the physiological function of opioid receptor oligomerization? Unlike other class A GPCRs, a vast number of ligands of various selectivity and efficacy at the  $\mu$ ,  $\delta$ , and  $\kappa$  opioid receptors have been used in a number of studies which suggest some cellular processes that may be influenced by oligomerization. One area of particular note is receptor desensitization and internalization at the molecular level, and how these processes relate to the development of opioid tolerance and dependence at the whole animal level.

Like most GPCRs, termination of opioid receptor signaling has been shown to involve the action of G protein receptor kinases (GRKs) and arrestins. Following agonist binding to the receptor, GRKs phosphorylate one or more specific residues on the receptor C-tail, at which point arrestin proteins can associate and sterically prevent G

protein coupling (166). Arrestin binding then mediates internalization, removing the receptor from the plasma membrane and effectively eliminating their capacity for transducing extracellular signals. Chronic opioid agonist exposure results in the development of tolerance (the need for higher doses to achieve equivalent responses) and dependence (a psychological craving and/or physiological reliance on a drug), and given the importance of these phenomena in the clinic considerable research has focused on understanding the molecular details of desensitization and internalization following prolonged MOR activation (167).

MOR desensitization begins with phosphorylation of Thr180 by GRK3 in response to agonist binding (168), which then promotes association with Arrestin3 (Arr3 /  $\beta$ -arrestin2) (169). Some research has shed light on the potential for MOR-DOR hetero-oligomers to influence opioid receptor internalization. By measuring time-courses of stimulated potassium current in oocytes expressing MOR and DOR, Lowe *et al.* showed that DOR signaling desensitized significantly faster than MOR (170). The authors additionally showed that the recruitment of Arr3 was the rate limiting step in desensitization, and increasing the amount of Arr3 in the oocytes could increase MOR desensitization rates closer to those seen for DOR.

These different MOR and DOR interactions with arrestin may prove to be very clinically important. The opioid receptor-arrestin interaction has been demonstrated to be involved in the development of opioid tolerance in an Arr3<sup>-/-</sup> knock-out mouse model. Mice lacking Arr3 displayed either no tolerance to morphine (171) or a greatly delayed induction of weaker tolerance (172). A traditional view of receptor function and development of tolerance to agonist signaling would hold that chronic opioid activity

results in increased receptor desensitization and internalization. This internalization would decrease the number of receptors at the cell surface and require higher doses of drug to elicit equivalent responses. Fitting nicely with this theory, the lack of arrestin would be expected to result in maintenance of receptor numbers at the plasma membrane, and a correlated lack of tolerance.

However, multiple studies have further complicated our understanding of tolerance development. While morphine treatment reproducibly produces tolerance *in vivo*, it is unable to efficiently promote GRK phosphorylation of MOR in cultured cells (173, 174), bringing into question how arrestins are recruited to a morphine activated receptor. Furthermore, chronic morphine treatment has been reported to decrease receptor number (175, 176), cause no change (177, 178), or increase MOR binding sites (179-181).

More recently, MOR oligomerization has been suggested to influence internalization in response to chronic morphine treatment. He *et al.* used immunocytochemistry methods to show that saturating morphine doses do not cause MOR internalization in HEK293 cells (182). This was also illustrated with immunohistochemistry on explanted rat spinal cord cultures. Surprisingly, if cells or animals were co-treated with a low dose of DAMGO which does not cause internalization on its own, a significant amount of MOR internalization was apparent. After showing that the induced internalization of MOR was not the result of increased local GRK and arrestin activity caused by DAMGO binding, the authors proposed that MOR was functioning in oligomeric complexes. These complexes were postulated to simultaneously bind both morphine and DAMGO, with DAMGO-bound receptors

internalizing and effectively ‘dragging’ the other morphine-bound receptors inside the cell. Further experiments in this work showed that morphine tolerance in rats could be prevented by co-administration of small doses of DAMGO. From these findings the authors concluded that internalization of MOR resulted in protection against the development of tolerance, rather than being the cause of tolerance. Others, however, have found no effect of DAMGO on MOR internalization in a state of morphine tolerance (183).

Intriguing studies have even suggested chronic morphine treatment results in specific up-regulation of putative MOR-DOR hetero-oligomers. The laboratories of Westfall, Rothman, and Holaday published a series of reports using [<sup>3</sup>H][D-Ala<sup>2</sup>, D-Leu<sup>5</sup>]enkephalin and [<sup>3</sup>H]naltrexone binding in rat brain preparations to describe the generation of unique binding sites when  $\mu$  and  $\delta$  receptors are in hetero-oligomeric complexes versus when they are not complexed (64, 67, 184). When analyzing these receptor populations in response to chronic morphine, the number of complex sites increased ~30-50% while the total receptor sites were minimally increased by ~10-15% (180, 181, 185-187). These findings may begin to explain the contradictory changes in MOR density seen by different groups during the development of morphine tolerance, as receptor density changes would be over or underestimated if the probing ligand binds different receptor complexes/populations with different affinities. More importantly, these results have suggested that MOR-DOR hetero-oligomers may play a role in either the development tolerance or its subsequent alterations in opioid signaling.

Finally, investigations of morphine tolerance in animals have revealed additional pieces to the puzzle of potential MOR and DOR interactions in vivo. The development of



morphine tolerance and dependence is reduced with co-administration of selective DOR antagonists (188-190). Moreover, the observation that the DOR knock-out mouse exhibits morphine analgesia, but no tolerance, provides strong evidence for a role of DOR in tolerance in vivo (191). As a result of these findings, many researchers have endeavored to create novel opioid compounds with both  $\mu$ -agonist and  $\delta$ -antagonist properties (192). After this mixed-opioid approach for eliciting analgesia while limiting tolerance and dependence was initially validated in animal models, many additional compounds incorporating various  $\mu$  and  $\delta$  pharmacophores and exhibiting various binding and activation profiles have been described (193).

All told, these data indicate that both MOR and DOR play pivotal roles in tolerance and suggest that there may be a direct interplay between the two receptors. In the end, however, much is still unclear regarding opioid receptor oligomerization. An ever growing number of studies have yielded few definitive answers regarding whether there are cellular functions which absolutely require opioid receptor oligomerization, versus functional processes which are fine-tuned by oligomerization. A better understanding of the tolerance phenomena will require more thorough research of the interaction between opioid receptors at a molecular level.

### **Direct analysis of opioid receptor organization in cells**

One issue with the studies discussed above is the nature of the experimental systems. A majority of investigations into opioid receptor function and oligomerization are performed in a heterologous over-expression cell culture system. With this approach the expressed receptors are often assumed to be a homogenous population. This could

represent a fundamental flaw when it comes to probing the function of receptor complexes, as it is possible that a mixed population of monomers, homodimers, heterodimers, or even higher order oligomers could all exist on the cell surface.

To address this possibility and begin to determine the nature of opioid receptor oligomerization at the membrane, we propose to further examine fluorescent ligand binding using single molecule total internal reflection fluorescence microscopy (SM-TIRF). Studies presented in Appendix A illustrate how reconstituted HDL particles can serve as a platform for the visualization of fluorescent-agonist binding to monomeric YMOR. The instrumentation for these assays is currently being adapted to visualize ligand binding to live cells. The usefulness of this approach has been shown in studies of opioid receptor desensitization and internalization in cultured HEK and locus ceruleus cells (194, 195). Grandy and co-workers showed plasma membrane localization of specific  $\mu$  and  $\delta$  agonists dermorphin and deltorphin which were labeled with Bodipy-TR (Figure 5-1). This technique can likely be expanded to visualize the binding of many different peptide opiate ligands, which will prove very useful in light of several studies that highlight the potential for bifunctional or oligomer selective ligands. Recent efforts to identify ligands which can selectively interact with opioid receptor oligomers may open new possibilities for visual analysis of opioid receptors.

As discussed earlier, an emerging branch of research in the opioid field is focused on the identification of bifunctional and bivalent ligands which display unique affinity and activity profiles for multiple receptor subtypes (75, 193). Waldhoer *et al.* have proposed just such a ligand for dimers between DOR and KOR with 6'-guanidinonaltrindole (196). In the efforts to combine  $\mu$ -agonist/ $\delta$ -antagonist

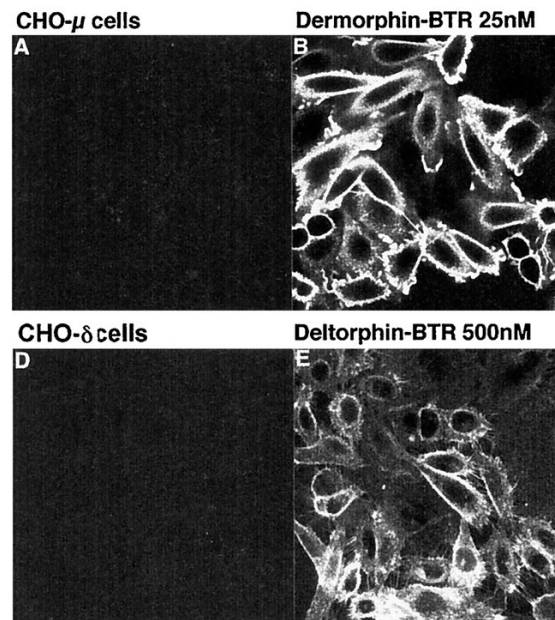


**Figure 5-1.** Visualization of Bodipy TR-conjugated opioids binding to live cells. CHO cells expressing either  $\mu$  or  $\delta$  opioid receptor were imaged with confocal laser microscopy before (A and D) and after a 5 min incubation with Bodipy TR-labeled dermorphin and deltorphin (B and E). Adapted from Arttamangkul *et al.* 2000, *Mol Pharmacol* 58:1570-80, with permission.

pharmacophores to create novel therapeutic compounds several bivalent molecules have been proposed. One particular compound, a combination of oxymorphone and aminonaltridole pharmacophores with 19 to 25 Å linkers, has been reported to simultaneously bind MOR and DOR in a heterodimer complex (197). Although these claims of heterodimer selective ligands need more rigorous testing, unique bifunctional ligands which exhibit enhanced or selective binding at heterodimers would prove useful for imaging approaches. Fluorescence microscopy of cells bound to fluorescent ligands highly selective for MOR or DOR could directly visualize gross receptor localization or organization. Comparison of receptor levels and organization with heterodimer-selective ligands may reveal the proportion of heterodimers compared to the total receptor population, as well as potential differences in subcellular localization between heterodimers and receptor homodimers/monomers.

## **Isolation and reconstitution of opioid receptor dimers**

Although the SM-TRIF approaches may allow for visual comparison of different types of opioid receptor oligomerization, it would still not allow for definitive characterization of their function. As discussed in Chapter 3, one of our ultimate goals with the reconstituted HDL particle system is to incorporate a GPCR dimer, allowing for direct functional comparison with a monomer in a number of biochemical assays. This thesis describes the extensive efforts to develop and validate the HDL approach for studying opioid receptor pharmacology and function, through which we have elucidated vital information regarding the function of monomeric MOR. Several different ways in which a MOR-DOR dimer could exhibit unique pharmacology have been outlined in this thesis, and reconstitution of active heterodimers can begin to address the molecular basis of altered ligand binding, G protein activation, GRK phosphorylation, and arrestin interactions. To this end, our laboratory has made significant progress in modifying the HDL reconstitution methodology to directly compare GPCR monomers to dimers. To allow for incorporation of two GPCRs the inner diameter of HDL particles has been increased by engineering apoA-1 with repeated helical domains. More importantly we have been able to develop a strategy for maintaining a parallel GPCR dimer orientation during the reconstitution process, in which two receptors are held together by interacting fusion proteins or by bivalent ligands, although further optimization of this approach is under development as the final yield of GPCR dimers compared to monomers is low.

Just as the work presented here required a new strategy for MOR purification, heterodimer reconstitution would require purification of DOR in appropriately high

yields. To this end, baculoviruses for both YFP- and CFP-tagged DOR constructs have been created in a similar fashion to YMOR. High Five<sup>TM</sup> cells expressed YDOR

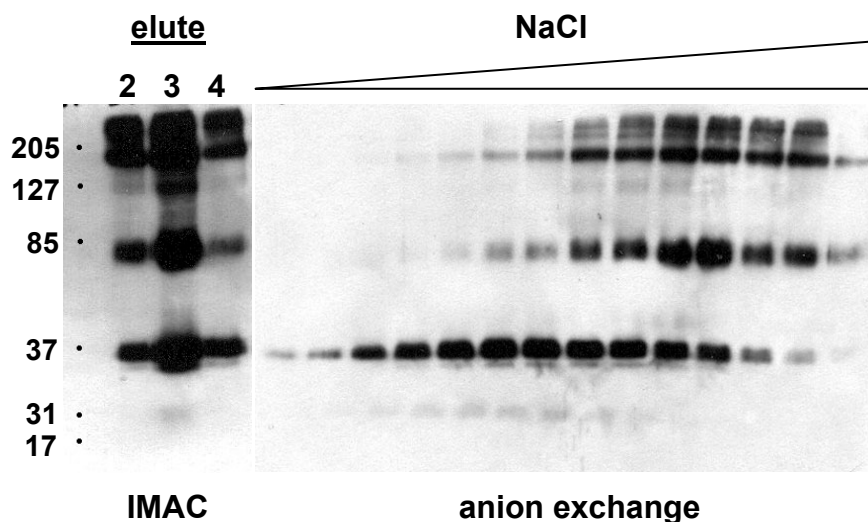


**Figure 5-2.** Anti-FLAG Western Blot analysis of YDOR enrichment. YDOR was expressed in High Five<sup>TM</sup> cells and extracted from membranes with 1% n-dodecyl- $\beta$ -D-maltoside and 0.1% cholesteryl hemissuccinate. The soluble fraction was enriched for His<sub>10</sub> tagged protein with a Talon<sup>TM</sup> immobilized metal affinity column followed by strong anion exchange chromatography. Column fractions were resolved with SDS-PAGE and YDOR content was determined by anti-FLAG Western Blot. Although full-length YDOR (~70 kDa) can be observed, the majority of FLAG reactivity corresponded to proteolysis products.

at relatively high amounts, approximately 15 pmol/mg of membrane protein and bound

[<sup>3</sup>H]diprenorphine with high affinity. Preliminary efforts have been made to purify

YDOR from High Five<sup>TM</sup> cells with the same strategy employed for YMOR.

Unfortunately, YDOR is apparently more susceptible to proteolysis during the

purification, as evidence by anti-FLAG Western Blot analysis of the Talon<sup>TM</sup> metal

affinity column and anion exchange column fractions (Figure 5-2). A significant

proportion of the enriched sample appeared to be a proteolysis product of ~36 kDa. This

may correspond to the N-terminal FLAG and His<sub>10</sub> tags plus the YFP fusion protein and approximately 80 residues of DOR. Unlike the proteolysis seen with YMOR, this amount of proteolysis for YDOR is high enough to prevent effective purification. Therefore future efforts to optimize preparation of mono-dispersed YDOR will be required before reconstitution attempts can be made.

Despite these technical hurdles, every effort should be made to accomplish the co-reconstitution of opioid receptor homo- and heterodimers. The growing push towards pharmacological manipulation of opioid receptor oligomers for therapeutic intervention emphasizes the absolute need for a better understanding of opioid receptor oligomerization. Only with a clear knowledge of the functional similarities and differences between opioid receptor monomers and oligomers can truly rational drug design be achieved. The work presented here not only illustrates that the requisite dimer theory of opioid receptor function must be re-evaluated, but has also lays the groundwork for directly assessing opioid receptor heterodimer function.

## APPENDIX A

As a means to further study agonist binding to monomeric YMOR, this appendix describes a novel method for imaging the binding of peptide-opiate ligands using single molecule total internal reflection fluorescence microscopy (198). Binding of a Cy3-labeled  $\mu$ -specific agonist, [Lys<sup>7</sup>, Cys<sup>8</sup>]dermorphin, was successfully visualized and confirmed to be dependent upon G protein coupling. Moreover, a 1:1 ligand to receptor binding ratio was observed. This unique approach to visualizing ligand binding is being developed further to expand our understanding GPCR oligomerization and organization in live cells.

### Results

#### Single particle visualization of agonist binding to rHDL•YMOR

The  $\mu$ -specific opioid [Lys<sup>7</sup>, Cys<sup>8</sup>]dermorphin (194, 199) was used as an agonist probe to visualize binding to monomeric YMOR in HDL at the single molecule level with total internal reflection (SM-TIRF) microscopy. [Lys<sup>7</sup>, Cys<sup>8</sup>]dermorphin was labeled with Cy3 fluorophore (Figure A-1 and A-2). [Lys<sup>7</sup>, Cys<sup>8</sup>]dermorphin-Cy3's ability to bind reconstituted YMOR+G<sub>i2</sub> with high affinity ( $K_i \sim 3.3$  nM) and stimulate G $\alpha_{i2}$  ( $EC_{50} = 32 \pm 9.1$  nM) was confirmed in [<sup>3</sup>H]DPN competition and [<sup>35</sup>S]GTP $\gamma$ S binding assays (Figure A-3). YMOR was reconstituted with biotinylated  $\Delta(1-43)$ -His<sub>6</sub>-apoA-1, enriched

on a FLAG affinity column, and added to G<sub>i2</sub> heterotrimer at a 30:1 G<sub>i2</sub>:YMOR molar ratio to ensure complete receptor coupling to G protein. This rHDL•YMOR+G<sub>i2</sub> sample was then incubated with a saturating concentration (500 nM) of [Lys<sup>7</sup>, Cys<sup>8</sup>]dermorphin-Cy3 for 45 min at 25°C prior to imaging with SM-TIRF. Fifty or one hundred picomolar rHDL or rHDL•YMOR+G<sub>i2</sub> (Figure A-4a, b) samples were continuously excited at 532 nm and fluorescence intensity traces (Figure A-4c) were analyzed for step photobleaching. Approximately 95% of the rHDL•YMOR+G<sub>i2</sub> fluorescence traces exhibited single-step photobleaching, suggesting that a single [Lys<sup>7</sup>, Cys<sup>8</sup>]dermorphin-Cy3 was localized within each fluorescent spot (Figure A-4d). Considering the rHDL particles contain a single receptor (Chapter 3), these photobleaching data indicates that only one dermorphin bound per receptor.

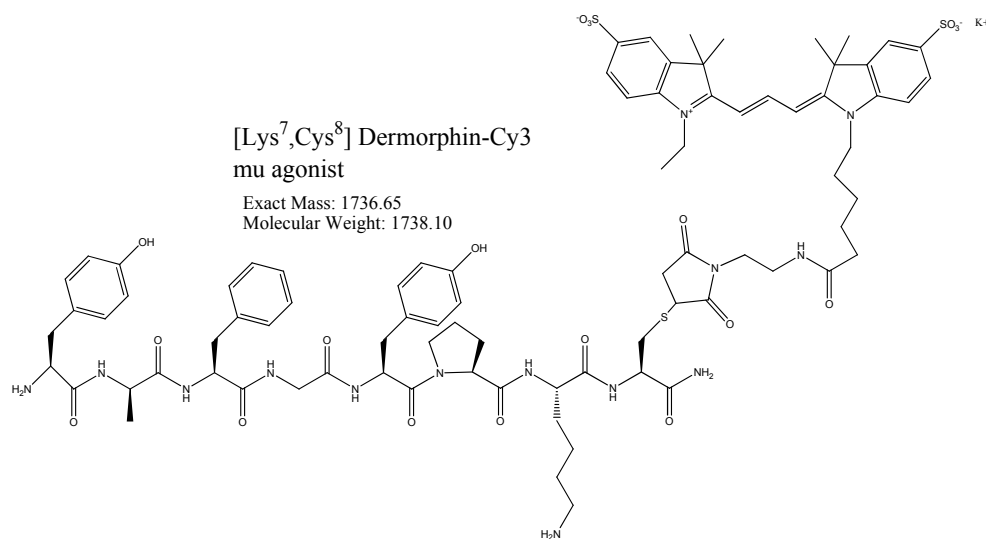


**Figure A-1.** [Lys<sup>7</sup>, Cys<sup>8</sup>]dermorphin-Cy3 structure. The  $\mu$ -opioid specific agonist dermorphin (NH<sub>2</sub>-Tyr-D-Ala-Phe-Gly-Tyr-Pro-CONH<sub>2</sub>) was synthesized with carboxyl lysine and cysteine extensions. Cy3 fluorescent dye was then added to the terminal cysteine via maleimide conjugation.



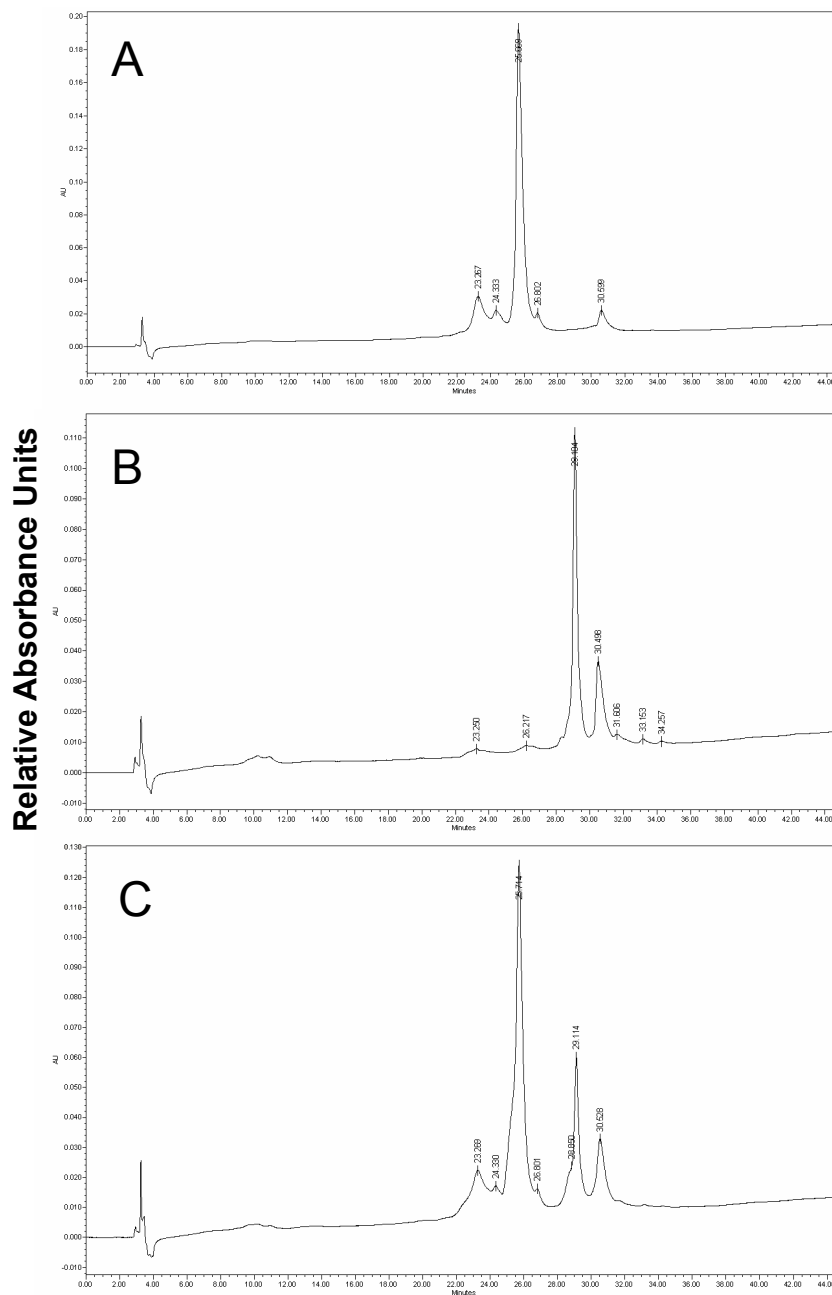


**Figure A-2.** [Lys<sup>7</sup>, Cys<sup>8</sup>]dermorphin-Cy3 preparation. [Lys<sup>7</sup>, Cys<sup>8</sup>]dermorphin was synthesized on Rink resin using an Applied Biosystems Peptide Synthesizer and Fmoc chemistry. Samples were resolved on a Waters reverse phase HPLC using a Vydac C18 10 micron column, run on a linear gradient of 0 to 45% acetonitrile containing 0.1% TFA in an aqueous phase containing 0.1% TFA at 35°C. Samples were monitored at 254 nm. [Lys<sup>7</sup>, Cys<sup>8</sup>]dermorphin (**A**) has a retention time of 25.9 min and was determined to be 98% pure before labeling. [Lys<sup>7</sup>, Cys<sup>8</sup>]dermorphin was labeled with Cy3-maleimide dye (GE Healthcare) at a ratio of 1.5:1 peptide:fluorophore. [Lys<sup>7</sup>, Cys<sup>8</sup>]dermorphin-Cy3 (**B**) has a retention time of 29.2 min and was determined to be 91.4% pure before use in binding assays and imaging experiments. A mixture and co-elution profile (**C**) shows that the two compounds are well separated. Peptide synthesis was performed by Jessica Anand (University of Michigan, Department of Medicinal Chemistry).

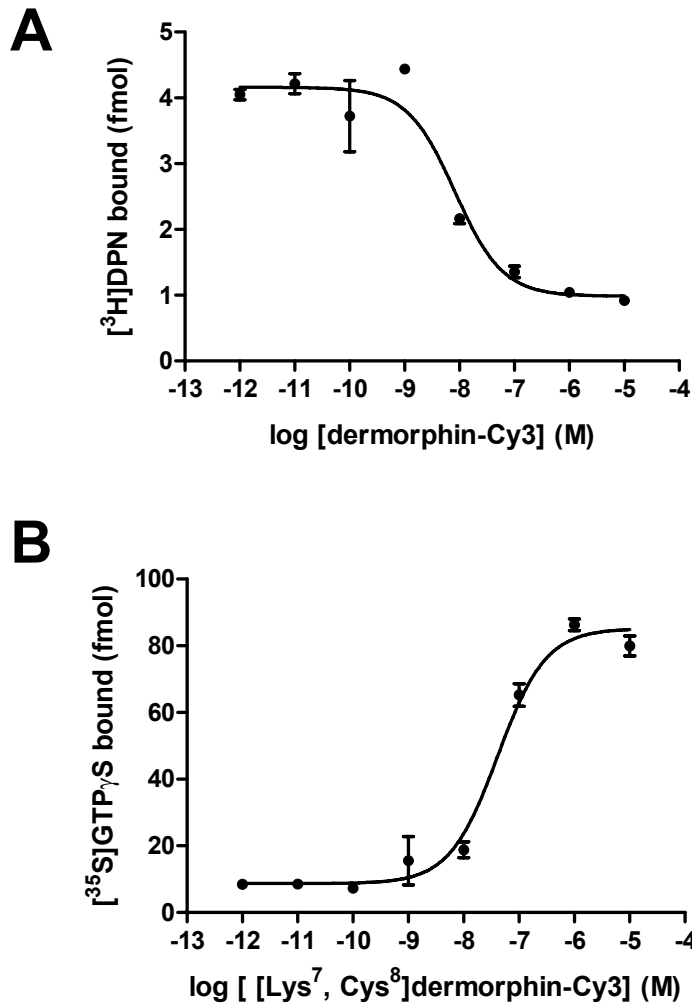


**Figure A-3.**  $[\text{Lys}^7, \text{Cys}^8]$ dermorphin-Cy3 retains agonist properties. Reconstituted HDL•YMOR was coupled to  $G_{i2}$  at a 30:1 molar ratio to ensure all YMOR was coupled to heterotrimer. **(A)** Binding of 0.75 nM  $[\text{H}]$ DPN to rHDL•YMOR+ $G_{i2}$  was competed with increasing concentrations of  $[\text{Lys}^7, \text{Cys}^8]$ dermorphin-Cy3. Binding data were fit to a one-site competition,  $K_i = 3.3 \pm 1.4$  nM. **(B)** Dose-response of  $[\text{S}]$ GTP $\gamma$ S binding to  $G_{\alpha_{i2}}$  coupled monomeric YMOR. An estimated 60 fmoles of reconstituted YMOR+ $G_{i2}$  were incubated with 100 nM  $[\text{S}]$ GTP $\gamma$ S in Tris•HCl, pH 7.4, 100 mM NaCl, 5 mM  $\text{MgCl}_2$ , 1  $\mu\text{M}$  GDP for 1 hr.  $[\text{Lys}^7, \text{Cys}^8]$ dermorphin-Cy3 stimulated  $[\text{S}]$ GTP $\gamma$ S binding with an  $\text{EC}_{50}$  of  $41 \pm 1.3$  nM. Data are representative of two independent experiments performed in replicate. Error bars represent the SEM. Experiments were performed by Jessica Anand (University of Michigan, Department of Medicinal Chemistry).

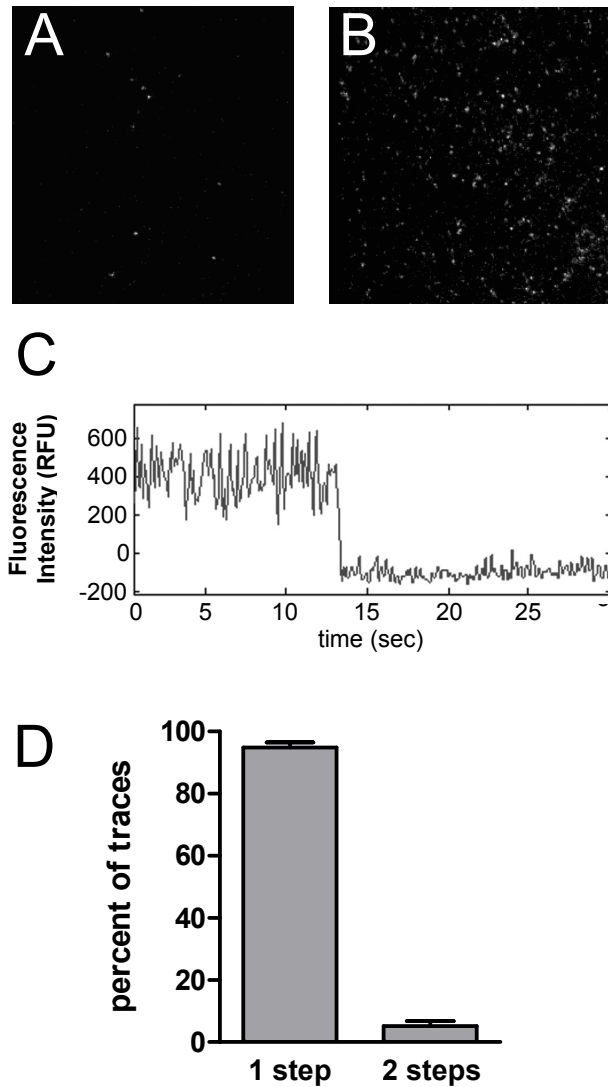


**Figure A-4.** Single molecule imaging of Cy3-labeled agonist binding to rHDL•YMOR coupled to  $G_{i2}$ . Binding of [Lys<sup>7</sup>, Cys<sup>8</sup>]dermorphin-Cy3, a fluorescently-labeled MOR-specific agonist, to rHDL•YMOR+ $G_{i2}$  was observed with SM-TIRF. YMOR was reconstituted into HDL particles using biotinylated apoA-1, followed by  $G_{i2}$  heterotrimer addition at a 30:1 G protein to receptor molar ratio. Reconstituted HDL (**A**) or rHDL•YMOR+ $G_{i2}$  (**B**) were then incubated with a saturating concentration (500 nM) of [Lys<sup>7</sup>, Cys<sup>8</sup>]dermorphin-Cy3, adhered to a streptavidin-coated quartz slide and washed with ice-cold 25 mM Tris•HCl, pH 7.7 buffer. Bound [Lys<sup>7</sup>, Cys<sup>8</sup>]dermorphin-Cy3 was continuously excited at 532 nm to observe photobleaching of the fluorophore. A representative fluorescence intensity trace for a one-step photobleach event is shown (**C**). (**D**) Quantification of photobleaching showed that approximately 95% of the bound [Lys<sup>7</sup>, Cys<sup>8</sup>]dermorphin-Cy3 bleached in a single step, suggesting that 95% of rHDL particles containing monomeric YMOR bind a single labeled agonist.

SM-TIRF analysis further showed the binding of [Lys<sup>7</sup>, Cys<sup>8</sup>]dermorphin-Cy3 to rHDL•YMOR+G<sub>i2</sub> was competitive and dependent upon G protein coupling. Samples were analyzed for step-photobleaching as before and total [Lys<sup>7</sup>, Cys<sup>8</sup>]dermorphin-Cy3 binding was measured as the combination of both one and two-step photobleaching traces. Binding of 500 nM [Lys<sup>7</sup>, Cys<sup>8</sup>]dermorphin-Cy3 to 50 pM rHDL•YMOR+G<sub>i2</sub> was reduced to levels approaching those seen in empty HDL particles when incubated in the presence of 5 μM naltrexone (Figure A-5a), indicating that the two ligands compete for the same binding site on YMOR.

Uncoupling of G<sub>i2</sub> from rHDL•YMOR also resulted in a loss of [Lys<sup>7</sup>, Cys<sup>8</sup>]dermorphin-Cy3 binding. One hundred picomolar rHDL•YMOR+G<sub>i2</sub> was incubated with 500 pM [Lys<sup>7</sup>, Cys<sup>8</sup>]dermorphin-Cy3 and total ligand binding was determined in three distinct slide regions. The sample was then treated with 10 μM GTPγS for 5 min and three different regions were analyzed for [Lys<sup>7</sup>, Cys<sup>8</sup>]dermorphin-Cy3 binding. Treatment with GTPγS completely eliminated [Lys<sup>7</sup>, Cys<sup>8</sup>]dermorphin-Cy3 binding, reducing the number of observed fluorescent signals to levels seen with empty rHDL particles (Figure A-5b). These data suggest that the binding of [Lys<sup>7</sup>, Cys<sup>8</sup>]dermorphin-Cy3, at the concentrations used here, is dependent upon G protein coupling.

## Discussion

In further efforts to characterize agonist behavior at YMOR, we used reconstitution into HDL as a platform for analysis of ligand binding using single molecule microscopy. In this study we examined the reversible binding of a μ-opioid receptor specific agonist [Lys<sup>7</sup>, Cys<sup>8</sup>]dermorphin-Cy3 with SM-TIRF. To the best of our

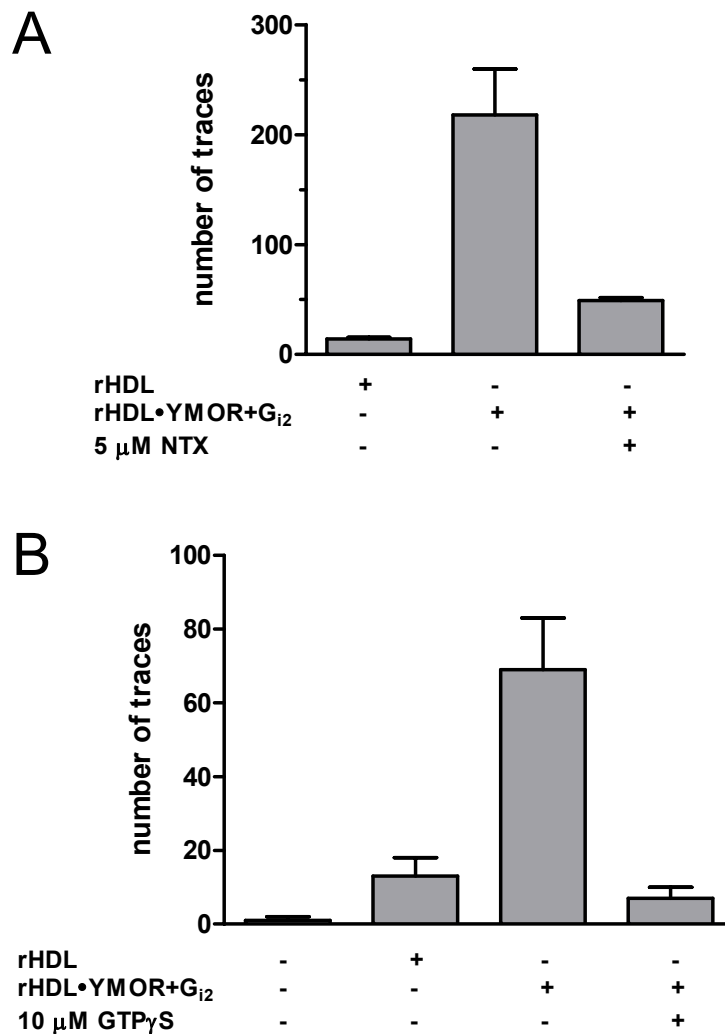


**Figure A-5.** Single molecule TIRF imaging of [Lys<sup>7</sup>, Cys<sup>8</sup>]dermorphin-Cy3 binding is competed by naltrexone and dependent on G protein coupling. Reconstituted HDL or rHDL•YMOR coupled to purified G<sub>i2</sub> heterotrimer (rHDL•YMOR+G<sub>i2</sub>) were incubated with [Lys<sup>7</sup>, Cys<sup>8</sup>]dermorphin-Cy3 for 45 min at 25°C in 25 mM Tris•HCl, pH 7.7. [Lys<sup>7</sup>, Cys<sup>8</sup>]dermorphin-Cy3 binding was measured as the total amount of one and two-step fluorescent photobleaching traces. At least three separate slide regions were analyzed for each condition. **(A)** 5 nM rHDL or rHDL•YMOR+G<sub>i2</sub> was incubated with 500 nM [Lys<sup>7</sup>, Cys<sup>8</sup>]dermorphin-Cy3 and diluted 100-fold prior to imaging. [Lys<sup>7</sup>, Cys<sup>8</sup>]dermorphin-Cy3 binding was significantly increased in reconstituted HDL samples containing YMOR+G<sub>i2</sub>. Addition of 5 μM NTX during the binding incubation ablated [Lys<sup>7</sup>, Cys<sup>8</sup>]dermorphin-Cy3 binding. **(B)** 100 nM rHDL or rHDL•YMOR+G<sub>i2</sub> was incubated with 500 nM [Lys<sup>7</sup>, Cys<sup>8</sup>]dermorphin-Cy3 and diluted 1,000-fold prior to imaging. [Lys<sup>7</sup>, Cys<sup>8</sup>]dermorphin-Cy3 binding to rHDL•YMOR+G<sub>i2</sub> particles was significantly decreased following a 5 min treatment with 10 μM GTPγS.

knowledge these data represent the first reported observation of a peptide agonist binding to an isolated GPCR in a lipid bilayer using single particle imaging. These imaging methods are currently being refined to resolve the kinetics of ligand binding to Y<sub>MOR</sub>. In addition, instrumentation is under development that will allow for visualizing ligand binding to opioid receptors in intact cells. Peptide receptors such as the opioid family are particularly amenable to fluorescence spectroscopy since the relatively large ligand size can tolerate the incorporation of fluorophores without drastically impairing binding affinities (194, 195). Additionally, bivalent ligands have been developed which are proposed to specifically bind opioid receptor oligomers (193, 196). This single molecule visual approach of studying ligand binding to opioid receptors, utilizing such bivalent labeled agonists and antagonists with unique binding affinities towards receptor homo- and heterodimers, may potentially address opioid receptor oligomerization in physiologically relevant tissue preparations.

## **Materials and Methods**

### **Materials**

Cy3-maleimide reactive dye was from GE Healthcare (Piscataway, NJ). Amino acids for peptide synthesis were from Advanced ChemTech (Louisville, KY) or Sigma-Alrich.

### **Synthesis of [Lys<sup>7</sup>, Cys<sup>8</sup>]dermorphin and labeling with Cy3 dye**

[Lys<sup>7</sup>, Cys<sup>8</sup>]dermorphin (Tyr-D-Ala-Phe-Gly-Tyr-Pro-Lys-Cys-NH<sub>2</sub>) was synthesized on Rink resin (solid support) using an Applied Biosystems 431A Peptide

Synthesizer and standard Fmoc chemistry. Samples were characterized on a Waters reverse phase HPLC using a Vydac C18 (Protein and Peptide) 10 micron column. Samples were run on a linear gradient of 0 to 45% acetonitrile in an aqueous phase containing 0.1% TFA at 35°C. Samples were monitored at 254 and 230 nm (Appendix Figure A-2). Peptides were similarly purified on a Waters semi-preparative RP-HPLC using a Vydac C18 10 micron column at room temperature. The purified peptide was labeled with Cy3-maleimide (GE Healthcare) according to the manufacturer's instructions using a ratio of 1.5:1 peptide to fluorophore and repurified by HPLC as before. The labeled peptide was further purified via semi-preparative HPCL using a 5 micron Vydac C18 column as described above. The potency and efficacy of [Lys<sup>7</sup>, Cys<sup>8</sup>]dermorphin-Cy3 at MOR were confirmed in radiolabeled [<sup>3</sup>H]DPN competition and [<sup>35</sup>S]GTPγS binding assays.

### **Prism-based Single Molecule TIRF and Step-Photobleaching analysis of [Lys<sup>7</sup>, Cys<sup>8</sup>]dermorphin-Cy3 binding to rHDL-YMOR+G<sub>i2</sub>**

Purified recombinant apoA-1 was biotinylated at a 3:1 molar ratio of biotin:apoA-1. Purified YMOR was then reconstituted with biotin-apoA-1, POPC, POPG, and brain lipid extract as above. Purified Gi<sub>2</sub> heterotrimer was added to reconstituted receptor and coupling was confirmed by observing high affinity competition of [<sup>3</sup>H]DPN binding by the agonist DAMGO. Five nanomolar biotin-rHDL-YMOR+G<sub>i2</sub> was then incubated with 5 μM [Lys<sup>7</sup>, Cys<sup>8</sup>]dermorphin-Cy3 for 45 min at 25°C in 25 mM Tris•HCl, pH 7.7. Samples were diluted 100- or 1000-fold in 25 mM Tris•HCl pH 7.7 and immediately injected into a microfluidic channel on a quartz slide, previously coated with

biotinylated-PEG and treated with 0.2 mg/mL streptavidin to generate a surface density of  $\sim 0.25$  molecules per  $\mu\text{m}^2$ . An oxygen scavenging system (OSS) of 10 mM trolox, 100 mM protocatechuic acid and 1  $\mu\text{M}$  protocatechuate-3,4-dioxygenase was included in the sample dilution (146). Following a 10 min incubation to allow binding of the biotin-rHDL•Cy-YMOR complex to the streptavidin coated slide, the channel was washed with ice cold 25 mM Tris•HCl pH 7.7 containing the OSS. An Olympus IX71 inverted microscope configured for prism-based total internal reflection fluorescence (TIRF) and coupled to an intensified CCD camera was used to image Cy3 and Cy5 fluorophores (CrystaLaser - 532 nm, Coherent CUBE laser - 638 nm, Chroma bandpass filters HQ580/60 and HQ710/130 nm). Fluorophore intensity time traces were collected for 30 to 100 s at 10 frames per s. Time traces were analyzed for photobleaching with MatLab 7.0 software.



## APPENDIX B

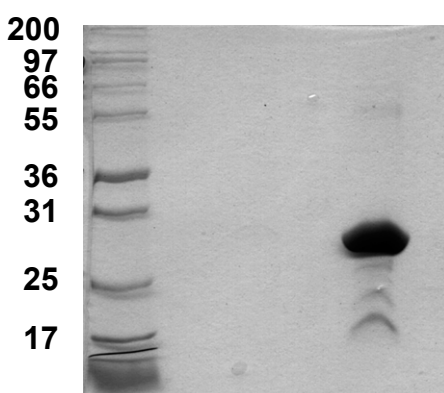


**Figure B-1.** Analysis of  $\Delta(1-43)\text{His}_6\text{-apoA-1}$  purification. *Escherichia coli* cells were transformed with a pET15b plasmid encoding an N-terminal truncated, His<sub>6</sub>-tagged apolipoproteinA-1. This construct was enriched on Ni-NTA gravity flow column and purified by size exclusion chromatography. After concentrating to  $\sim 9.7$  mg/mL, an estimated 19  $\mu\text{g}$  of total protein was resolved on SDS-PAGE and visualized with Coomassie stain.  $\Delta(1-43)\text{-His}_6\text{-ApoA-1}$  was prepared to approximately 85-90% purity and runs at the expected size of  $\sim 28.5$  kDa. Both higher weight contaminants and lower weight degradation products/contaminants are observed at the protein amount loaded here.

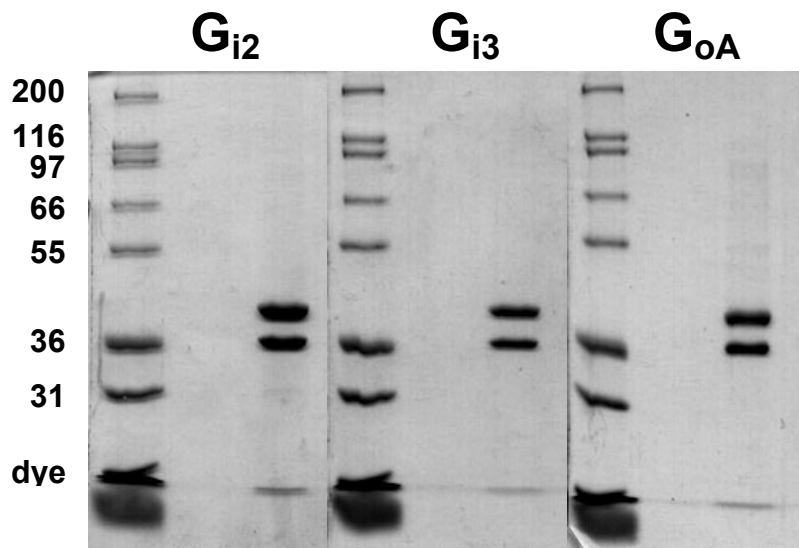


**Figure B-2.** Analysis of  $G_{i2}$ ,  $G_{i3}$ , and  $G_{oA}$  heterotrimer purifications. G protein heterotrimers were expressed in *Spodoptera frugiperda Sf9* insect cells via infection with three baculoviruses encoding the individual subunits. Heterotrimers were purified according to the method of Kozasa (147). Final purified samples were resolved on SDS-PAGE and visualized with Coomassie staining. Each subunit appeared at the expected molecular weight:  $G\alpha$  ~40 kDa, His<sub>6</sub>-Gβ<sub>1</sub> ~37 kDa,  $G\gamma_2$  ~7 kDa (unresolved and weakly stained in the dye front).

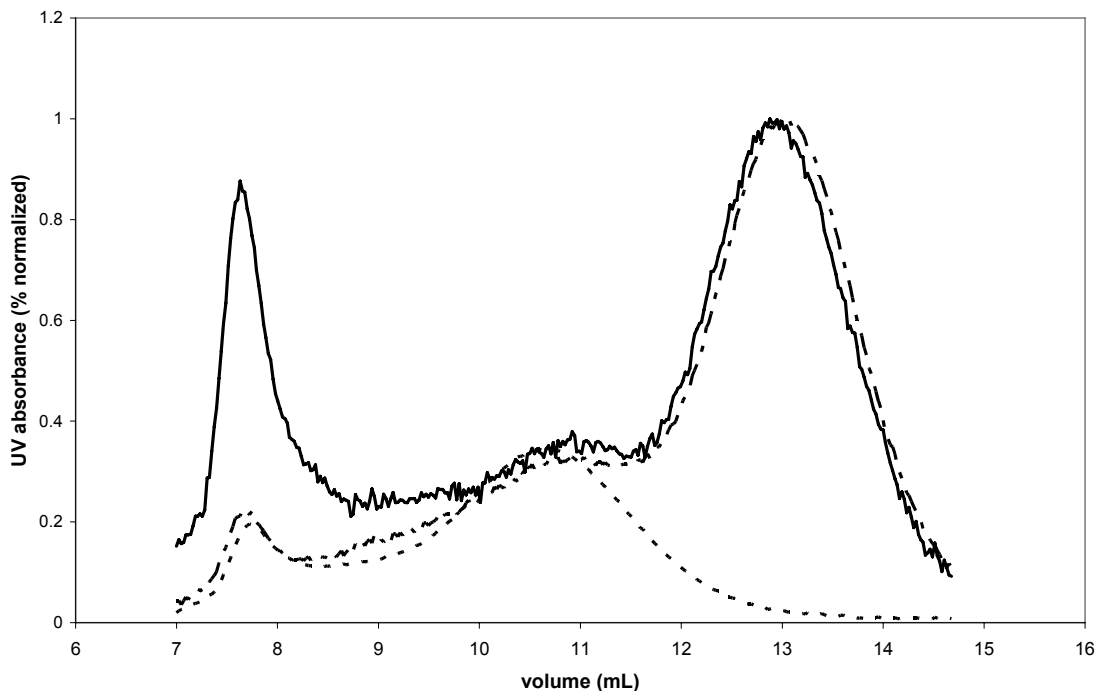


**Figure B-3.** Size exclusion chromatography resolution of rHDL•YMOR particles. Purified YMOR was reconstituted into HDL particles as described in Chapter 3. A sample of this rHDL•YMOR sample was resolved by size exclusion chromatography (SEC), represented by the dotted line. The main HDL particle peak elutes off the column at approximately 10.8 mL. A void volume peak of protein aggregate is also present at ~7.7 mL. The remainder of the rHDL•YMOR sample was then enriched on a FLAG affinity column. The enrichment was performed in the presence of 0.1% BSA to decrease non-specific protein binding of the rHDL•YMOR. When the FLAG enriched sample was separated by SEC (dashed line) a peak corresponding to BSA (~13 mL) was readily identified along with the same rHDL•YMOR and protein aggregate peaks. Purified G<sub>12</sub> protein heterotrimers were then added to the FLAG enriched rHDL•YMOR sample at a 10:1 G protein to receptor molar ratio. Detergent removal by Bio-Beads™ (Bio-Rad) incubation promoted coupling of G proteins to YMOR in the HDL lipid bilayer. When this rHDL•YMOR+G<sub>12</sub> sample was resolved on SEC (solid line) the profile was identical to the FLAG enrichment with the exception of a void volume protein aggregate. This aggregate likely corresponds to the G protein heterotrimer which precipitated during detergent removal (Chapter 4 and Whorton *et al.* (78)).

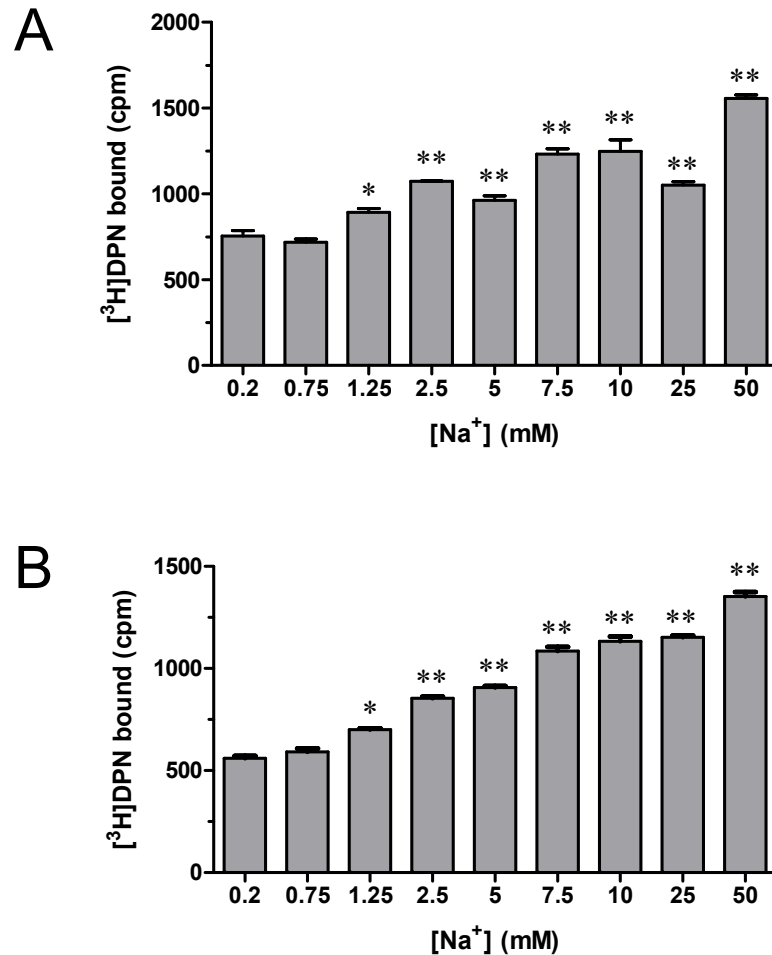
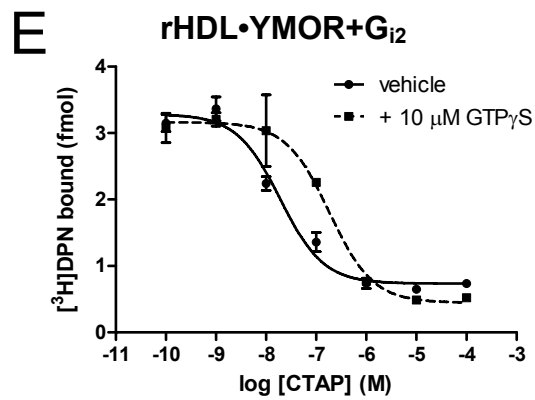
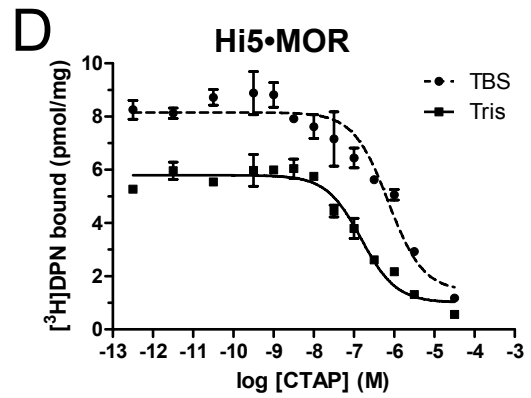
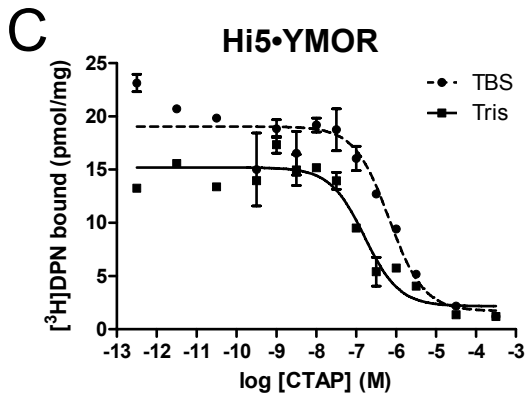
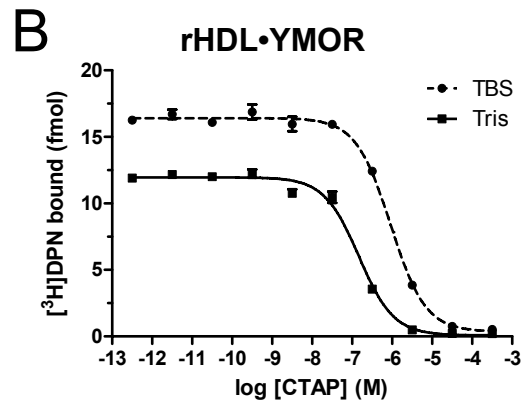
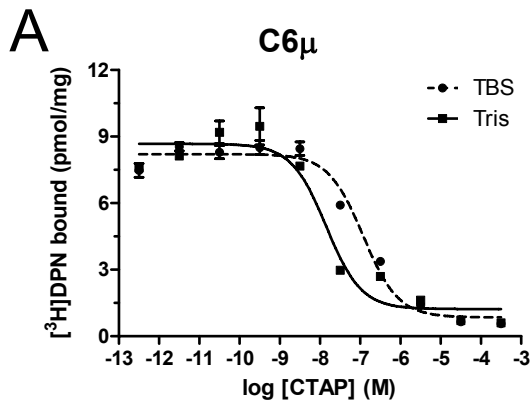


**Figure B-4.** Na<sup>+</sup> ions modulate [<sup>3</sup>H]DPN binding to monomeric YMOR. Binding of 0.75 nM [<sup>3</sup>H]DPN to rHDL•YMOR+G<sub>oA</sub> particles was determined in the presence of increasing concentrations of NaCl. [<sup>3</sup>H]DPN binding increased nearly two-fold as NaCl increased from 0.2 mM to 50 mM both in the absence (**A**) and presence (**B**) of 10 μM GTPγS. This ability of Na<sup>+</sup> ions to potentiate the binding of antagonists to MOR has been well established in several cellular systems (37-39, 44, 200). These results in the HDL reconstituted YMOR samples indicate that the receptor is effected by Na<sup>+</sup> in an appropriate manner, and also suggest that Na<sup>+</sup> effects the receptor monomer directly, as opposed to modulating oligomers in some fashion. \*P<0.05, \*\*P<0.01, significantly different from 0.2 mM Na<sup>+</sup> as calculated by a Student's t-test.

**Figure B-5.** Allosteric regulation of CTAP binding to YMOR. CTAP (D-Phe-Cys-Tyr-D-Trp-Arg-Thr-Pen-Thr-NH<sub>2</sub>) is a peptide ligand which is highly selective for MOR (201) and behaves as a surmountable antagonist in assays measuring analgesia in mice (202). The observation of lower than expected affinities for CTAP binding to YMOR when in a TBS solution containing 136 mM Na<sup>+</sup> (Figure 3-7) prompted further analysis of its ability to compete [<sup>3</sup>H]DPN binding. **(A)** CTAP competes [<sup>3</sup>H]DPN binding with a K<sub>i</sub> of ~7 nM in membranes of C6 glioma cells which stably express MOR (C6μ). The binding of CTAP is influenced by sodium, as performing the assay in TBS solution increases the K<sub>i</sub> to ~60 nM. Further competition assays thus compared the K<sub>i</sub> of CTAP in 25 mM Tris•HCl, pH 7.7 buffer versus TBS, pH 7.7 (25 mM Tris•HCl, 136 mM NaCl, 2.7 mM KCl). **(B and C)** While performing the assays in Tris did indeed reveal a higher affinity for CTAP binding to HDL reconstituted YMOR (rHDL•YMOR) and High Five<sup>TM</sup> membranes containing YMOR (Hi5•YMOR), it was still substantially lower than the affinity observed in C6μ cells. **(D)** The YFP fusion protein may interfere with CTAP binding, and this was tested by repeating the competitions in High Five<sup>TM</sup> membranes expressing MOR without the YFP (but retaining the FLAG and His<sub>10</sub> tags). As can be seen, the N-terminal YFP was not the cause of the low affinity for CTAP, as it bound MOR in an identical fashion to YMOR in the absence and presence of sodium. Another potential difference between MOR in C6μ cells and YMOR in High Five<sup>TM</sup> cells or rHDL was the presence of G proteins. Presumably, MOR in C6μ membranes is coupled to endogenous G<sub>i/o</sub> heterotrimers. We have observed that the endogenous G proteins of High Five<sup>TM</sup> cells do not effectively couple the over-expressed YMOR and the rHDL•YMOR used in the previous experiments did not include G proteins. Therefore the affinity of CTAP was determined on rHDL•YMOR samples which were coupled to purified G<sub>i2</sub> heterotrimer in Tris buffer **(E)**. Strikingly, the presence of G<sub>i2</sub> revealed a ~9 nM K<sub>i</sub> for CTAP, well in line with the ~7 nM K<sub>i</sub> seen in C6μ membranes. Uncoupling of G<sub>i2</sub> with 10 μM GTPγS resulted in a K<sub>i</sub> to ~92 nM for CTAP, very similar to what was seen for rHDL•YMOR. All binding data were fit to a one-site competition curve using Prism 5.0 software (GraphPad). Experiments were performed in duplicate and error bars represent the SEM. The higher amount of [<sup>3</sup>H]DPN binding seen in TBS is due to the Na<sup>+</sup> effect described in Figure B-4. These data suggest that CTAP binding to MOR is allosterically regulated by both Na<sup>+</sup> ions and G proteins in a similar fashion to MOR agonists, and echo recent reports of G protein coupling to MOR influencing CTAP binding in transfected CHO cells (203) and C6μ glioma cells (204).



CTAP K <sub>i</sub> values (nM) against [ <sup>3</sup> H]DPN		
	TBS	Tris
C6 $\mu$	60	7.2
rHDL•YMOR	307	50
Hi5•YMOR	335	81
Hi5•MOR	360	76
	Tris	
	Vehicle	+GTP $\gamma$ S
rHDL•YMOR+G <sub>12</sub>	9.5	92

## References

1. Gutstein, H. and Akil, H. (2006) Opioid Analgesics. In: L. L. Brunton, Lazo, J.S., and Parker, K.L. (ed). *The Pharmacological Basis of Therapeutics*, 11 Ed., McGraw-Hill, New York
2. Trescot, A. M., Datta, S., Lee, M. and Hansen, H. (2008) *Opioid pharmacology*. Pain Physician **11**(2 Suppl), S133-53
3. Pert, C. B. and Snyder, S. H. (1973) *Opiate receptor: demonstration in nervous tissue*. Science **179**(77), 1011-4
4. Simon, E. J., Hiller, J. M. and Edelman, I. (1973) *Stereospecific Binding of Potent Narcotic Analgesic [H-3]Etorphine to Rat-Brain Homogenate*. Proceedings of the National Academy of Sciences of the United States of America **70**(7), 1947-1949
5. Terenius, L. (1973) *Stereospecific Interaction between Narcotic Analgesics and a Synaptic Plasma-Membrane Fraction of Rat Cerebral-Cortex*. Acta Pharmacologica Et Toxicologica **32**(3-4), 317-320
6. Akil, H., Watson, S. J., Young, E., Lewis, M. E., Khachaturian, H. and Walker, J. M. (1984) *Endogenous Opioids - Biology and Function*. Annual Review of Neuroscience **7**, 223-255
7. Martin, W. R., Eades, C. G., Thompson, J. A., Huppler, R. E. and Gilbert, P. E. (1976) *The effects of morphine- and nalorphine- like drugs in the nondependent and morphine-dependent chronic spinal dog*. J Pharmacol Exp Ther **197**(3), 517-32
8. Chen, Y., Mestek, A., Liu, J., Hurley, J. A. and Yu, L. (1993) *Molecular-Cloning and Functional Expression of a Mu-Opioid Receptor from Rat-Brain*. Molecular Pharmacology **44**(1), 8-12
9. Kieffer, B. L., Befort, K., Gaveriauxruff, C. and Hirth, C. G. (1992) *The Delta-Opioid Receptor - Isolation of a Cdna by Expression Cloning and Pharmacological Characterization*. Proceedings of the National Academy of Sciences of the United States of America **89**(24), 12048-12052
10. Evans, C. J., Keith, D. E., Morrison, H., Magendzo, K. and Edwards, R. H. (1992) *Cloning of a Delta Opioid Receptor by Functional Expression*. Science **258**(5090), 1952-1955
11. Yasuda, K., Raynor, K., Kong, H., Breder, C. D., Takeda, J., Reisine, T. and Bell, G. I. (1993) *Cloning and Functional Comparison of Kappa-Opioid and Delta-*

*Opioid Receptors from Mouse-Brain*. Proceedings of the National Academy of Sciences of the United States of America **90**(14), 6736-6740

12. Bunzow, J. R., Saez, C., Mortrud, M., Bouvier, C., Williams, J. T., Low, M. and Grandy, D. K. (1994) *Molecular cloning and tissue distribution of a putative member of the rat opioid receptor gene family that is not a mu, delta or kappa opioid receptor type*. FEBS Lett **347**(2-3), 284-8
13. Jordan, B. A., Cvejic, S. and Devi, L. A. (2000) *Opioids and their complicated receptor complexes*. Neuropsychopharmacology **23**(4 Suppl), S5-S18
14. Wolozin, B. L. and Pasternak, G. W. (1981) *Classification of multiple morphine and enkephalin binding sites in the central nervous system*. Proc Natl Acad Sci U S A **78**(10), 6181-5
15. Pasternak, G. W. and Wood, P. J. (1986) *Multiple mu opiate receptors*. Life Sci **38**(21), 1889-98
16. Traynor, J. (1989) *Subtypes of the kappa-opioid receptor: fact or fiction?* Trends Pharmacol Sci **10**(2), 52-3
17. Rodbell, M., Krans, H. M., Pohl, S. L. and Birnbaumer, L. (1971) *The glucagon-sensitive adenylyl cyclase system in plasma membranes of rat liver. IV. Effects of guanylnucleotides on binding of 125I-glucagon*. J Biol Chem **246**(6), 1872-6
18. Gilman, A. G. (1987) *G-Proteins - Transducers of Receptor-Generated Signals*. Annual Review of Biochemistry **56**, 615-649
19. Johnston, C. A. and Siderovski, D. P. (2007) *Receptor-mediated activation of heterotrimeric G-proteins: current structural insights*. Mol Pharmacol **72**(2), 219-30
20. Meng, F., Ueda, Y., Hoversten, M. T., Thompson, R. C., Taylor, L., Watson, S. J. and Akil, H. (1996) *Mapping the receptor domains critical for the binding selectivity of delta-opioid receptor ligands*. Eur J Pharmacol **311**(2-3), 285-92
21. DeWire, S. M., Ahn, S., Lefkowitz, R. J. and Shenoy, S. K. (2007) *Beta-arrestins and cell signaling*. Annu Rev Physiol **69**, 483-510
22. Mervine, S. M., Yost, E. A., Sabo, J. L., Hynes, T. R. and Berlot, C. H. (2006) *Analysis of G protein betagamma dimer formation in live cells using multicolor bimolecular fluorescence complementation demonstrates preferences of beta1 for particular gamma subunits*. Mol Pharmacol **70**(1), 194-205
23. Simon, M. I., Strathmann, M. P. and Gautam, N. (1991) *Diversity of G-Proteins in Signal Transduction*. Science **252**(5007), 802-808



24. Sprang, S. R. (1997) *G protein mechanisms: insights from structural analysis*. *Annu Rev Biochem* **66**, 639-78
25. Tesmer, J. J., Sunahara, R. K., Gilman, A. G. and Sprang, S. R. (1997) *Crystal structure of the catalytic domains of adenylyl cyclase in a complex with G $\alpha$ .GTP $\gamma$ S*. *Science* **278**(5345), 1907-16
26. Sunahara, R. K., Tesmer, J. J., Gilman, A. G. and Sprang, S. R. (1997) *Crystal structure of the adenylyl cyclase activator G $\alpha$* . *Science* **278**(5345), 1943-7
27. Sharma, S. K., Klee, W. A. and Nirenberg, M. (1977) *Opiate-dependent modulation of adenylyl cyclase*. *Proc Natl Acad Sci U S A* **74**(8), 3365-9
28. Watts, V. J. and Neve, K. A. (2005) *Sensitization of adenylyl cyclase by G $\alpha$  i/o-coupled receptors*. *Pharmacol Ther* **106**(3), 405-21
29. Hescheler, J., Rosenthal, W., Trautwein, W. and Schultz, G. (1987) *The GTP-binding protein, Go, regulates neuronal calcium channels*. *Nature* **325**(6103), 445-7
30. North, R. A., Williams, J. T., Surprenant, A. and Christie, M. J. (1987) *Mu and delta receptors belong to a family of receptors that are coupled to potassium channels*. *Proc Natl Acad Sci U S A* **84**(15), 5487-91
31. Ikeda, S. R. (1996) *Voltage-dependent modulation of N-type calcium channels by G-protein beta gamma subunits*. *Nature* **380**(6571), 255-258
32. Valenzuela, D., Han, X., Mende, U., Fankhauser, C., Mashimo, H., Huang, P., Pfeiffer, J., Neer, E. J. and Fishman, M. C. (1997) *G alpha(o) is necessary for muscarinic regulation of Ca<sup>2+</sup> channels in mouse heart*. *Proc Natl Acad Sci U S A* **94**(5), 1727-32
33. Law, P. Y., Wong, Y. H. and Loh, H. H. (2000) *Molecular mechanisms and regulation of opioid receptor signaling*. *Annu Rev Pharmacol Toxicol* **40**, 389-430
34. Gaibelet, G., Meilhoc, E., Riond, J., Saves, I., Exner, T., Liaubet, L., Nurnberg, B., Masson, J. M. and Emorine, L. J. (1999) *Nonselective coupling of the human mu-opioid receptor to multiple inhibitory G-protein isoforms*. *Eur J Biochem* **261**(2), 517-23
35. Pineyro, G. and Archer-Lahlou, E. (2007) *Ligand-specific receptor states: implications for opiate receptor signalling and regulation*. *Cell Signal* **19**(1), 8-19

36. May, L. T., Leach, K., Sexton, P. M. and Christopoulos, A. (2007) *Allosteric modulation of G protein-coupled receptors*. *Annu Rev Pharmacol Toxicol* **47**, 1-51
37. Blume, A. J., Lichtshtein, D. and Boone, G. (1979) *Coupling of opiate receptors to adenylate cyclase: requirement for Na<sup>+</sup> and GTP*. *Proc Natl Acad Sci U S A* **76**(11), 5626-30
38. Pfeiffer, A., Sadee, W. and Herz, A. (1982) *Differential regulation of the mu-, delta-, and kappa-opiate receptor subtypes by guanyl nucleotides and metal ions*. *J Neurosci* **2**(7), 912-7
39. Frances, B., Moisand, C. and Meunier, J. C. (1985) *Na<sup>+</sup> ions and Gpp(NH)p selectively inhibit agonist interactions at mu- and kappa-opioid receptor sites in rabbit and guinea-pig cerebellum membranes*. *Eur J Pharmacol* **117**(2), 223-32
40. Werling, L. L., Puttfarcken, P. S. and Cox, B. M. (1988) *Multiple agonist-affinity states of opioid receptors: regulation of binding by guanyl nucleotides in guinea pig cortical, NG108-15, and 7315c cell membranes*. *Mol Pharmacol* **33**(4), 423-31
41. Ott, S. and Costa, T. (1989) *Guanine nucleotide-mediated inhibition of opioid agonist binding. Modulatory effects of ions and of receptor occupancy*. *Biochem Pharmacol* **38**(12), 1931-9
42. Richardson, A., Demoliou-Mason, C. and Barnard, E. A. (1992) *Guanine nucleotide-binding protein-coupled and -uncoupled states of opioid receptors and their relevance to the determination of subtypes*. *Proc Natl Acad Sci U S A* **89**(21), 10198-202
43. Alves, I. D., Ciano, K. A., Boguslavski, V., Varga, E., Salamon, Z., Yamamura, H. I., Hruby, V. J. and Tollin, G. (2004) *Selectivity, cooperativity, and reciprocity in the interactions between the delta-opioid receptor, its ligands, and G-proteins*. *J Biol Chem* **279**(43), 44673-82
44. Pert, C. B. and Snyder, S. H. (1974) *Opiate Receptor-Binding of Agonists and Antagonists Affected Differentially by Sodium*. *Molecular Pharmacology* **10**(6), 868-879
45. Zajac, J. M. and Roques, B. P. (1985) *Differences in binding properties of mu and delta opioid receptor subtypes from rat brain: kinetic analysis and effects of ions and nucleotides*. *J Neurochem* **44**(5), 1605-14
46. Szucs, M., Spain, J. W., Oetting, G. M., Moudy, A. M. and Coscia, C. J. (1987) *Guanine nucleotide and cation regulation of mu, delta, and kappa opioid receptor*

- binding: evidence for differential postnatal development in rat brain.* J Neurochem **48**(4), 1165-70
47. Horstman, D. A., Brandon, S., Wilson, A. L., Guyer, C. A., Cragoe, E. J. and Limbird, L. E. (1990) *An Aspartate Conserved among G-Protein Receptors Confers Allosteric Regulation of Alpha-2-Adrenergic Receptors by Sodium.* Journal of Biological Chemistry **265**(35), 21590-21595
  48. Neve, K. A., Cox, B. A., Henningsen, R. A., Spanoyannis, A. and Neve, R. L. (1991) *Pivotal Role for Aspartate-80 in the Regulation of Dopamine-D2 Receptor Affinity for Drugs and Inhibition of Adenylyl Cyclase.* Molecular Pharmacology **39**(6), 733-739
  49. Warne, T., Serrano-Vega, M. J., Baker, J. G., Moukhametzianov, R., Edwards, P. C., Henderson, R., Leslie, A. G. W., Tate, C. G. and Schertler, G. F. X. (2008) *Structure of a beta(1)-adrenergic G-protein-coupled receptor.* Nature **454**(7203), 486-U2
  50. Heron, D., Israeli, M., Hershkowitz, M., Samuel, D. and Shinitzky, M. (1981) *Lipid-Induced Modulation of Opiate Receptors in Mouse-Brain Membranes.* European Journal of Pharmacology **72**(4), 361-364
  51. Lazar, D. F. and Medzihradsky, F. (1992) *Altered microviscosity at brain membrane surface induces distinct and reversible inhibition of opioid receptor binding.* J Neurochem **59**(4), 1233-40
  52. Emmerson, P. J., Clark, M. J., Medzihradsky, F. and Remmers, A. E. (1999) *Membrane microviscosity modulates mu-opioid receptor conformational transitions and agonist efficacy.* J Neurochem **73**(1), 289-300
  53. Hasegawa, J., Loh, H. H. and Lee, N. M. (1987) *Lipid requirement for mu opioid receptor binding.* J Neurochem **49**(4), 1007-12
  54. Remmers, A. E., Nordby, G. L. and Medzihradsky, F. (1990) *Modulation of opioid receptor binding by cis and trans fatty acids.* J Neurochem **55**(6), 1993-2000
  55. Pin, J. P., Kniazeff, J., Liu, J., Binet, V., Goudet, C., Rondard, P. and Prezeau, L. (2005) *Allosteric functioning of dimeric class C G-protein-coupled receptors.* Febs Journal **272**(12), 2947-2955
  56. Overton, M. C. and Blumer, K. J. (2000) *G-protein-coupled receptors function as oligomers in vivo.* Curr Biol **10**(6), 341-4
  57. Angers, S., Salahpour, A., Joly, E., Hilairet, S., Chelsky, D., Dennis, M. and Bouvier, M. (2000) *Detection of beta 2-adrenergic receptor dimerization in living*

- cells using bioluminescence resonance energy transfer (BRET)*. Proc Natl Acad Sci U S A **97**(7), 3684-9
58. Wang, D., Sun, X., Bohn, L. M. and Sadee, W. (2005) *Opioid receptor homo- and heterodimerization in living cells by quantitative bioluminescence resonance energy transfer*. Mol Pharmacol **67**(6), 2173-84
  59. James, J. R., Oliveira, M. I., Carmo, A. M., Iaboni, A. and Davis, S. J. (2006) *A rigorous experimental framework for detecting protein oligomerization using bioluminescence resonance energy transfer*. Nat Methods **3**(12), 1001-6
  60. Hazum, E., Chang, K. J. and Cuatrecasas, P. (1979) *Opiate (Enkephalin) Receptors of Neuro-Blastoma Cells - Occurrence in Clusters on the Cell-Surface*. Science **206**(4422), 1077-1079
  61. Fields, H. L., Emson, P. C., Leigh, B. K., Gilbert, R. F. T. and Iversen, L. L. (1980) *Multiple Opiate Receptor-Sites on Primary Afferent-Fibers*. Nature **284**(5754), 351-353
  62. Egan, T. M. and North, R. A. (1981) *Both Mu and Delta-Opiate Receptors Exist on the Same Neuron*. Science **214**(4523), 923-924
  63. Zieglgansberger, W., French, E. D., Mercuri, N., Pelayo, F. and Williams, J. T. (1982) *Multiple Opiate Receptors on Neurons of the Mammalian Central Nervous-System - Invivo and Invitro Studies*. Life Sciences **31**(20-2), 2343-2346
  64. Rothman, R. and Westfall, T. C. (1983) *Further evidence for an opioid receptor complex*. J Neurobiol **14**(5), 341-51
  65. Rothman, R. B., Bowen, W. D., Schumacher, U. K. and Pert, C. B. (1983) *Effect of beta-FNA on opiate receptor binding: preliminary evidence for two types of mu receptors*. Eur J Pharmacol **95**(1-2), 147-8
  66. Rothman, R. B., Danks, J. A., Jacobson, A. E., Burke, T. R., Jr. and Rice, K. C. (1985) *Leucine enkephalin noncompetitively inhibits the binding of [3H]naloxone to the opiate mu-recognition site: evidence for delta----mu binding site interactions in vitro*. Neuropeptides **6**(4), 351-63
  67. Rothman, R. B., Pert, C. B., Jacobson, A. E., Burke, T. R., Jr. and Rice, K. C. (1984) *Morphine noncompetitively inhibits [3H]leucine enkephalin binding to membranes lacking type-II delta binding sites: evidence for a two-site allosteric model*. Neuropeptides **4**(3), 257-60
  68. Rothman, R. B. and Westfall, T. C. (1983) *Interaction of leucine enkephalin with (3H)naloxone binding in rat brain: evidence for an opioid receptor complex*. Neurochem Res **8**(7), 913-31

69. Cvejić, S. and Devi, L. A. (1997) *Dimerization of the delta opioid receptor: implication for a role in receptor internalization*. J Biol Chem **272**(43), 26959-64
70. Jordan, B. A. and Devi, L. A. (1999) *G-protein-coupled receptor heterodimerization modulates receptor function*. Nature **399**(6737), 697-700
71. George, S. R., Fan, T., Xie, Z., Tse, R., Tam, V., Varghese, G. and O'Dowd, B. F. (2000) *Oligomerization of mu- and delta-opioid receptors. Generation of novel functional properties*. J Biol Chem **275**(34), 26128-35
72. Martin, N. A. and Prather, P. L. (2001) *Interaction of co-expressed mu- and delta-opioid receptors in transfected rat pituitary GH(3) cells*. Mol Pharmacol **59**(4), 774-83
73. Hasbi, A., Nguyen, T., Fan, T., Cheng, R., Rashid, A., Alijaniam, M., Rasenick, M. M., O'Dowd, B. F. and George, S. R. (2007) *Trafficking of preassembled opioid mu-delta heterooligomer-Gz signaling complexes to the plasma membrane: coregulation by agonists*. Biochemistry **46**(45), 12997-3009
74. Rozenfeld, R. and Devi, L. A. (2007) *Receptor heterodimerization leads to a switch in signaling: beta-arrestin2-mediated ERK activation by mu-delta opioid receptor heterodimers*. Faseb J **21**(10), 2455-65
75. Levac, B. A., O'Dowd, B. F. and George, S. R. (2002) *Oligomerization of opioid receptors: generation of novel signaling units*. Curr Opin Pharmacol **2**(1), 76-81
76. Leitz, A. J., Bayburt, T. H., Barnakov, A. N., Springer, B. A. and Sligar, S. G. (2006) *Functional reconstitution of Beta2-adrenergic receptors utilizing self-assembling Nanodisc technology*. Biotechniques **40**(5), 601-2, 604, 606, passim
77. Bayburt, T. H., Leitz, A. J., Xie, G., Oprian, D. D. and Sligar, S. G. (2007) *Transducin activation by nanoscale lipid bilayers containing one and two rhodopsins*. J Biol Chem **282**(20), 14875-81
78. Whorton, M. R., Bokoch, M. P., Rasmussen, S. G., Huang, B., Zare, R. N., Kobilka, B. and Sunahara, R. K. (2007) *A monomeric G protein-coupled receptor isolated in a high-density lipoprotein particle efficiently activates its G protein*. Proc Natl Acad Sci U S A **104**(18), 7682-7
79. Whorton, M. R., Jastrzebska, B., Park, P. S., Fotiadis, D., Engel, A., Palczewski, K. and Sunahara, R. K. (2008) *Efficient coupling of transducin to monomeric rhodopsin in a phospholipid bilayer*. J Biol Chem **283**(7), 4387-94
80. Banerjee, S., Huber, T. and Sakmar, T. P. (2008) *Rapid incorporation of functional rhodopsin into nanoscale apolipoprotein bound bilayer (NABB) particles*. J Mol Biol **377**(4), 1067-81

81. Rothman, R. B. and Westfall, T. C. (1983) *Multiple opioid receptors: an examination of the dissociation of [3H]leucine enkephalin from rat brain membranes*. *Neurochem Res* **8**(2), 179-84
82. Nishimura, S. L., Recht, L. D. and Pasternak, G. W. (1984) *Biochemical characterization of high-affinity 3H-opioid binding. Further evidence for Mu1 sites*. *Mol Pharmacol* **25**(1), 29-37
83. Xu, H., Partilla, J. S., de Costa, B. R., Rice, K. C. and Rothman, R. B. (1993) *Differential binding of opioid peptides and other drugs to two subtypes of opioid delta ncx binding sites in mouse brain: further evidence for delta receptor heterogeneity*. *Peptides* **14**(5), 893-907
84. Cho, T. M., Ge, B. L. and Loh, H. H. (1985) *Isolation and purification of morphine receptor by affinity chromatography*. *Life Sci* **36**(11), 1075-85
85. Jin, Y. C., Ye, C. Y., Li, Y., Suo, C. L., Li, L. Y., Liu, M. Q., Jin, X. M. and Mao, Z. M. (1989) *Solubilization and purification of opioid receptor molecules of rat brain*. *Proc Chin Acad Med Sci Peking Union Med Coll* **4**(1), 1-7
86. Li, L. Y., Zhang, Z. M., Su, Y. F., Watkins, W. D. and Chang, K. J. (1992) *Purification of opioid receptor in the presence of sodium ions*. *Life Sci* **51**(15), 1177-85
87. Loukas, S., Mercouris, M., Panetsos, F. and Zioudrou, C. (1994) *Purification to homogeneity of an active opioid receptor from rat brain by affinity chromatography*. *Proc Natl Acad Sci U S A* **91**(10), 4574-8
88. Weems, H. B., Chalecka-Franaszek, E. and Cote, T. E. (1996) *Solubilization of high-affinity, guanine nucleotide-sensitive mu-opioid receptors from rat brain membranes*. *J Neurochem* **66**(3), 1042-50
89. Gioannini, T. L., Howard, A. D., Hiller, J. M. and Simon, E. J. (1985) *Purification of an active opioid-binding protein from bovine striatum*. *J Biol Chem* **260**(28), 15117-21
90. Ueda, H., Harada, H., Misawa, H., Nozaki, M. and Takagi, H. (1987) *Purified opioid mu-receptor is of a different molecular size than delta- and kappa-receptors*. *Neurosci Lett* **75**(3), 339-44
91. Cho, T. M., Ge, B. L., Yamato, C., Smith, A. P. and Loh, H. H. (1983) *Isolation of opiate binding components by affinity chromatography and reconstitution of binding activities*. *Proc Natl Acad Sci U S A* **80**(17), 5176-80

92. Cote, T. E., Gosse, M. E. and Weems, H. B. (1993) *Solubilization of high-affinity, guanine nucleotide-sensitive mu-opioid receptors from 7315c cell membranes*. J Neurochem **61**(3), 973-8
93. Talmont, F., Sidobre, S., Demange, P., Milon, A. and Emorine, L. J. (1996) *Expression and pharmacological characterization of the human mu-opioid receptor in the methylotrophic yeast Pichia pastoris*. FEBS Lett **394**(3), 268-72
94. Sarramegna, V., Demange, P., Milon, A. and Talmont, F. (2002) *Optimizing functional versus total expression of the human mu-opioid receptor in Pichia pastoris*. Protein Expr Purif **24**(2), 212-20
95. Sarramegna, V., Talmont, F., Sere de Roch, M., Milon, A. and Demange, P. (2002) *Green fluorescent protein as a reporter of human mu-opioid receptor overexpression and localization in the methylotrophic yeast Pichia pastoris*. J Biotechnol **99**(1), 23-39
96. Sarramegna, V., Muller, I., Mousseau, G., Froment, C., Monsarrat, B., Milon, A. and Talmont, F. (2005) *Solubilization, purification, and mass spectrometry analysis of the human mu-opioid receptor expressed in Pichia pastoris*. Protein Expr Purif **43**(2), 85-93
97. O'Reilly, D. R., Miller, L.K., Lucklow, V.A. (1992) *Baculovirus expression vectors: a laboratory manual*, W.H. Freeman & Co., New York
98. Raynor, K., Kong, H., Mestek, A., Bye, L. S., Tian, M., Liu, J., Yu, L. and Reisine, T. (1995) *Characterization of the cloned human mu opioid receptor*. J Pharmacol Exp Ther **272**(1), 423-8
99. Emmerson, P. J., Clark, M. J., Mansour, A., Akil, H., Woods, J. H. and Medzihradsky, F. (1996) *Characterization of opioid agonist efficacy in a C6 glioma cell line expressing the mu opioid receptor*. J Pharmacol Exp Ther **278**(3), 1121-7
100. Alt, A., Mansour, A., Akil, H., Medzihradsky, F., Traynor, J. R. and Woods, J. H. (1998) *Stimulation of guanosine-5'-O-(3-[<sup>35</sup>S]thio)triphosphate binding by endogenous opioids acting at a cloned mu receptor*. J Pharmacol Exp Ther **286**(1), 282-8
101. Clark, M. J., Furman, C. A., Gilson, T. D. and Traynor, J. R. (2006) *Comparison of the relative efficacy and potency of mu-opioid agonists to activate Galpha(i/o) proteins containing a pertussis toxin-insensitive mutation*. J Pharmacol Exp Ther **317**(2), 858-64
102. Kenakin, T. (2004) *Principles: receptor theory in pharmacology*. Trends Pharmacol Sci **25**(4), 186-92

103. Liu-Chen, L. Y., Chen, C. and Phillips, C. A. (1993) *Beta-[3H]funaltrexamine-labeled mu-opioid receptors: species variations in molecular mass and glycosylation by complex-type, N-linked oligosaccharides*. *Mol Pharmacol* **44**(4), 749-56
104. Obermeier, H., Wehmeyer, A. and Schulz, R. (1996) *Expression of mu-, delta- and kappa-opioid receptors in baculovirus-infected insect cells*. *Eur J Pharmacol* **318**(1), 161-6
105. Massotte, D., Baroche, L., Simonin, F., Yu, L., Kieffer, B. and Pattus, F. (1997) *Characterization of delta, kappa, and mu human opioid receptors overexpressed in baculovirus-infected insect cells*. *J Biol Chem* **272**(32), 19987-92
106. Kempf, J., Snook, L. A., Vonesch, J. L., Dahms, T. E., Pattus, F. and Massotte, D. (2002) *Expression of the human mu opioid receptor in a stable Sf9 cell line*. *J Biotechnol* **95**(2), 181-7
107. Massotte, D., Pereira, C. A., Pouliquen, Y. and Pattus, F. (1999) *Parameters influencing human mu opioid receptor over-expression in baculovirus-infected insect cells*. *J Biotechnol* **69**(1), 39-45
108. Perret, B. G., Wagner, R., Lecat, S., Brillet, K., Rabut, G., Bucher, B. and Pattus, F. (2003) *Expression of EGFP-amino-tagged human mu opioid receptor in Drosophila Schneider 2 cells: a potential expression system for large-scale production of G-protein coupled receptors*. *Protein Expr Purif* **31**(1), 123-32
109. Guan, X. M., Kobilka, T. S. and Kobilka, B. K. (1992) *Enhancement of membrane insertion and function in a type IIIb membrane protein following introduction of a cleavable signal peptide*. *J Biol Chem* **267**(31), 21995-8
110. Kobilka, B. K. (1995) *Amino and carboxyl terminal modifications to facilitate the production and purification of a G protein-coupled receptor*. *Anal Biochem* **231**(1), 269-71
111. Hanson, M. A., Cherezov, V., Griffith, M. T., Roth, C. B., Jaakola, V. P., Chien, E. Y., Velasquez, J., Kuhn, P. and Stevens, R. C. (2008) *A specific cholesterol binding site is established by the 2.8 Å structure of the human beta2-adrenergic receptor*. *Structure* **16**(6), 897-905
112. Cherezov, V., Liu, J., Griffith, M., Hanson, M. A. and Stevens, R. C. (2008) *LCP-FRAP Assay for Pre-Screening Membrane Proteins for in Meso Crystallization*. *Cryst Growth Des* **8**(12), 4307-4315
113. Zukin, R. S., Sugarman, J. R., Fitz-Syage, M. L., Gardner, E. L., Zukin, S. R. and Gintzler, A. R. (1982) *Naltrexone-induced opiate receptor supersensitivity*. *Brain Res* **245**(2), 285-92



114. Cote, T. E., Izenwasser, S. and Weems, H. B. (1993) *Naltrexone-induced upregulation of mu opioid receptors on 7315c cell and brain membranes: enhancement of opioid efficacy in inhibiting adenylyl cyclase*. *J Pharmacol Exp Ther* **267**(1), 238-44
115. Yao, Z. and Kobilka, B. (2005) *Using synthetic lipids to stabilize purified beta2 adrenoceptor in detergent micelles*. *Anal Biochem* **343**(2), 344-6
116. Rosenbaum, D. M., Cherezov, V., Hanson, M. A., Rasmussen, S. G., Thian, F. S., Kobilka, T. S., Choi, H. J., Yao, X. J., Weis, W. I., Stevens, R. C. and Kobilka, B. K. (2007) *GPCR engineering yields high-resolution structural insights into beta2-adrenergic receptor function*. *Science* **318**(5854), 1266-73
117. Baneres, J. L., Mesnier, D., Martin, A., Joubert, L., Dumuis, A. and Bockaert, J. (2005) *Molecular characterization of a purified 5-HT4 receptor: a structural basis for drug efficacy*. *J Biol Chem* **280**(21), 20253-60
118. Lazar, D. F. and Medzihradsky, F. (1993) *Altered transition between agonist- and antagonist-favoring states of mu-opioid receptor in brain membranes with modified microviscosity*. *J Neurochem* **61**(3), 1135-40
119. Ruprecht, J. J., Mielke, T., Vogel, R., Villa, C. and Schertler, G. F. (2004) *Electron crystallography reveals the structure of metarhodopsin I*. *Embo J* **23**(18), 3609-20
120. Cherezov, V., Rosenbaum, D. M., Hanson, M. A., Rasmussen, S. G., Thian, F. S., Kobilka, T. S., Choi, H. J., Kuhn, P., Weis, W. I., Kobilka, B. K. and Stevens, R. C. (2007) *High-resolution crystal structure of an engineered human beta2-adrenergic G protein-coupled receptor*. *Science* **318**(5854), 1258-65
121. Ramon, E., Marron, J., del Valle, L., Bosch, L., Andres, A., Manyosa, J. and Garriga, P. (2003) *Effect of dodecyl maltoside detergent on rhodopsin stability and function*. *Vision Res* **43**(28), 3055-61
122. Chae, P. S., Wander, M. J., Bowling, A. P., Laible, P. D. and Gellman, S. H. (2008) *Glycotripod amphiphiles for solubilization and stabilization of a membrane-protein superassembly: importance of branching in the hydrophilic portion*. *Chembiochem* **9**(11), 1706-9
123. Bradford, M. M. (1976) *A rapid and sensitive method for the quantitation of microgram quantities of protein utilizing the principle of protein-dye binding*. *Anal Biochem* **72**, 248-54
124. Sambrook, J., Fritsch, E.F., Maniatis, T. (2001) *Molecular Cloning, A Laboratory Manual*, 3 Ed., Cold Spring Harbor Laboratory Press, Cold Springs Harbor

125. Waldhoer, M., Bartlett, S. E. and Whistler, J. L. (2004) *Opioid receptors*. *Annu Rev Biochem* **73**, 953-90
126. Bai, M. (2004) *Dimerization of G-protein-coupled receptors: roles in signal transduction*. *Cell Signal* **16**(2), 175-86
127. Milligan, G., Canals, M., Padiani, J. D., Ellis, J. and Lopez-Gimenez, J. F. (2006) *The role of GPCR dimerisation/oligomerisation in receptor signalling*. *Ernst Schering Found Symp Proc* (2), 145-61
128. Gomes, I., Jordan, B. A., Gupta, A., Trapaidze, N., Nagy, V. and Devi, L. A. (2000) *Heterodimerization of mu and delta opioid receptors: A role in opiate synergy*. *J Neurosci* **20**(22), RC110
129. Gomes, I., Filipovska, J., Jordan, B. A. and Devi, L. A. (2002) *Oligomerization of opioid receptors*. *Methods* **27**(4), 358-65
130. Nath, A., Atkins, W. M. and Sligar, S. G. (2007) *Applications of phospholipid bilayer nanodiscs in the study of membranes and membrane proteins*. *Biochemistry* **46**(8), 2059-69
131. Liang, Y., Fotiadis, D., Filipek, S., Saperstein, D. A., Palczewski, K. and Engel, A. (2003) *Organization of the G protein-coupled receptors rhodopsin and opsin in native membranes*. *J Biol Chem* **278**(24), 21655-62
132. Fotiadis, D., Liang, Y., Filipek, S., Saperstein, D. A., Engel, A. and Palczewski, K. (2003) *Atomic-force microscopy: Rhodopsin dimers in native disc membranes*. *Nature* **421**(6919), 127-8
133. Jastrzebska, B., Fotiadis, D., Jang, G. F., Stenkamp, R. E., Engel, A. and Palczewski, K. (2006) *Functional and structural characterization of rhodopsin oligomers*. *J Biol Chem* **281**(17), 11917-22
134. Remmers, A. E. and Medzihradsky, F. (1991) *Reconstitution of high-affinity opioid agonist binding in brain membranes*. *Proc Natl Acad Sci U S A* **88**(6), 2171-5
135. Traynor, J. R. and Elliott, J. (1993) *delta-Opioid receptor subtypes and cross-talk with mu-receptors*. *Trends Pharmacol Sci* **14**(3), 84-6
136. Pasternak, G. W. (2001) *Insights into mu opioid pharmacology the role of mu opioid receptor subtypes*. *Life Sci* **68**(19-20), 2213-9
137. Clark, J. A., Liu, L., Price, M., Hersh, B., Edelson, M. and Pasternak, G. W. (1989) *Kappa opiate receptor multiplicity: evidence for two U50,488-sensitive*

- kappa 1 subtypes and a novel kappa 3 subtype.* J Pharmacol Exp Ther **251**(2), 461-8
138. Cerione, R. A. and Ross, E. M. (1991) *Reconstitution of receptors and G proteins in phospholipid vesicles.* Methods Enzymol **195**, 329-42
139. Mansoor, S. E., Palczewski, K. and Farrens, D. L. (2006) *Rhodopsin self-associates in asolectin liposomes.* Proc Natl Acad Sci U S A **103**(9), 3060-5
140. Ueda, H., Harada, H., Nozaki, M., Katada, T., Ui, M., Satoh, M. and Takagi, H. (1988) *Reconstitution of rat brain mu opioid receptors with purified guanine nucleotide-binding regulatory proteins, Gi and Go.* Proc Natl Acad Sci U S A **85**(18), 7013-7
141. Frey, E. A., Gosse, M. E. and Cote, T. E. (1989) *Reconstitution of the solubilized mu-opioid receptor coupled to a GTP-binding protein.* Eur J Pharmacol **172**(4-5), 347-56
142. Fan, L. Q., Gioannini, T. L., Wolinsky, T., Hiller, J. M. and Simon, E. J. (1995) *Functional reconstitution of a highly purified mu-opioid receptor protein with purified G proteins in liposomes.* J Neurochem **65**(6), 2537-42
143. Scheideler, M. A. and Zukin, R. S. (1990) *Reconstitution of solubilized delta-opiate receptor binding sites in lipid vesicles.* J Biol Chem **265**(25), 15176-82
144. Gomes, I., Gupta, A., Filipovska, J., Szeto, H. H., Pintar, J. E. and Devi, L. A. (2004) *A role for heterodimerization of mu and delta opiate receptors in enhancing morphine analgesia.* Proceedings of the National Academy of Sciences of the United States of America **101**(14), 5135-5139
145. Jonas, A. (1986) *Reconstitution of high-density lipoproteins.* Methods Enzymol **128**, 553-82
146. Patil, P. V. and Ballou, D. P. (2000) *The use of protocatechuate dioxygenase for maintaining anaerobic conditions in biochemical experiments.* Anal Biochem **286**(2), 187-92
147. Kozasa, T. (1999) Purification of Recombinant G Protein alpha and beta-gamma Subunits from Sf9 Cells. In: D. R. Manning (ed). *G Proteins: Techniques of Analysis*, CRC Press LLC, Boca Raton
148. Panetta, R. and Greenwood, M. T. (2008) *Physiological relevance of GPCR oligomerization and its impact on drug discovery.* Drug Discov Today **13**(23-24), 1059-66

149. Fichna, J., do-Rego, J. C., Kosson, P., Schiller, P. W., Costentin, J. and Janecka, A. (2006) *[(35)S]GTPgammaS binding stimulated by endomorphin-2 and morphiceptin analogs*. *Biochem Biophys Res Commun* **345**(1), 162-8
150. Clark, M. J. and Traynor, J. R. (2006) *Mediation of adenylyl cyclase sensitization by PTX-insensitive GalphaoA, Galphai1, Galphai2 or Galphai3*. *J Neurochem* **99**(6), 1494-504
151. Chakrabarti, S., Prather, P. L., Yu, L., Law, P. Y. and Loh, H. H. (1995) *Expression of the Mu-Opioid Receptor in CHO Cells - Ability of Mu-Opioid Ligands to Promote Alpha-Azidoanilido [P-32] Gtp Labeling of Multiple G-Protein Alpha-Subunits*. *Journal of Neurochemistry* **64**(6), 2534-2543
152. Alt, A., Clark, M. J., Woods, J. H. and Traynor, J. R. (2002) *Mu and Delta opioid receptors activate the same G proteins in human neuroblastoma SH-SY5Y cells*. *Br J Pharmacol* **135**(1), 217-25
153. Saidak, Z., Blake-Palmer, K., Hay, D. L., Northup, J. K. and Glass, M. (2006) *Differential activation of G-proteins by mu-opioid receptor agonists*. *Br J Pharmacol* **147**(6), 671-80
154. Stanasila, L., Lim, W. K., Neubig, R. R. and Pattus, F. (2000) *Coupling efficacy and selectivity of the human mu-opioid receptor expressed as receptor-Galpa fusion proteins in Escherichia coli*. *J Neurochem* **75**(3), 1190-9
155. Kleineke, J., Duls, C. and Soling, H. D. (1979) *Subcellular Compartmentation of Guanine-Nucleotides and Functional Relationships between the Adenine and Guanine-Nucleotide Systems in Isolated Hepatocytes*. *Febs Letters* **107**(1), 198-202
156. Peveri, P., Heyworth, P. G. and Curnutte, J. T. (1992) *Absolute Requirement for Gtp in Activation of Human Neutrophil NADPH Oxidase in a Cell-Free System - Role of Atp in Regenerating Gtp*. *Proceedings of the National Academy of Sciences of the United States of America* **89**(6), 2494-2498
157. McKee, E. E., Bentley, A. T., Smith, R. M. and Ciaccio, C. E. (1999) *Origin of guanine nucleotides in isolated heart mitochondria*. *Biochemical and Biophysical Research Communications* **257**(2), 466-472
158. Wang, Z. J., Segredo, V. and Sadee, W. (1994) *Constitutive Mu-Opioid Receptor Activation as a Regulatory Mechanism in Narcotic Tolerance and Dependence*. *Faseb Journal* **8**(4), A379-a379
159. Burford, N. T., Wang, D. X. and Sadee, W. (2000) *G-protein coupling of mu-opioid receptors (OP3): elevated basal signalling activity*. *Biochemical Journal* **348**, 531-537

160. Liu, J. G., Ruckle, M. B. and Prather, P. L. (2001) *Constitutively active mu-opioid receptors inhibit adenylyl cyclase activity in intact cells and activate G-proteins differently than the agonist [D-Ala<sup>2</sup>,N-MePhe<sup>4</sup>,Gly-ol<sup>5</sup>]enkephalin*. J Biol Chem **276**(41), 37779-86
161. Liu, J. G. and Prather, P. L. (2001) *Chronic exposure to mu-opioid agonists produces constitutive activation of mu-opioid receptors in direct proportion to the efficacy of the agonist used for pretreatment*. Mol Pharmacol **60**(1), 53-62
162. Liu, J. G. and Prather, P. L. (2002) *Chronic agonist treatment converts antagonists into inverse agonists at delta-opioid receptors*. J Pharmacol Exp Ther **302**(3), 1070-9
163. Wang, D., Raehal, K. M., Bilsky, E. J. and Sadee, W. (2001) *Inverse agonists and neutral antagonists at mu opioid receptor (MOR): possible role of basal receptor signaling in narcotic dependence*. J Neurochem **77**(6), 1590-600
164. Burgisser, E., De Lean, A. and Lefkowitz, R. J. (1982) *Reciprocal modulation of agonist and antagonist binding to muscarinic cholinergic receptor by guanine nucleotide*. Proc Natl Acad Sci U S A **79**(6), 1732-6
165. Snook, L. A., Milligan, G., Kieffer, B. L. and Massotte, D. (2008) *Co-expression of mu and delta opioid receptors as receptor-G protein fusions enhances both mu and delta signalling via distinct mechanisms*. J Neurochem **105**(3), 865-73
166. Pitcher, J. A., Freedman, N. J. and Lefkowitz, R. J. (1998) *G protein-coupled receptor kinases*. Annual Review of Biochemistry **67**, 653-692
167. Zuo, Z. (2005) *The role of opioid receptor internalization and beta-arrestins in the development of opioid tolerance*. Anesth Analg **101**(3), 728-34, table of contents
168. Celver, J. P., Lowe, J., Kovoov, A., Gurevich, V. V. and Chavkin, C. (2001) *Threonine 180 is required for G-protein-coupled receptor kinase 3- and beta-arrestin 2-mediated desensitization of the mu-opioid receptor in Xenopus oocytes*. J Biol Chem **276**(7), 4894-900
169. Oakley, R. H., Laporte, S. K., Holt, J. A., Caron, M. G. and Barak, L. S. (2000) *Differential affinities of visual arrestin, beta arrestin1, and beta arrestin2 for G protein-coupled receptors delineate two major classes of receptors*. Journal of Biological Chemistry **275**(22), 17201-17210
170. Lowe, J. D., Celver, J. P., Gurevich, V. V. and Chavkin, C. (2002) *mu-Opioid receptors desensitize less rapidly than delta-opioid receptors due to less efficient activation of arrestin*. J Biol Chem **277**(18), 15729-35

171. Bohn, L. M., Gainetdinov, R. R., Lin, F. T., Lefkowitz, R. J. and Caron, M. G. (2000) *Mu-opioid receptor desensitization by beta-arrestin-2 determines morphine tolerance but not dependence*. *Nature* **408**(6813), 720-3
172. Bohn, L. M., Lefkowitz, R. J. and Caron, M. G. (2002) *Differential mechanisms of morphine antinociceptive tolerance revealed in (beta)arrestin-2 knock-out mice*. *J Neurosci* **22**(23), 10494-500
173. Blake, A. D., Bot, G., Freeman, J. C. and Reisine, T. (1997) *Differential opioid agonist regulation of the mouse mu opioid receptor*. *Journal of Biological Chemistry* **272**(2), 782-790
174. Zhang, J., Ferguson, S. S. G., Barak, L. S., Bodduluri, S. R., Laporte, S. A., Law, P. Y. and Caron, M. G. (1998) *Role for G protein-coupled receptor kinase in agonist-specific regulation of mu-opioid receptor responsiveness*. *Proceedings of the National Academy of Sciences of the United States of America* **95**(12), 7157-7162
175. Bernstein, M. A. and Welch, S. P. (1998) *mu-Opioid receptor down-regulation and cAMP-dependent protein kinase phosphorylation in a mouse model of chronic morphine tolerance*. *Brain Res Mol Brain Res* **55**(2), 237-42
176. Tao, P. L., Han, K. F., Wang, S. D., Lue, W. M., Elde, R., Law, P. Y. and Loh, H. H. (1998) *Immunohistochemical evidence of down-regulation of mu-opioid receptor after chronic PL-017 in rats*. *Eur J Pharmacol* **344**(2-3), 137-42
177. De Vries, T. J., Tjon Tien Ril, G. H., Van der Laan, J. W., Mulder, A. H. and Schoffelmeer, A. N. (1993) *Chronic exposure to morphine and naltrexone induces changes in catecholaminergic neurotransmission in rat brain without altering mu-opioid receptor sensitivity*. *Life Sci* **52**(21), 1685-93
178. Werling, L. L., McMahon, P. N. and Cox, B. M. (1989) *Selective changes in mu opioid receptor properties induced by chronic morphine exposure*. *Proc Natl Acad Sci U S A* **86**(16), 6393-7
179. Brady, L. S., Herkenham, M., Long, J. B. and Rothman, R. B. (1989) *Chronic morphine increases mu-opiate receptor binding in rat brain: a quantitative autoradiographic study*. *Brain Res* **477**(1-2), 382-6
180. Rothman, R. B., Bykov, V., Long, J. B., Brady, L. S., Jacobson, A. E., Rice, K. C. and Holaday, J. W. (1989) *Chronic administration of morphine and naltrexone up-regulate mu-opioid binding sites labeled by [3H][D-Ala2,MePhe4,Gly-ol5]enkephalin: further evidence for two mu-binding sites*. *Eur J Pharmacol* **160**(1), 71-82

181. Rothman, R. B., Long, J. B., Bykov, V., Xu, H., Jacobson, A. E., Rice, K. C. and Holaday, J. W. (1991) *Upregulation of the opioid receptor complex by the chronic administration of morphine: a biochemical marker related to the development of tolerance and dependence*. *Peptides* **12**(1), 151-60
182. He, L., Fong, J., von Zastrow, M. and Whistler, J. L. (2002) *Regulation of opioid receptor trafficking and morphine tolerance by receptor oligomerization*. *Cell* **108**(2), 271-82
183. Bailey, C. P., Couch, D., Johnson, E., Griffiths, K., Kelly, E. and Henderson, G. (2003) *Mu-opioid receptor desensitization in mature rat neurons: lack of interaction between DAMGO and morphine*. *J Neurosci* **23**(33), 10515-20
184. Rothman, R. B., Danks, J. A., Herkenham, M., Jacobson, A. E., Burke, T. R., Jr. and Rice, K. C. (1985) *Evidence that the delta-selective alkylating agent, fit, alters the mu-noncompetitive opiate delta binding site*. *Neuropeptides* **6**(3), 227-37
185. Danks, J. A., Tortella, F. C., Bykov, V., Jacobson, A. E., Rice, K. C., Holaday, J. W. and Rothman, R. B. (1986) *Upregulation of the mu-noncompetitive delta binding site by chronic morphine administration: effect of preincubating membranes in 400 nM sodium chloride*. *NIDA Res Monogr* **75**, 93-6
186. Rothman, R. B., McLean, S., Bykov, V., Lessor, R. A., Jacobson, A. E., Rice, K. C. and Holaday, J. W. (1987) *Chronic morphine upregulates a mu-opiate binding site labeled by [3H]cycloFOXY: a novel opiate antagonist suitable for positron emission tomography*. *Eur J Pharmacol* **142**(1), 73-81
187. Danks, J. A., Tortella, F. C., Long, J. B., Bykov, V., Jacobson, A. E., Rice, K. C., Holaday, J. W. and Rothman, R. B. (1988) *Chronic administration of morphine and naltrexone up-regulate [3H][D-Ala2,D-leu5]enkephalin binding sites by different mechanisms*. *Neuropharmacology* **27**(9), 965-74
188. Abdelhamid, E. E., Sultana, M., Portoghese, P. S. and Takemori, A. E. (1991) *Selective blockage of delta opioid receptors prevents the development of morphine tolerance and dependence in mice*. *J Pharmacol Exp Ther* **258**(1), 299-303
189. Fundytus, M. E., Schiller, P. W., Shapiro, M., Weltrowska, G. and Coderre, T. J. (1995) *Attenuation of morphine tolerance and dependence with the highly selective delta-opioid receptor antagonist TIPP[psi]*. *Eur J Pharmacol* **286**(1), 105-8
190. Hepburn, M. J., Little, P. J., Gingras, J. and Kuhn, C. M. (1997) *Differential effects of naltrindole on morphine-induced tolerance and physical dependence in rats*. *J Pharmacol Exp Ther* **281**(3), 1350-6

191. Zhu, Y., King, M. A., Schuller, A. G., Nitsche, J. F., Reidl, M., Elde, R. P., Unterwald, E., Pasternak, G. W. and Pintar, J. E. (1999) *Retention of supraspinal delta-like analgesia and loss of morphine tolerance in delta opioid receptor knockout mice*. *Neuron* **24**(1), 243-52
192. Ananthan, S. (2006) *Opioid ligands with mixed mu/delta opioid receptor interactions: an emerging approach to novel analgesics*. *Aaps J* **8**(1), E118-25
193. Schiller, P. W. (2009) *Bi- or multifunctional opioid peptide drugs*. *Life Sci*
194. Arttamangkul, S., Alvarez-Maubecin, V., Thomas, G., Williams, J. T. and Grandy, D. K. (2000) *Binding and internalization of fluorescent opioid peptide conjugates in living cells*. *Mol Pharmacol* **58**(6), 1570-80
195. Alvarez, V. A., Arttamangkul, S., Dang, V., Salem, A., Whistler, J. L., Von Zastrow, M., Grandy, D. K. and Williams, J. T. (2002) *mu-Opioid receptors: Ligand-dependent activation of potassium conductance, desensitization, and internalization*. *J Neurosci* **22**(13), 5769-76
196. Waldhoer, M., Fong, J., Jones, R. M., Lunzer, M. M., Sharma, S. K., Kostenis, E., Portoghese, P. S. and Whistler, J. L. (2005) *A heterodimer-selective agonist shows in vivo relevance of G protein-coupled receptor dimers*. *Proc Natl Acad Sci U S A* **102**(25), 9050-5
197. Daniels, D. J., Lenard, N. R., Etienne, C. L., Law, P. Y., Roerig, S. C. and Portoghese, P. S. (2005) *Opioid-induced tolerance and dependence in mice is modulated by the distance between pharmacophores in a bivalent ligand series*. *Proc Natl Acad Sci U S A* **102**(52), 19208-13
198. Axelrod, D. (1981) *Cell-Substrate Contacts Illuminated by Total Internal-Reflection Fluorescence*. *Journal of Cell Biology* **89**(1), 141-145
199. Attila, M., Salvadori, S., Balboni, G., Bryant, S. D. and Lazarus, L. H. (1993) *Synthesis and receptor binding analysis of dermorphin hepta-, hexa- and pentapeptide analogues. Evidence for one- and two-side binding models for the mu-opioid receptor*. *Int J Pept Protein Res* **42**(6), 550-9
200. Puttfarcken, P., Werling, L. L., Brown, S. R., Cote, T. E. and Cox, B. M. (1986) *Sodium regulation of agonist binding at opioid receptors. I. Effects of sodium replacement on binding at mu- and delta-type receptors in 7315c and NG108-15 cells and cell membranes*. *Mol Pharmacol* **30**(2), 81-9
201. Pelton, J. T., Kazmierski, W., Gulya, K., Yamamura, H. I. and Hruby, V. J. (1986) *Design and synthesis of conformationally constrained somatostatin analogues with high potency and specificity for mu opioid receptors*. *J Med Chem* **29**(11), 2370-5



202. Kramer, T. H., Shook, J. E., Kazmierski, W., Ayres, E. A., Wire, W. S., Hruby, V. J. and Burks, T. F. (1989) *Novel peptidic mu opioid antagonists: pharmacologic characterization in vitro and in vivo*. J Pharmacol Exp Ther **249**(2), 544-51
203. Szucs, M., Boda, K. and Gintzler, A. R. (2004) *Dual effects of DAMGO [D-Ala<sup>2</sup>,N-Me-Phe<sup>4</sup>,Gly<sup>5</sup>-ol]-enkephalin and CTAP (D-Phe-Cys-Tyr-D-Trp-Arg-Thr-Pen-Thr-NH<sub>2</sub>) on adenylyl cyclase activity: implications for mu-opioid receptor Gs coupling*. J Pharmacol Exp Ther **310**(1), 256-62
204. Divin, M. F., Bradbury, F. A., Carroll, F. I. and Traynor, J. R. (2009) *Neutral antagonist activity of naltrexone and 6beta-naltrexol in naive and opioid-dependent C6 cells expressing a micro-opioid receptor*. Br J Pharmacol **156**(7), 1044-53